Title
Resource Limits and Conversion Efficiency with Implications for Climate Change

Author
Croft, Gregory Donald

Publication Date
2009

Peer reviewed|Thesis/dissertation

Resource Limits and Conversion Efficiency with Implications for Climate Change and California's Energy Supply

by

Gregory Donald Croft

A dissertation submitted in partial satisfaction of the
requirements for the degree of
Doctor of Philosophy

in

Engineering - Civil and Environmental Engineering

in the

GRADUATE DIVISION
of the
UNIVERSITY OF CALIFORNIA, BERKELEY

Committee in charge:

Professor Tadeusz W. Patzek, Chair
Professor James W. Rector
Professor Richard Norgaard
Professor Nicholas Sitar

Fall 2009

Resource Limits and Conversion Efficiency with Implications for Climate Change and California's Energy Supply,
The dissertation of Gregory Donald Croft is approved:

Chair ________________________ Date __________

________________________ Date __________

________________________ Date __________

________________________ Date __________

University of California, Berkeley
Fall 2009

Resource Limits and Conversion Efficiency with Implications for Climate Change and California's Energy Supply

Abstract

Resource Limits and Conversion Efficiency with Implications for Climate Change and California's Energy Supply

by

Gregory Donald Croft
Doctor of Philosophy in Engineering - Civil and Environmental Engineering

University of California, Berkeley

Professor Tadeusz W. Patzek, Chair

There are two commonly-used approaches to modeling the future supply of mineral resources. One is to estimate reserves and compare the result to extraction rates, and the other is to project from historical time series of extraction rates. Perceptions of abundant oil supplies in the Middle East and abundant coal supplies in the United States are based on the former approach. In both of these cases, an approach based on historical production series results in a much smaller resource estimate than aggregate reserve numbers. This difference is not systematic; natural gas production in the United States shows a strong increasing trend even though modest reserve estimates have resulted in three decades of worry about the gas supply. The implication of a future decline in Middle East oil production is that the market for transportation fuels is facing major changes, and that alternative fuels should be analyzed in this light. Because the U.S. holds very large coal reserves, synthesizing liquid hydrocarbons from coal has been suggested as an alternative fuel supply. To assess the potential of this process, one has to look at both the resource base and the net efficiency. The three states with the largest coal production declines in the 1996 to 2006 period are among the top 5 coal reserve holders, suggesting that gross coal reserves are a poor indicator of future production. Of the three categories of coal reserves reported by the U.S. Energy Information Administration, reserves at existing mines is the narrowest category and is approximately the equivalent of proved developed oil reserves. By this measure, Wyoming has the largest coal reserves in the U.S., and it accounted for all of U.S. coal production growth over the 1996 to 2006 time period. In Chapter 2, multi-cycle Hubbert curve analysis of historical data of coal production from 1850 to 2007 demonstrates that U.S. anthracite and bituminous coal are past their production peak. This result contradicts estimates based on aggregated reserve numbers. In Chapter 4, a similar analysis of world coal results in a peak production year of 2011.

Electric power generation consumes 92 percent of U.S. coal production. Natural gas competes with coal as a baseload power generation fuel with similar or slightly better generation efficiency. Fischer-Tropsch synthesis, described in Chapter 2, creates transportation fuel from coal with an efficiency of less than 45 percent. Claims of higher efficiencies are based on waste heat recovery, since this is a highly exothermic process. The yield of liquid fuel as a proportion of the energy content of the coal input is always less than 45 percent. Compressed natural gas can be used for vehicle fuel with efficiency greater than 98 percent. If we view Fischer-Tropsch synthesis as a form of arbitrage between markets for electricity and transportation fuel, coal cannot simultaneously compete with natural gas for both transportation fuel and electric power. This is because Fischer-Tropsch synthesis is a way to turn power generation fuel into transportation fuel with low efficiency, while natural gas can be converted to transportation fuel with much greater efficiency. For this reason, Fischer-Tropsch synthesis will be an uneconomic source of transportation fuel as long as natural gas is economic for power generation. This conclusion holds even without the very high capital cost of coal-to-liquids plants.

The Intergovernmental Panel on Climate Change (IPCC) has generated forty carbon production and emissions scenarios, see the IPCC Special Report on Emissions Scenarios (2000). Chapter 4 develops a base-case scenario for global coal production based on the physical multi-cycle Hubbert analysis of historical production *data*. Areas with large resources but little production history, such as Alaska or Eastern Siberia, can be treated as sensitivities on top of this base case. The value of our approach is that it provides a reality check on the magnitude of carbon emissions in a business-as-usual (BAU) scenario. The resulting base case is significantly below 36 of the 40 carbon emission scenarios from the IPCC, and the global peak of coal production from existing coalfields is predicted to occur about the year 2011. The peak coal production rate calculated here is 160 EJ/y, and the associated peak carbon emissions from coal burning are 4.5 Gt C per year. After 2011, the production rates of coal and CO_2 decline, reaching 1990 levels by the year 2037, and reaching 50% of the peak value in the year 2047. It is unlikely that future mines will reverse the trend predicted in the base case scenario here, and current efforts to sequester carbon or to convert coal into liquid fuels should be reexamined in light of resource limits.

California provides a good example of the implications of scarcity-driven changes in the fuel supply, and the limited policy options available to deal with them. Once a great oil producer, California is becoming increasingly dependent on oil from the Middle East and Ecuador. Middle East production is not increasing, yet oil cargoes from the Middle East have to pass growing Asian markets to reach California. Alaska and Mexico also supply oil to the Pacific Basin, but are facing production declines. The effect of rising Asian demand on Pacific Basin oil markets is already visible, with significant amounts of oil coming to California from Atlantic Basin sources such as Angola, Brazil and Argentina. Policy options that could affect California's oil supply security include increased oil development in Alaska or offshore California, development of additional heavy oil pipeline outlets on Canada's Pacific Coast or substituting natural gas for oil when possible. The proposed low-carbon fuel standard will negatively impact California's energy supply security.

Contents

Acknowledgments

The author has been supported by 2 years of the Jane Lewis Fellowship from U.C. Berkeley.

Chapter 1

Literature Review and Discussion

1.1 Introduction

Coal drove the expansion of Britain in the nineteenth century, and concern about future coal supply was first expressed by Jevons [1866]. His analysis was based on trends in working depth of coal mines, since reserve data were not available at that time. The importance of petroleum supplies for warfare was first recognized when the British decided to convert the Royal Navy from coal to oil in the first decade of the twentieth century, and again during the First World War (Yergin [1991]). About this same time, there was enough interest in U.S. coal resources that the United States Geologic Survey was asked to undertake a resource evaluation. A U.S. coal evaluation was produced in 1913 and an oil evaluation in 1919 (Schurr and Netschert [1960]). This early oil evaluation predicted shortages which did not materialize, so resource evaluation was off to a bad start. All of these early USGS efforts were based on estimating reserves and aggregating them.

Projections of future production of mineral resources can be made using qualitative factors, by calculating reserves or by projecting historical data. Examples of qualitative factors are coal mine depth, coal seam thickness or water production in oil fields. The first production extrapolation approach that was not simply a linear or exponential projection was developed by Marion King Hubbert (Hubbert [1956]) when he worked at Shell Development. Hubbert's prediction that U.S. oil production would reach a peak around 1970 was not well-received, but now appears remarkably prescient. The actual peak in U.S. oil production did occur in 1970 and the USGS did not predict it. The Arab Oil Embargo of 1974 made oil supply a popular issue and Hubbert's work suddenly attracted broad interest. There was a perception that economic power had shifted from the developed countries to resource-rich eveloping countries. This view is eloquently described in Vallenilla [1975].

The interest in resource limits declined with oil prices after 1985, but the surge in oil prices since 1999 has elevated Hubbert almost to the status of a cult figure, which discourages the kind of critical analysis that Hubbert himself favored. Along with higher oil prices has come a discussion of the implications of a peak in world oil production, with U.S. government sponsorship of the Hirsch, Bezdek and Wendling [2005] study. Current concerns about climate change have added another important reason, besides energy security, to evaluate fossil fuel resources. It appears that interest in resource modelling is largely driven by fear of either too little or too much of a resource.

1.2 The Hubbert Model of Mineral Resource Depletion

The best known production extrapolation method is Hubbert analysis, named for Marion King Hubbert, who developed and published multiple versions of his model over time. Hubbert's early work (Hubbert [1956]) involved production extrapolation by manually fitting a Gaussian curve to ultimate recovery (reserves plus cumulative production) figures. Approximating the Gaussian curve with a logistic function allows fitting a single cycle to historical production data without incorporating any asumptions about reserve volumes. This approach is referred to as Hubbert Linearization because it involves fitting a straight line to a graph of the ratio of current to cumulative production plotted as a function of cumulative production. It was first published in Hubbert [1982]. The relation between the Gaussian and logistic functions is described in section 4.10 of this work.

1.2.1 Assumptions and Limitations of the Hubbert Model

The critical assumptions of the Hubbert method are that the discovery function is normally distributed, the individual production functions are independent, and that a large number of production units are being aggregated without any one dominating. If all of these conditions are satisfied, then the Central Limit Theorem applies. The economic implication of the individual production functions being independent is that, once the discovery function is established, price is irrelevant. This doesn't mean that economics and technology are not involved; they control the discovery function. The reason for a multi-cyclic Hubbert approach is that there are numerous historical examples of multiple discovery functions driven in most cases by technological change. Discovery function may be misleading terminology because the function represents economic, not geological discovery. Gas shales are an example; even National Geographic mentioned in the seventies how vast amounts of gas were locked up in Devonian shales in the eastern United States (Hodgson [1978]). The new Hubbert cycle, which may be larger than the one for conventional natural gas, was triggered not by this geological awareness but by Mitchell Energy's economic success in Texas' Barnett Shale in the nineties.

Price being irrelevant sounds strange, but what it means in practice is that, once a producing unit has started, production is not suspended until exhaustion. The reason that actual oil fields and coal mines tend to fit this model are that capital costs per unit of production are typically much greater than unit marginal production costs. Deferred production in both cases often commences near the end of the unit's operating life. Coal mine de-watering is a major cost element that must continue while production is suspended if the unit is to be re-opened. All of these factors result in a reluctance to shut in production over the range of prices one normally encounters over the life of a project. That can't be true over all possible prices, but Figures 2.5 and 4.22 of this work suggest that it was true for anthracite coal from 1850 to 2007, except for the Depression, and for oil prices from 1971 through 2007. Note that the lost coal production from the Depression appears to have been deferred.

A recent comparison of Hubbert and other curves fitting to historical oil production appears in Brandt [2007]. Three symmetric and three asymmetric models were tested. The conclusion of extensive curve fitting to historical oil production was that the Hubbert model was the most widely useful symmetrical model, but an exponential growth and decline model provided a better fit when asymmetry was allowed. The question asked by Brandt, which is what is the best fit to historical data after the peak, is not the same as asking how to predict the peak. Of the models he tested, only the symmetric Hubbert model has any predictive value before the peak.

Brandt [2007] also observes that many oil production peaks are higher and narrower than a gaussian curve. This latter factor is the reason that the cuspate exponential growth and decline function was often a better fit. Brandt raises the issue of multiple cycles and shows Ohio as an excellent example, but does not attempt to fit multiple cycles.

Brandt [2007] also raises the issue of the extent to which Hubbert analysis can be justified by the Central Limit Theorem, arguing that it cannot. The emergence of Hubbert cycles from the Central Limit Theorem is discussed in Chapter 4. As Brandt points out, the Central Limit Theorem assumes summation of independent functions. The issue of independence is a problem when one considers the extent to which oil and coal prices affect production. For the Central Limit Theorem to apply, production from individual mines or oil fields must be independent of temporal price variations. Why this is normally the case is discussed in section 1.2 below. Brandt also attempts to determine whether a greater degree of data aggregation improves the Hubbert curve fit, which it should if it is an application of the Central Limit Theorem. He concludes that it does not, but uses cumulative production and land area as proxies for degree of aggregation. These are both probably a poor proxies for the degree of statistical aggregation. Looking at the United States for examples, Alaska has large cumulative oil production and the largest area, yet most of its oil production has come from a single field (see Figure 5.4). Many states such as Indiana, Kentucky or Nebraska are minor oil producers but produce from numerous fields and would have a greater degree of aggregation than Alaska.

1.2.2 Variations and Alternative Approaches

There are a number of variations and alternatives to the Hubbert model. The need for multiple cycles was suggested by Hubbert, but the first published multi-Hubbert cycle analysis of oil production was Laherrere [1997], who showed how two cycles accurately model the historical oil production of France, and three provide a good fit for the Netherlands. The methodology of the coal studies presented in Chapters 2 and 4 of this work is most similar to that of Imam, Startzman and Barrufet [2004]. The authors subdivide world natural gas production by region, apply a multicyclic Hubbert model to each region, and sum the results. Their conclusion is that world natural gas production will peak in 2019. This conclusion is vulnerable to the non-uniqueness of the solution. If a major new cycle is in its early stages, will it be recognized? This question is particularly pertinent in the case of natural gas because recent advances in producing gas from volumetrically large shale formations have produced a huge surge in US gas production. This development may still be lost in the noise outside of North America.

One variation on the Hubbert model is to use an asymmetric curve. A model with the peak at 60 percent of ultimate production, rather then 50 percent, was published in Hallock et al [2004]. The analysis of historical production data in Brandt [2007] found that production curves were typically asymmetric, but there was no evidence for the consistent degree of asymmetry assumed by the Hallock model.

An alternative approach to modelling world oil production was developed in the statistics department of the University of Padua. The approach is described in Guseo, Dalla Valle and Guidolin [2006] using what the authors describe as a generalized Bass model. This is a diffusion model with a general perturbation introduced by mutiplying by an integrable function x(t). The result is regressive but nonlinear. This approach has the advantages of not necessarily being unimodal and, importantly, being independent of published reserve figures, which the authors describe as fundamentally flawed. Their model produces a peak in world oil production in 2007 and a rapid decline thereafter.

An intruiging alternative approach based on qualitative and cost data on U.S. copper, coal and oil production is Dale [1984], which argues that depletion is more a phenomenon of declining quality of the remaining resource, rather than declining quantity because mineral resource quantities are very large. Three models of depletion are presented; a simple model based on Hotelling [1931], a quality depletion model with increasing costs and a technological change model with decreasing costs. The paper examines historical trends in coal seam thickness and depth and depletion costs, defined as exploration plus production, for oil and copper. It also examines historical royalty rates and concludes that they are a leading indicator of resource depletion.

1.2.3 Applications of the Hubbert Model to Mining

Besides his well-known analysis of U.S. oil production, Dr. Hubbert also looked at coal and uranium (Hubbert [1956]). Hubbert's conclusion that U.S. coal production would peak between 2100 and 2200 was based on very large USGS coal reserve estimates that have since been revised downward by an amount much greater than U.S. coal production from 1956 through 2008.

Most recent published examples of Hubbert analysis apply it to oil production, but several recent publications have applied it to mining. A Hubbert analysis of copper and gold production in the United States, Canada and Australia was published in Mudd and Ward [2008]. Their conclusion was that copper production was accurately modeled by a single Hubbert curve, but gold production presented an entirely unsatisfactory fit. This relation held in all three countries, and the authors developed an energy-based model of gold depletion to address the problem. The conclusion that the Hubbert approach works for some mineral commodities but not for others raises the question of its applicability to coal production, but this conclusion may be an artifact of restricting the fit to a single cycle. The historical gold production curves would require four Hubbert cycles to achieve a good fit. This is because three very different types of deposits are involved; shallow alluvial deposits, deep veins and disseminated deposits that can be mined by open-cast methods. Gold production peaks are associated with surface alluvial deposits at discovery, improvements in deep mining of vein deposits around 1900, low labor costs in the Depression, and with surface mining of disseminated deposits around 2000. California's historical gold production shows the same peaks, and the explanations for all but the last peak are from Clark [1970]. The choice of a multicyclic symmetrical (Hubbert) model for the analysis of U.S. coal production in the following chapter is based on a good fit to the history of anthracite production as well as the need for few enough degrees of freedom to constrain the model.

At the same time the article which appears in Chapter 2 was published, an analysis of American coal appeared in the Journal of Coal Geology (Hook and Aleklett [2009]). The analysis by Hook and Aleklett fits two Hubbert cycles to historical coal production and reserves, both estimated recoverable reserves and demonstrated reserve base. This approach yields a unique result, but is subject to the quality of the estimate of recoverable reserves or demonstrated reserve base. Because the demonstrated reserve base has not had a recovery factor applied to it, it is inappropriate to use it for either a production projection or a reserve-to-production ratio. Both the history of past revisions of the estimated recoverable reserves and the poor correlation between large estimated recoverable reserves and production growth at a state level give reason to question the validity of production projections based on them, but they do represent an estimate of future production, unlike the demonstrated reserve base.

An analysis of Appalachian Basin coal reserves and historical production trends is presented in Milici [2000]. This paper looks at both data sets in more detail than most by looking at a regional or even county level. The paper concludes that an Appalachian Basin coal production shortfall of 200 million tons per year will appear by the middle of this century. The Appalachian Basin has historically been the most important coal-producing area in the U.S., so this result is significant in terms of the potential for liquids production from coal.

A projection of global coal production is found in Zittel and Schindler [2007]. The authors of this study examine reserves of major coal-producing regions, develop their own estimates, and then fit a single Hubbert cycle to remaining reserves. Their conclusion is that the peak in world coal production will occur in 2025 at about 30 percent above 2007 levels. The authors also emphasize that this projection represents an upper bound rather than a most-likely outcome.

Perhaps the most interesting recent projection of coal production is found in Mohr and Evans [2009]. The authors develop and tabulate two sets of national coal ultimate recoverable resource estimates, one based on Hubbert linearization and the other based on published reserves plus cumulative production. These values are then input into an iterative equilibrium model to produce a forecast. Not surprisingly, the two approaches to resource estimation produce very different numbers which produce very different forecasts in turn. The Hubbert linearization approach produces a peak in world coal production by tonnage in 2010 and by energy content in 2011. Official reserves produce a peak in world coal production by tonnage in 2048 and by energy content in 2047. By volume, the United States had the largest difference between the two approaches. Mohr and Evans separated historical coal production by rank, similar to the following study, but restricted themselves to a single Hubbert cycle since Hubbert linearization is a way to produce a best-fit single Hubbert cycle. A multicyclic approach to this global dataset is presented in Chapter 4 of this work.

A fine example of Hubbert linearization applied to oil and coal with implications for climate change is Rutledge [2009]. This work has not been published as a paper, but is significant because the residuals from the Hubbert fit are analyzed in order to establish confidence intervals. This is done by finding a Hubbert curve that produces uncorrelated residuals, which is not always possible, and then using a random number generator to create a large number of replications. The replications produce a probability distribution. The conclusion is that all of the IPCC scenarios fall outside of the 90 percent confidence interval. Chapter 4 of this dissertation differs from the work of Rutledge in two ways; geologic and qualitative information is examined to getermine whether it supports the conclusions and a multi-Hubbert cycle approach is used.

1.2.4 Predictive Ability of Multi-Hubbert Method: U.S. Coal

If one is to analyze the accuracy of what the multi-cyclic Hubbert method would have predicted in the past, the standard for comparison should be the actual historical predictions made by reserve-based methods. The historical U.S. production of hard coal, defined as anthracite plus bituminous, was used for this purpose because data are available back to 1850 and the peak occurred in 1990, so there is an event to test for. The test was to truncate the data series at 1973 because the United States Geological Survey did a major assessment of U.S. coal reserves as of January 1, 1974 which can be used for comparison purposes.

The best four-cycle Hubbert fit to the U.S. hard coal data from 1850 through 2007 appears in Figure 1.1. Although the actual year of peak production was 1990, the best-fitting fourth cycle has a peak in 1988. Removing all data after 1973 and fitting four cycles again produces a similar result, but the peak of the last cycle is moved forward by one year. This result is shown in Figure 1.2. The fit to the cumulative production curve appears in figure 1.3. This similarity in the Hubbert models breaks down if the historical data are truncated such that the last cycle does not manifest itself, a problem that will occur if the data are truncated much before 1970. In this case, we appear to be able to predict a peak up to twenty years in advance.

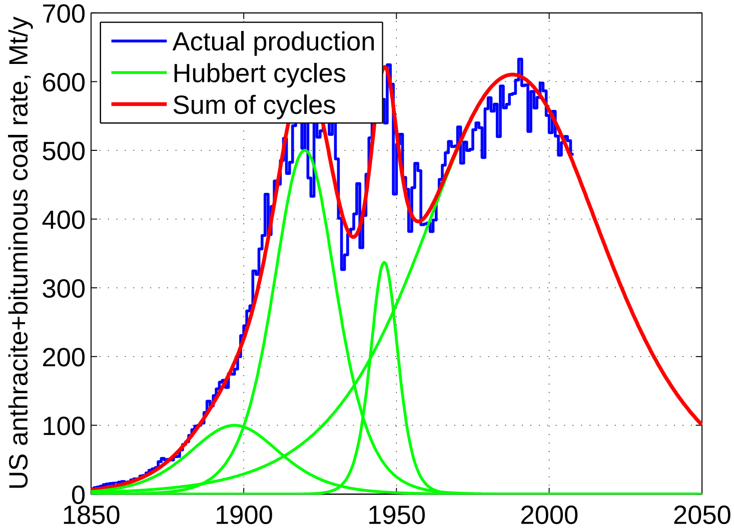

Figure 1.1: The production rate of anthracite plus bituminous coal in the U.S. from 1850 through 2007 can be modeled with four Hubbert curves. The production data are from EIA and Schurr & Netschert (1960).

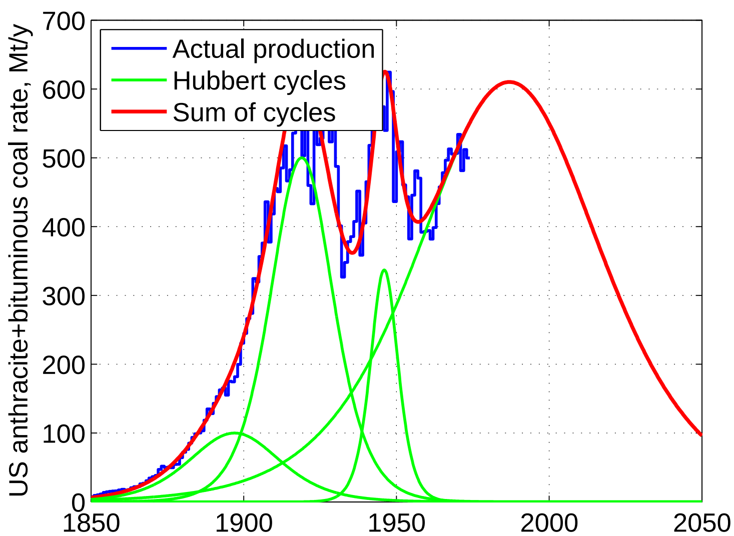

Figure 1.2: The production rate of anthracite plus bituminous coal in the U.S. from 1850 through 1973 fit with four Hubbert curves.

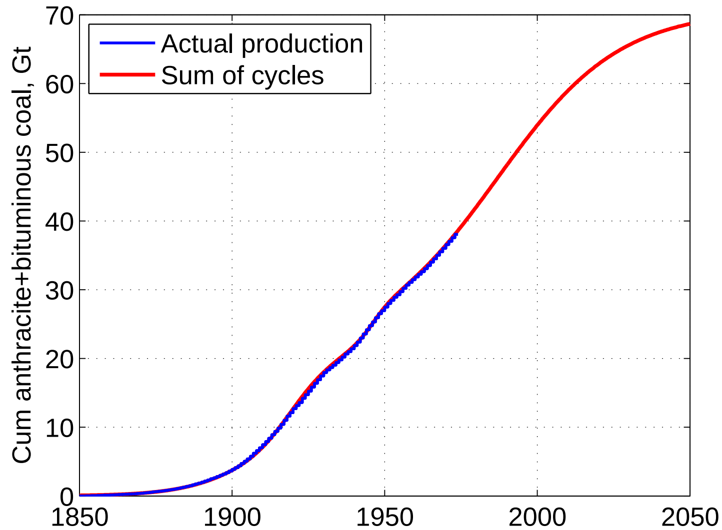

Figure 1.3: The cumulative production of coal in the U.S. from 1850 through 1973 with the Four-cycle fit shown in the previous figure.

1.3 Predictive Value of U.S. Coal Reserves

The United States Geological Survey did a major assessment of U.S. coal reserves as of January 1, 1974 which can be used for comparison purposes. According to Schurr and Netschert [1960] and Averitt [1969], all earlier reserve estimates were based on work done by Campbell of the U.S. Geological Survey in 1909 and 1913, so Averitt [1975] was the first modern asessment of U.S. coal. The USGS classification scheme at that time had two categories; identified resources are all coal in the ground subject to depth and seam thickness limits, while reserves are the proportion deemed economically recoverable. As of January 1, 1974, the U.S. reserve base of all ranks of coal was 424 billion tons and the identified resources of bituminous and anthracite coal were 767 billion tons. The report does not contain a production projection, but dividing these figures by 1973 production gives a reserve life of 708 years and a 1,394-year life for identified resources of bituminous and anthracite coal. Such long reserve lives are not consistent with a production peak before 2100, let alone in 1990. As of 2007, coal reserves were estimated to be 263 billion tons (Anonymous [2009]) and coal production from 1974 through 2007 was 32 billion tons, so downward revisions were 129 billion tons over the time period. Put another way, four tons of coal were revised away for each ton of coal that was mined.

The Energy Information Administration uses three categories of reserves; proved reserves at existing mines, estimated recoverable reserves, and demonstrated reserve base. Proved reserves at existing mines are reported by mine owners, while the demonstrated reserve base is calculated from all known anthracite and bituminous coal seams exceeding 28 inches in thickness and all sub-bituminous and lignite seams that both can be surface mined and exceed 60 inches in thickness. Thinner seams are included if they are currently mined or there is evidence that they could be mined commercially. The estimated recoverable reserves are produced by multiplying the demonstrated reserve base by a recovery factor, which depends on the mining method to be used. This methodology is described in Anonymous [1999]. The three reserve categories have been reported annually by state in the EIA annual coal report since 2001. In 2008, the proved reserves at existing mines were 17.875 billion short tons, representing 15.3 years of production, and the estimated recoverable reserves were 261.573 billion short tons, representing 223 years of production. This latter figure is the source of the popular claim that we have 200 years of coal supply. The demonstrated reserve base was 487.678 billion tons in 2008. In addition to these three reserve categories, the EIA also lists identified resources, which are all known coal in the ground, and total resources, which include undiscovered resources. The values of each of these categories is shown in table 1.1.

To see how broader reserve categories fail to indicate production declines, let us look at an area that appears to be declining. The states of Colorado and Utah produce low-sulfur bituminous coal from underground mines. In 2001, the estimated recoverable reserves of Colorado were 9.905 billion short tons, equivalent to 297 years of production. The equivalent figures for Utah were 2.819 billion tons and 105 years of production. Mine depth trends give a qualitative indication that this area is declining. To demonstrate that essentially no reserves are moving from the estimated recoverable reserve category to the recoverable reserves at active mines category, one needs to look at how production and recoverable reserves at active mines change with time. If there were no revisions and no reserves were upgraded into the recoverable reserves at active mines category, the sum of the recoverable reserves at active mines plus the cumulative production would be constant. Figures 1.4 and 1.5 show that this has very nearly been the case in Colorado and Utah over the last ten years. As of 2008, the estimated recoverable reserves of Colorado were 9.661 billion short tons, representing 302 years of production, and the estimated recoverable reserves of Utah were 2.652 billion short tons, representing 109 years of production. In what is arguably the fastest-depleting coal province in the U.S., reserve-to-production ratios actually increased at a time when narrowly defined reserves fell by nearly half.

Table 1.1: U.S. Coal Reserves and Resources, January 1, 1997
Data Source:EIA

Category	Billion Short Tons
Recoverable Reserves at Active Mines	19.4
Estimated Recoverable Reserves	275.1
Demonstrated Reserve Base	507.7
Identified Resources	1730.9
Total Resources	3968.3

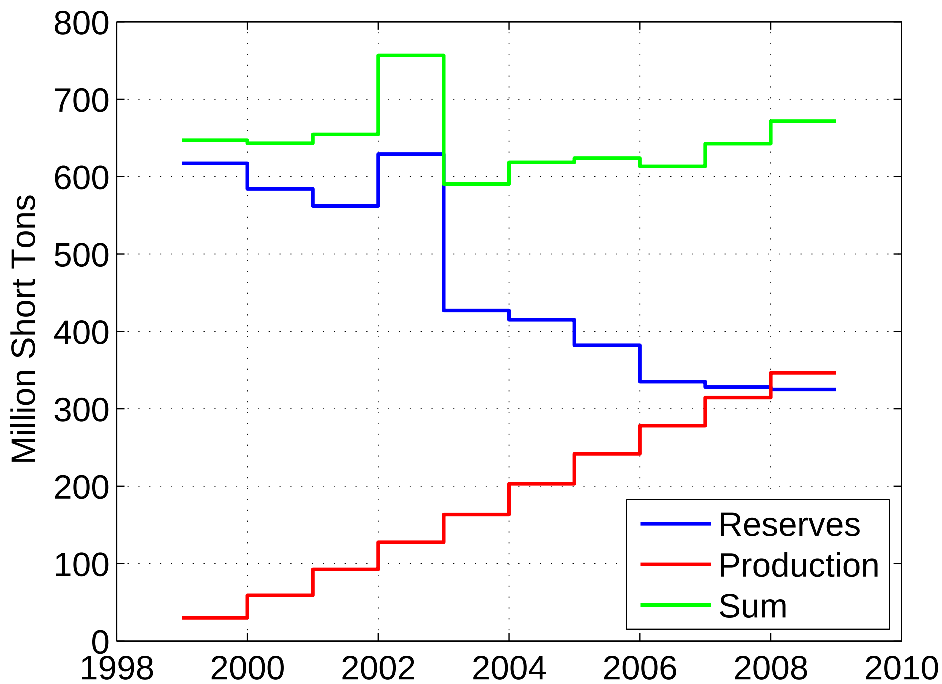

Figure 1.4: Mine Reserves and Cumulative Production, Colorado, 1999 through 2008
Data Source: EIA

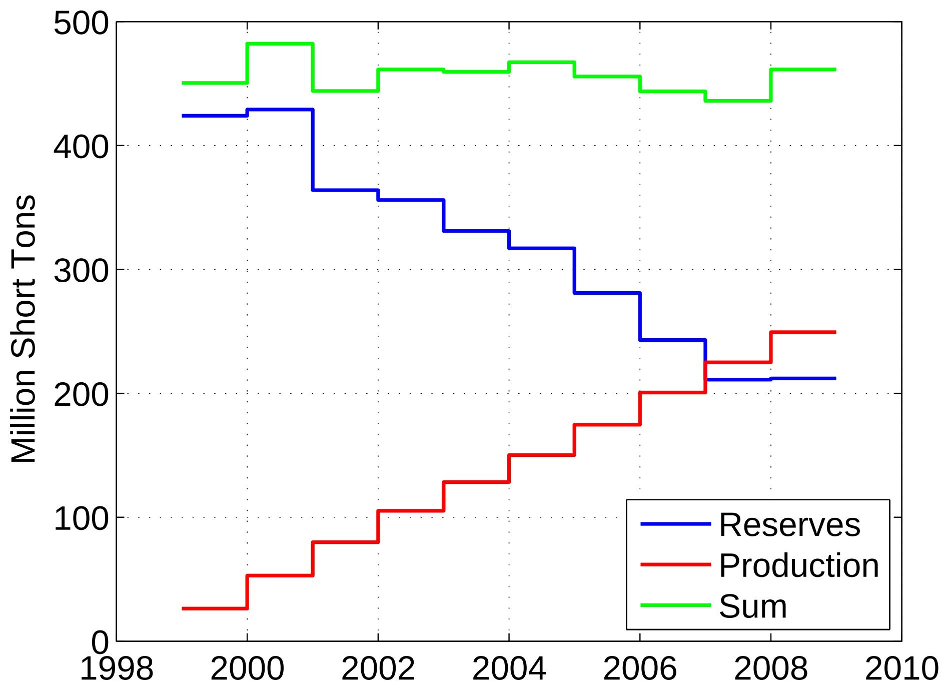

Figure 1.5: Mine Reserves and Cumulative Production, Utah, 1999 through 2008
Data Source: EIA

1.4 Coal to Liquids Conversion

The concept of coal-to-liquids technology fueling a transition from oil has been widely discussed. The issue of the efficiency of the process is related to the concept that coal supplies are limited because the remaining coal will be directed to its most valuable use. The analysis in Chapter 3 concludes that electric power generation is the most valuable use of coal. Additional issues with coal to liquids conversion include carbon emissions and water usage.

A graph showing a cost-volume relationship between conventional oil, coal-to-liquids and other synthetic fuels was published in Farrell and Brandt [2006]. A second, more alarming graph shows carbon emissions associated with the same technologies. Both graphs were based on published literature on costs and conversion efficiencies of current technologies. Their conclusion that the oil transition brings more long-term environmental concerns than long-term economic or security threats is based on published world coal reserve estimates. As a result, the volume increment shown for coal-to-liquids is the largest of any of the technologies described. This dissertation differs from the work of Farrell and Brandt in that the next chapter questions U.S. coal reserve estimates and the following chapter looks at the relative value of coal for electric power generation versus transportation fuels.

The policy issues associated with producing liquid fuels from coal are discussed in Bartis et al [2008]. The study claims that coal is a better source of liquid fuels than tar sands, oil shale or biomass because it is the world's most abundant fossil fuel. No attempt is made to verify the resource estimates or reconcile them with production trends. The problem of a two-fold increase in unit carbon emissions is mentioned, but is brushed aside with a comment about improving capture and sequestration technology.

Economic scenarios for coal-to-liquids plants were presented in Robinson and Tatterson [2008] and Robinson and Tatterson [2007]. Their worst-case scenario for a 10,733 ton-per-day plant in their more recent article used an oil price of $75 per barrel and a carbon dioxide value of $2 per thousand standard cubic feet for enhanced oil recovery, while their best-case scenario used an oil price of $135 per barrel and a carbon dioxide value of $5 per thousand standard cubic feet. The worst-case scenario had an internal rate of return of 12%. While their worst-case oil price may look like the most likely case a year later, the more questionable assumption is that one could obtain such a high price for the carbon dioxide at the plant gate. Their hypothetical plant is to use Montana Rosebud coal, so the carbon dioxide would have to be transported to enhanced oil recovery sites, probably in western North Dakota. The article does not discuss the cost of this transportation.

The analysis of mitigation of the peak in world oil production in Hirsch, Bezdek and Wendling [2005] advocates aggressive development coal-to-liquids technology, but addresses neither the inefficiency of the process nor the limits to coal resources. The example of South Africa's Sasol-3 plant, which was constructed on a crash basis in response to the Iranian revolution, is cited to demonstrate how quickly an experienced team can construct a new coal-to-liquids plant. The authors estimate that world coal-to-liquids capacity can be increased by five 100,000 barrel-per-day plants each year once a crash program is started.

There is an abundance of literature on the efficiency of coal-fired power plants. The current state of the art in Denmark, a country which has emphasized plant efficiency, is described in Bugge, Kjaer and Blum [2006]. The power plant at Nordjylandvaerket, which was the most efficient coal-fired power plant in Europe when it was comissioned in 1998, has actually achieved an efficiency in excess of 47 percent. The goal of the EU-financed AD700 project is to achieve efficiencies as high as 54 percent, which can be obtained if the steam temperature is increased to 700 degrees C and the pressure to 350 bar. This exceeds the maximum theoretical efficieny of Fischer-Tropsch conversion from coal, so electric power generation will continue to be a more valuable use for coal than conversion to liquid fuels.

1.5 The IPCC Carbon Emissions Scenarios

If world coal resources are substantially overstated, this raises the question of whether the carbon emissions scenarios in Pachauri and Reisinger [2007] are physically realizable. This is an issue of critical importance at a time when there are demands for drastic and costly measures to mitigate carbon emissions. The IPCC emission scenarios are described in Nakicenovic et al. [2000] and are based on a survey of emissions projections in published literature. The problem with this approach is that probably all of the surveyed projections are based on various government estimates of coal resources and on Saudi estimates of their oil resources. Chapters 2 and 4 will discuss why the former are fundamentally flawed, and problems with the latter have been publicized by Simmons [2005] and by Schindler and Zittel [2008], and will be discussed in Chapter 5 of this dissertation.

The process of generating the scenarios is described in Anonymous [2000]. There are four families of scenarios, designed around the following descriptions:

> The A1 storyline and scenario family describes a future world of very rapid economic growth, global population that peaks in mid-century and declines thereafter, and the rapid introduction of new and more efficient technologies. Major underlying themes are convergence among regions, capacity building, and increased cultural and social interactions, with a substantial reduction in regional differences in per capita income. The A1 scenario family develops into three groups that describe alternative directions of technological change in the energy system. The three A1 groups are distinguished by their technological emphasis: fossil intensive (A1FI), non-fossil energy sources (A1T), or a balance across all sources (A1B).
>
> The A2 storyline and scenario family describes a very heterogeneous world. The underlying theme is self-reliance and preservation of local identities. Fertility patterns across regions converge very slowly, which results in continuously increasing global population. Economic development is primarily regionally oriented and per capita economic growth and technological change are more fragmented and slower than in other storylines.
>
> The B1 storyline and scenario family describes a convergent world with the same global population that peaks in midcentury and declines thereafter, as in the A1 storyline, but with rapid changes in economic structures toward a service and information economy, with reductions in material intensity, and the introduction of clean and resource-efficient technologies. The emphasis is on global solutions to economic,

> social, and environmental sustainability, including improved equity, but without additional climate initiatives.
>
> The B2 storyline and scenario family describes a world in which the emphasis is on local solutions to economic, social, and environmental sustainability. It is a world with continuously increasing global population at a rate lower than A2, intermediate levels of economic development, and less rapid and more diverse technological change than in the B1 and A1 storylines. While the scenario is also oriented toward environmental protection and social equity, it focuses on local and regional levels.

Note that resource limits are not addressed in any of the scenario descriptions. Of the IPCC emissions scenarios, the lowest are the B1 and A1T groups. One of the A1T scenarios (A1T Maria) has coal usage declining, but the A1T scenarios include large increases in oil and natural gas production.

The nine B1 scenarios have peak coal production ranging from below current levels (B1 Maria) to as high as 403 exajoules per year (B1 ASF). The mean peak coal production value of the B1 scenarios is 167 exajoules per year. By comparison, Mohr and Evans [2009] have a coal peak of 145 exajoules based on Hubbert linearization and 177 exajoules based on published reserves. The studies by Zittel and Schindler [2007] and Hook and Aleklett [2009] also conclude that coal is not as abundant as is widely believed. The B1 and A1T scenarios are the only scenarios that are consistent with published coal reserves and even they are higher than a Hubbert methodology would produce. The other scenarios appear to be an excercise in fantasy; A2 AIM has coal production of 1016 exajoules per year in 2100.

The potential impact of fossil-fuel peaking on carbon emissions was addressed by Brecha [2008], who concluded that atmospheric carbon dioxide levels as high as 550 ppm might still occur. Two resource-limited scenarios are presented, one with 2 trillion barrels of ultimate oil recovery and one with 3 trillion. Ultimate recoverable natural gas resources are 6200 Tcf in the low case and 9300 Tcf in the high case. Both scenarios use an ultimate coal recovery of 1.3 trillion tonnes, but the high scenario has coal production increasing 4 percent per year to a peak in 2035, while the low scenario has it increasing 2 percent per year to 2050. The low scenario is very close to the B1 message scenario from the IPCC. The higher scenario results in a peak of carbon dioxide emissions in 2035 at about twice 2009 levels. This projection is dependent on published reserve numbers with additional reserve growth. While the author was right to impose some resource constraints on carbon emissions, this dissertation will argue that his resource estimates are far too high.

The following study, along with three other studies based on a similar methodology, concludes that coal resources are greatly overstated. While some of the efforts to mitigate climate change can also help mitigate a shortage of fossil fuels, there is reason to question whether large-scale investment in carbon capture and storage will add value, especially if this technology is not widely applied until after the peak in global carbon emissions. Exaggerated resource estimates could also render cap-and-trade approaches ineffective because the cap would be set too high. Combining this problem with an international cap-and-trade scheme could produce the unfortunate situation described in Baer et al [2000]:

> A long-term agreement based on historical levels would allow higher emitters to impose environmental damages, potentially large, on other countries, in violation of

the widely accepted 'polluter pays' principle. This imposition directly contravenes international environmental law.

1.6 The Supply of Transportation Fuels to California

The implications of oil resource limits for the state of California are likely to be greater then for the U.S. as a whole. This is because California is more dependent on Middle East oil. The issue of Middle East oil reserves has drawn public scrutiny in recent years because production has not grown in the manner repeatedly forecast by groups such as the IEA and the EIA. The Integrated Energy Policy Report from the California Energy Commission (California Energy Commission [2007]) is a comprehensive report that is published every two years. It includes information on the source of California's oil imports, but does not discuss likely oil production scenarios in those areas.

1.6.1 Middle East Oil Supply Outlook

The issue of future Middle East oil production is critical to California's energy security and concerns about future Saudi oil production have been raised by several authors, notably Simmons [2005]. Simmons' work is based on extensive review of technical papers by Saudi Aramco personnel. Most of these were presented to the Society of Petroleum Engineers, and they chronicle various late-stage production problems. Simmons' conclusion is that Saudi Arabia will soon face a decline, if not a collapse, in oil production. This conclusion is consistent with the fact that Saudi Arabia's oil production (excluding natural gas liquids) has never regained its 1981 level in spite of high oil prices and claims of excess capacity.

An alternative to looking at reported production problems is to develop reserve estimates of individual fields, starting with a calculation of the original oil in place. A compilation of such calculations for the world's largest hydrocarbon accumulations was published by Roadifer [1986], and a full set of reservoir parameters for all of the major Saudi oil fields can be found in Croft [2002] for those who would like to perform their own reserve calculations. Recoverable reserve estimates for giant oil fields worldwide were published in Nehring [1978], but that compilation does not include oil in place figures and tends to underestimate the size of Russian oil fields. Beydoun [1988] includes recoverable reserve estimates and geologic descriptions for all of the major Middle East oil fields. The reserve calculation approach independently leads to the same conclusion as Simmons' work, namely that Middle East national oil reserve figures are exaggerated. National oil reserve estimates were used to develop the production projections in Schindler and Zittel [2008], but these estimates were revised by the authors based on alternative sources of information. As an important example, this study uses a figure of 181 billion barrels for Saudi Arabia's remaining oil reserves, as compared to 264.3 billion barrels reported in the Oil and Gas Journal. The resulting regional projections are displayed in a series of figures with the 2004 and 2006 World Energy Outlook projections superimposed on them. The difference is striking.

Although Middle East oil producing nations are now quite secretive about the technical aspects of their oil fields, that was not always the case. It is also important to remember that the major Middle East oil fields are not new discoveries. By the time Saudi Arabia's supergiant Ghawar field was described in Arabian American Oil Company Staff [1959], more than 200 wells had been cored through the reservoir interval. The productive area of Ghawar is listed in Alsharhan and Kendall [1986] as 693,000 acres. Combining that figure with the reservoir data in Croft [2002] or Appendix B of Simmons [2005] gives an original oil in place of about 114 billion barrels. When one realizes that more than half of that oil has already been produced, it becomes clear that the oil field that has supplied more than half of Saudi Arabia's production is entering a declining phase.

Kuwait has not been as secretive as Saudi Arabia and a geologic description of the supergiant Burgan field, generally accepted as the second largest in the Middle East, can be found in Brennan [1990]. A description of Raudhatain field, Kuwait's second largest, is presented in Brennan [1990] and structural maps of the major Kuwait oil fields are available in Carman [1996]. Once again, the available geologic information supports a near-term peak in oil production.

The important Bab and Bu Hasa oil fields onshore Abu Dhabi are described in Hajash [1967] and the offshore Abu Dhabi fields are covered in Hassan and Azer [1985]. A geologic description of the major Iran oil fields can be found in Hull and Warman [1968] and Iran's Agha Jari field, one of the first of the major Middle East oil fields to be discovered, is described in Ion, Elder and Pedder [1951]. Iran's Gachsaran and Bibi Hakimeh fields are covered in detail in McQuillan [1985]. A description of Iraq's supergiant Kirkuk oil field appears in Dunnington [1958]. The information provided in all of these papers generally agrees with the values in Roadifer [1986]. The point is that a sufficient amount of geological information is available in the published literature to make a reasonable assessment of the Middle East oil reserves.

The overstatement of Middle East oil reserves and the implications of the peaking of world oil production are discussed at length in Deffeyes [2001]. The purpose of this book appears to be to sound a warning about an impending world oil supply crisis. A well-known article that also fits into the warning category is Campbell and Laherrere [1998]. This article largely presents results, but was the result of a detailed study conducted by the authors for Petroconsultants. Both the data and the calculations were checked by a team at the University of Reading. The conclusions of this checking are reported in Bently [2002]. It was determined that the Petroconsultants database was adequate for the task and that the Hubbert approach is robust, but there are several large uncertainties. The two most important uncertainties were deemed to be the size of Middle East oil reserves and the size of Russian oil reserves.

Although supported by independent lines of reasoning, the conclusion that Middle East oil reserves are overstated is controversial. One paper that takes an opposing view is Jackson [2006], who claims that world oil production will not peak before 2030. Much of Jackson's arguments are based on the upward revision of oil reserves over time because he attacks the dependence of the Hubbert method on reserve estimates. Two problems with this argument are that methods such as Hubbert linearization or the multicyclic fit used in Chapters 2 and 4 of this work are not dependent on reserve estimates, and that most of the upward revisions in the 1995 to 2003 time period he described have no supporting documentation because they are from national oil companies in the Middle East. Jackson further states that there is no credible technical analysis that we are aware of that demonstrates that its productive capacity will suddenly fall in the near term. Matthew Simmons would not agree with that statement. One interesting way that this paper differs from the others cited here is in its definition of oil, which includes natural gas liquids such as ethane that are not liquid under standard conditions. The analysis of U.S. oil versus gas well energy production in Chapter 5 combines gas liquids with natural gas because they are mostly a by-product of gas production and tend to compete with natural gas for the same applications.

1.6.2 California, Alaska and Canada

The California Division of Oil and Gas does not publish projections of future oil production, but the important issue of California and Alaska offshore oil potential is addressed in Syms and Voskanian [2007]. These resource estimates are well-constrained in California because of extensive past exploration, but are hampered offshore Alaska by a lack of data. The potential in the Alaska Natinal Wildlife Refuge is addressed in United States Geological Survey [2001], but the most important well was not available for the study. When looking at the range of possible exploration outcomes for a group of structures, one must address both how full the structures are and the mix of oil and gas that they are filled with. The conclusions of this study are based on the structures being entirely full and the hydrocarbon charge being entirely oil even though the nearest known accumulation is a gas-condensate field. Such a case represents an end member of the range of possibilities rather than the most likely outcome.

The likely impact of the Canadian oil sands on world oil markets is discussed in the context of overall U.S. energy security in Levi [2009]. Levi's conclusion that the Canadian oil sands will not have a large effect on world oil prices is based on the fact that they are not expected to account for more than 5 percent of world oil production by 2030. This conclusion omits the important benefit that the U.S. receives from pipeline reversal; when oil flowed from the Gulf Coast to Chicago, oil prices in Chicago were world prices plus a pipeline charge. Now that the oil flows the other way, oil prices in Chicago are world prices less a pipeline tariff. This provides a substantial economic benefit in a heavily industrialized part of the United States. For California to receive a similar benefit would require a reversal of one or more of current seaborne oil routes. Replacing all of the Middle East oil coming into the U.S. West Coast with Canadian oil would have such an effect, and is conceivable if enough pipeline capacity is built to Canada's West Coast.

1.6.3 Energy Security and the Low Carbon Fuel Standard

The security implications of California's proposed low carbon fuel standard are not dicussed in Farrell and Sperling [2007], which is primarily focussed on environmental issues and the formidable task of implementing such a standard. Recent criticism of the concept of a low carbon fuel standard is found in Dachis [2009], who concludes that a low carbon fuel standard is less likely to reduce total greenhouse gas emissions than would a comprehensive cap-and-trade system. The lack of discussion of the energy security implications of proposed low carbon fuel standards is probably due to the belief that there will continue to be an abundant supply of Middle East oil. A good discussion of the energy security implications of the peak in world oil production is found in Hirsch, Bezdek and Wendling [2005]. This paper recommends an aggressive mitigation program, but its advocacy of gas-to-liquids and coal-to-liquids technologies addresses neither the inefficiency of the process nor the limits to those resources. Hirsch devotes an entire chapter to learning from the U.S. natural gas experience, but the article came out immediately before improvements in gas production technology caused the earlier forecasts that he criticizes to come true, and now natural gas production has increased at prices half that of oil on an energy-equivalent basis. That such a detailed study could be so far in error after only four years illustrates the unifying concept of this dissertation, which is that production projections based on historical time series are more accurate than those based on aggregated reserve data. The values for coal resources were too high and those for natural gas were far too low, but production trends tell a different story in both cases.

1.7 Objectives of this Research

The conclusion that neither oil nor coal are as abundant as is widely believed has major implications. The next four chapters look at specific issues associated with coal and oil resource depletion. Chapter 2 (Croft and Patzek [2009]) examines whether U.S. coal reserves are adequate to support a major coal-to-liquids conversion industry, and concludes that they are not. A Hubbert linearization projection of U.S. coal production is included in Mohr and Evans [2009], but this is the first paper to use a multi-Hubbert cycle approach that is independent of reserve estimates. Chapter 3 (Patzek and Croft [2009]) then argues that, because of these resource limits, coal will be diverted to its most valuable use, which is electric power generation for most grades of coal. This paper differs from other published work on coal-to-liquid conversion in examining the relative value of different uses of coal and alternative fuels. Chapter 4 applies a multi-Hubbert cycle approach to model global coal resources and concludes they are insufficient to create the level of carbon emissions in 36 of the 40 scenarios from the Intergovernmental Panel on Climate Change. This differs from Mohr and Evans [2009] and Rutledge [2009] by using a multi-Hubbert cycle approach and by including qualitative geologic information as a check on results. Chapter 5 analyzes the oil supply outlook in the regions that supply California and how it will evolve over time. This work is based on an extensive review of published literature, as well as the author's 26 years of experience in oil and natural gas exploration. It differs from the work of the California Energy Commission by examining supply security issues, and it differs from Deffeyes [2001] and Simmons [2005] in specifically addressing the impact on California. In each of these examples, resource limits fundamentally alter the conclusions.

Bibliography

Alsharhan, Abdulrahman S. and Kendall, Christopher G. St. C., *Precambrian to Jurassic Rocks of Arabian Gulf and Adjacent Areas: Their Facies, Depositional Setting, and Hydrocarbon Habitat*, Bulletin of the American Association of Petroleum Geologists, volume 70, No. 8, 1986

Anonymous 1999, *U.S. Coal Reserves: 1997 Update*, Coal Reserves Report DOE/EIA-0529(97), Energy Information Administration, Washington, DC.

Anonymous, *Emissions Scenarios Summary for Policymakers*, 2000, Intergovernmental Panel on Climate Change, ISBN: 92-9169-113-5 27 p.

Anonymous, *Recoverable Coal Reserves at Producing Mines, Estimated Recoverable Reserves, and Demonstrated Reserve Base by Mining Method, 2007*, Energy Information Administration http://www.eia.doe.gov/cneaf/coal/reserves/reserves.html, downloaded October 30, 2009

Arabian American Oil Company Staff, *Ghawar Oil Field, Saudi Arabia*, Bulletin of the American Association of Petroleum Geologists, Volume 43, No. 2, 1959

Averitt, Paul, *Coal Resources of the United States, January 1, 1967*, United States Geological Survey Bulletin 1275, Washington, 1969, 116 p

Averitt, Paul, *Coal Resources of the United States, January 1, 1974*, United States Geological Survey Bulletin 1412, Washington, 1975, 131 p

Paul Baer, John Harte, Barbara Haya, Antonia V. Herzog, John Holdren, Nathan E. Hultman, Daniel M. Kammen, Richard B. Norgaard and Leigh Raymond, *Equity and Greenhouse Gas Responsibility*, Science, Vol 289, Issue 5488, 2287 , 29 September 2000

Bartis, James T, Camm, Frank and Ortiz, David S., *Producing Liquid Fuels from Coal*, RAND Corporation, ISBN: 978-0-8330-4511-9

Bently, R. W., *Global oil and gas depletion:an overview*, Energy Policy, volume 30, 2002, pp 189 to 205

Beydoun, Z. R., *The Middle East: Regional Geology and Petroleum Resources*, Scientific Press Ltd., Beaconsfield, UK, 1988

Brandt, A.R., *Testing Hubbert*, Energy Policy, 35, 3074, 2007

Brecha, Robert J., *Emissions scenarios in the face of fossil-fuel peaking*, Energy Policy, 36, 3492-3504, 2008

Brennan, P., *Greater Burgan Field*, in Treatise of Petroleum Geology, Structural Traps I, American Association of Petroleum Geologists, Tulsa, 1990

Brennan, P., *Raudhatain Field, Kuwait*, in Treatise of Petroleum Geology, Structural Traps V, American Association of Petroleum Geologists, Tulsa, 1991

Bugge, Jorgen, Kjaer, Sven and Blum, Rudolph *High-efficiency coal-fired power plants development and perspectives*, ENERGY, volume 31, 2006, pp 1437 to 1445

California Energy Commission, *2007 Integrated Energy Policy Report*, CEC-100-2007-008-CMF, California Energy Commission, Sacramento CA

Campbell, Colin J, and Laherrere, Jean H. *The End of Cheap Oil*, Scientific American, March 1998, pp 78 to 83

Carman, George J., *Structural Elements of Onshore Kuwait*, Geoarabia, Volume 1 No. 2, 1996

Clark, William B., *Gold Districts of California*, California Division of Mines and Geology Bulletin 193, Sacramento, 1970, 186 p

Croft, Gregory D. *Oil Fields of the Gulf Region: An Illustrated Atlas*, Greg Croft Inc., San Leandro, 2002

G. D. Croft, T. W. Patzek, Potential for Coal-to-Liquids Conversion in the U.S. – Resource Base, Natural Resources Research J. 18 (3) (2009) 173 – 180, dOI: 10.1007/s11053-009-9097-x.

Dachis, Benjamin *Low-Carbon Fuel Standards: Driving in the Wrong Direction*, C. D. Howe Institute (2009), www.cdhowe.org

Dale, Larry L. *The Pace of Mineral Depletion in the United States*, Land Economics, volume 60, no. 3 (August 1984), pp 255 to 267

Deffeyes, Kenneth S. *Hubbert;s Peak*, Princeton University Press, 2001

Dunnington, H. V., *Oil in Northern Iraq,* in Habitat of Oil, American Association of Petroleum Geologists, Tulsa, 1958

Farrell, A. E. and Brandt, A.R., *Risks of The Oil Transition*, Environmental Research Letters 1 (2006) 014004

Farrell, Alexander E. and Sperling, Daniel, *A Low-Carbon Fuel Standard for California, Part 1: Technical Analysis, 2007*, University of California, Berkeley CA

Guseo, R., Dalla Valle, A. and and Guidolin, M. *World Oil Depletion Models: Price effects compared with strategic or technological interventions*, Technological Forecasting and Social Change, volume 74, 2007, pp 452 to 469

Hajash, G. M., *The Abu Sheikdom - The Onshore Oilfields History of Exploration and Development*, World Petroleum Congress, 1967

Hassan, T. H., and Azer, S., *The Occurrence and Origin of Oil in Offshore Abu Dhabi*, in Proceedings of the Fourth Middle East Oil Technical Conference, Society of Petroleum Engineers, 1985

Hallock, John L. Jr., Thakaran, Pradeep J., Hall, Charles A.S., Jefferson, Michael and Wu, Wei, *Forecasting the limits to the availability and diversity of global conventional oil supply*, ENERGY, volume 29 (2004) pp 1673-1696

Hirsch, Robert L., Bezdek, Roger and Wendling, Robert *Peaking of World Oil Production: Impacts, Mitigation, and Risk Management*, U.S. Department of Energy, National Energy Technology Laboratory. February 2005.

Hodgson, Bryan *Natural Gas: The Search Goes On*, National Geographic November 1978, pp 632-651

Hook, Mikael and Aleklett, Kjell *Historical Trends in American Coal Production and a Possible Future Outlook*, International Journal of Coal Geology Volume 78, Issue 3, 1 May 2009, Pages 201-216 http://dx.doi.org/10.1016/j.coal.2009.03.002

Hotelling, Harold *The Economics of Exhaustible Resources*, Journal of Political Economy, volume 39, April 1931, pp 137 to 175

Hubbert, M. K., *Nuclear Energy and the Fossil Fuels*, Proceedings Spring Meeting, Southern District, Division of Production, American Petroleum Institute, San Antonio, Texas, USA, 1956, 57 p.

Hubbert, M. K., *Techniques of Prediction as Applied to the Production of Oil and Gas, in the collection Oil and Gas Supply Modeling*, edited by Saul I. Gass (published as NBS Special Publication 631), 1982

Hull, Cedric E. and Warman, Harry R., *Asmari Oil Fields of Iran*, in Geology of Giant Petroleum Fields, American Association of Petroleum Geologists Memoir 14, 1968

Ion, D. C., Elder, S., and Pedder, A. E., *The Agha Jari Oil Field, Southwest Persia*, in Proceedings of the Third World Petroleum Congress, 1951

Jackson, Peter M. *Why the "Peak Oil" Theory Falls Down: Myths, Legends, and the Future of Oil Resources*, Cambridge Energy Research Associates (2006)

Imam, Asher, Startzman, Richard A. and Barrufet, Maria *Multicyclic Hubbert model shows global conventional gas output peaking in 2019*, Oil and Gas Journal, August 16, 2004

Jevons, William S. *The Coal Question: An Inquiry Concerning the Progress of the Nation, and the Probable Exhaustion of Our Coal-Mines*, Macmillan and Co., London, 2, revised edn., www.eoearth.org/article/The_Coal_Question%3A_Preface, 1866.

Laherrere, Jean *Muti-Hubbert Modeling*, http://www.hubbertpeak.com/laherrere/multihub.htm, Downloaded November 17, 2009

Levi, Michael A. *The Canadian Oil Sands, Energy Security vs. Climate Change* Council on Foreign Relations Council Special Report No. 47, May 2009

McQuillan, H., *Gachsaran and Bibi Hakimeh Fields*, in Carbonate Petroleum Reservoirs (Roehl and Choquette eds), Springer-Verlag, New York, 1985

Milici, Robert C. *Depletion of Appalachian coal reserves - how soon?* Journal of Coal Geology, volume 44, 2000, pp 251 - 266

Mohr, S.H. and Evans, G. M. *Forecasting coal production until 2100*, Fuel (2009), fuel 2009.01.032

Mudd, G.M. and Ward, J. D. *Will Sustainability Constraints Cause Peak Minerals ?*, Proceedings 3rd International Conference on Sustainability Engineering Science : Blueprints for Sustainable Infrastructure, Auckland, New Zealand 9-12 Dec. 2008

Nebojsa Nakicenovic and Rob Swart (Eds.), *Emissions Scenarios*, IPCC, Cambridge University Press, UK. 570 p.

Nehring, Richard *Giant Oil Fields and World Oil Resources*, Rand Corporation, Report R-2284-CIA, June 1978

Pachauri, R.K. and Reisinger, A. (Eds.) *Contribution of Working Groups I, II and III to the Fourth Assessment Report of the Intergovernmental Panel on Climate Change*, IPCC, Geneva, Switzerland. 104 p.

T. W. Patzek, G. D. Croft, Potential for Coal-to-Liquids Conversion in the U.S. – Fischer-Tropsch Synthesis, Natural Resources Research J. 18 (3) (2009) 181 – 191, dOI: 10.1007/s11053-009-9098-9.

Roadifer, R. E., *How Heavy Oil Occurs Worldwide*, Oil and Gas Journal, March 3, 1986, Pennwell Publishing, Tulsa OK

Robinson, Ken K. and Tatterson, David F., *Fischer-Tropsch Oil from Coal Promising as Transport Fuel*, Oil and Gas Journal, February 26, 2007, p 20

Robinson, Ken K. and Tatterson, David F., *Economics on Fischer-Tropsch Coal-to-Liquids Method Updated*, Oil and Gas Journal, October 27, 2008, pp 22-26

Rutledge, David *Hubbert's Peak, The Coal Question, and Climate Change*, slide presentation, http://rutledge.caltech.edu/

Schindler, Jorg and Zittel, Dr. Werner, *Crude Oil The Supply Outlook*, Energy Watch Group (2008), EWG-Paper No. 2008/02/11, 102 p.

Schurr, S. H. and Netschert, B. C. 1960, *Energy in the American Economy, 1850-1975*, Chapt. Statistical Appendix to Part 1, pp 492 – 493, Johns Hopkins Press, Baltimore.

Simmons, Matthew R. *Twilight in the Desert* John Wiley and Sons, Hoboken, NJ, 422 p, May 2005

Syms, Harold E. and Voskanian, Armen, *Estimated Oil and Gas Reserves Pacific Outer Continental Shelf*, OCS Report MMS 2007-012, 2007, Minerals Management Service, Washington DC

United States Geological Survey, *Arctic National Wildlife Refuge, 1002 Area, Petroleum Assessment, 1998, Including Economic Analysis*, USGS Fact Sheet FS-028-01, 2001, United States Geological Survey, Washington DC

Vallenilla, Luis, *Oil: The Making of a New Economic Order*, McGraw-Hill, New York, 1975

Yergin, Daniel, *The Prize*, Touchstone Press, New York, 1991

Zittel, Dr. Werner and Schindler, Jorg *Coal: Resources and Future Production*, Energy Watch Group (2007), EWG-Paper No. 1/07, 47 p.

Chapter 2

Potential for Coal-to-Liquids Conversion in the U.S., Part I – Resource Base

2.1 Abstract

In Part I of this paper we apply the multi-Hubbert curve analysis to coal production in the U.S. We demonstrate that anthracite production can be modeled with a single Hubbert curve that extends to the practical end of commercial production of this highest-rank coal. The production of bituminous coal from existing mines is about 80% complete and can be carried out at the current rate for the next 20 years. The production of subbituminous coal from existing mines can be carried out at the current rate for 40 – 45 years. Significant new investment to extend the existing mines and build new ones would have to commence almost now to sustain the current rate of coal production, 1 billion tons per year, to 2029. In view of the existing data, we conclude that there is no spare coal production capacity of the size required for massive coal conversion to liquid transportation fuels. Our analysis in Part I is independent of other factors that will prevent large-scale coal liquefaction projects: the inefficiency of the process and either emissions of greenhouse gases or the energy cost of sequestration. These other factors will be addressed in Part II. The lack of water, environmental problems with coal ash, and high investment costs are also serious issues.

2.2 Introduction

There is a popular belief that coal production in the U.S. may continue practically forever at the current rate of about 1 billion tons per year. For example, a U.S. coal industry website states the following facts about coal:

> The United States has enormous coal "resources" and "recoverable reserves[1]." The most reliable information about coal is published by the Energy

[1] Defined in the next section.

> Information Administration (EIA). The most recent figures available from the EIA, show that America's estimated recoverable reserves of coal stand at 275 billion tons, an amount that is greater than [those for] any other nation in the world. These recoverable reserves [are] capable of meeting domestic demand for more than 250 years at current rates of consumption[2].

While this statement may be true in principle, our analysis of historical coal production data shows that the existing U.S. mines can continue producing bituminous coal at the current rate for the next 20 years and subbituminous coal for about 20 years more. To extend the next four decades of coal production at today's rate to over 250 years, will require the costly and environmentally unacceptable expansions of existing mines and the opening of new mines that will operate at ever greater depths in ever thinner coal seams.

The goal of Part I of this paper is to characterize the near-future of coal production in the U.S. and demonstrate that there is no large spare production capacity that could be used to create mega-scale conversion of coal to liquid transportation fuels. In Part II, we will investigate what would it take to carry on such a conversion in the only theoretically possible location in the U.S., southeastern Montana.

Here, we first characterize the coal resource base in the U.S., and then perform a multi-Hubbert curve analysis of anthracite, bituminous, and all coal production in the U.S.

2.3 Coal Resources

U.S. coal resources are generally regarded as very large, which is the premise for the development of large-scale coal-to-liquids (CTL) conversion. The size and distribution of these resources bears examination. The United States has three major coal-producing areas; the Appalachian Basin, the Illinois Basin, and the Rocky Mountain area. Figure 2.1 shows the major coal-producing regions of the United States and figure 2.2 shows a more detailed view of the Powder River Basin. Coal reserves reported by the U.S. Geological Survey are based on seam thickness and depth, and do not necessarily represent economic reserves (Fettweiss [1979]).

There are three categories of coal reserves reported by the EIA, demonstrated reserve base, estimated recoverable reserves, and recoverable reserves at producing mines. Table 2.1 shows these categories for selected coal-producing states. As one can see, the relationship between reserves and production is not clear. The broader reserve categories put the most coal in Montana, Illinois and Wyoming, but the producing mines category reflects Wyoming's dominant position in coal production. Coal reserves are not comparable with oil reserves, except that the category of recoverable reserves at producing coal mines is approximately equivalent to proved developed oil reserves.

Coal production trends tell a simpler story; production is declining in the Appalachian and Illinois Basins, and is increasing in Wyoming and Colorado. Elsewhere in the Rocky Mountain area, production is about constant. Tables 2.2 and 2.3 show the states with the

[2] *About Coal, America's most abundant energy resource and a source of chemicals, fertilizer, and power worldwide*, www.clean-energy.us/facts/coal.htm.

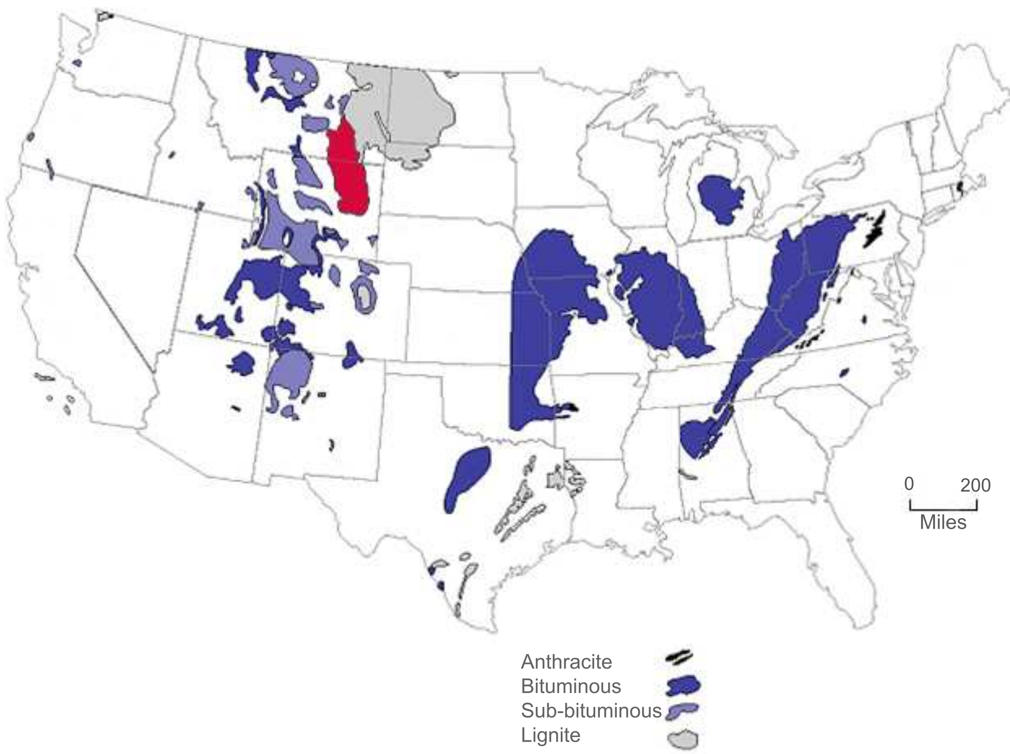

Figure 2.1: Map of Coal-Producing Regions of the United States, Powder River Basin Shown in Red, Source: EIA

Table 2.1: Coal Reserves and Production, Selected States

State	Recoverable Reserves million short tons	Mine reserves million short tons	2007 Production million short tons
Montana	74,856	1,251	43.4
Wyoming	39,674	7,330	453.6
Illinois	37,957	1,286	32.4
West Virginia	17,669	1,828	153.5
Kentucky	14,682	1,182	115.3

largest ten-year coal production increases and decreases. Huge growth in Wyoming coal production comes from surface mining of subbituminous coal in Campbell and Converse Counties in the Powder River Basin. Coal production in Colorado is mostly underground mining of bituminous coal west of the Continental Divide, in the Colorado River watershed.

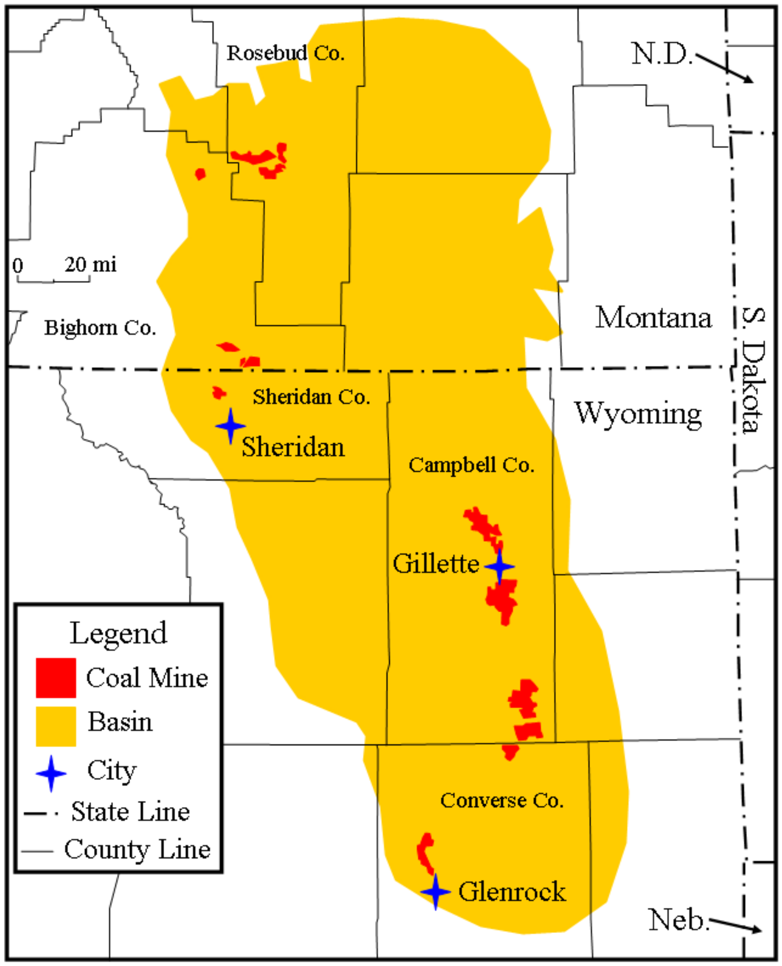

Figure 2.2: Map of the Powder River Basin with Mines Shown in Red, Adapted from Flores and Bader [1999]

Table 2.2: States with Greatest Coal Production Increases, 1997-2007

State	Production Increase 1997-2007
	thousand short tons
Wyoming	171,687
Colorado	8,935
Montana	2,385
Arkansas	65
Kansas	60

Table 2.3: States with Greatest Coal Production Decreases, 1997-2007

State	Production Decrease 1997-2007
	thousand short tons
Kentucky	-40,573
West Virginia	-20,263
Texas	-11,380
Pennsylvania	-11,150
Virginia	-10,491
Illinois	-8,714

Coal is classified by rank, going from anthracite (highest) to lignite (lowest). In the U.S., anthracite and bituminous coal are mostly produced from underground mines, while subbituminous coal and lignite are produced almost exclusively from surface mines. U.S. coal production shows a clear trend of declining production of high-rank coals and rapidly increasing production of subbituminous coal, the second-lowest rank. Lignite resources in North Dakota and Montana are enormous, but air-quality and other environmental and technological considerations have limited the use of lignite. **Figure 2.3** shows historical U.S. coal production by rank.

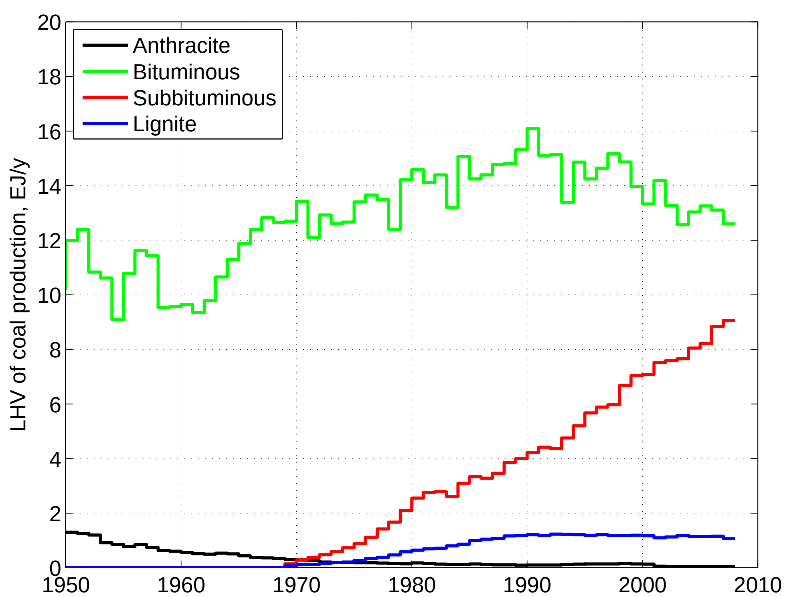

Figure 2.3: United States historical coal production by rank. Note that currently the U.S. uses around 110 exajoules (EJ) of primary energy per year (Patzek, 2008). Data source: EIA.

Another way of classifying coal is sulfur content. The Wyoming, Montana, and Colorado coals are lower in sulfur than those of comparable rank from east of the Mississippi River Anonymous [1999]. This has been an important factor in the development of western coal in recent years because power plants have been under pressure to reduce their emissions of sulfur oxides.

Yet another way of classifying coal is by heat yield. This classification is similar to rank, with anthracite higher than bituminous coal, which is higher than subbituminous, which is higher than lignite. The difference is that large ranges of values are found within the bituminous and subbituminous categories, and there is some overlap. By this classification, the Wyoming and Montana coals are at the low end of the subbituminous range with heat yields of about 8,200 btu per pound (19 MJ kg^{-1}). By comparison, anthracite yields up to 15,000 btu per pound (35 MJ kg^{-1}). The 1997 EIA coal reserves review lists reserves by state, divided into heat yield and sulfur content ranges Anonymous [1999].

Concentrated resources are desirable for CTL conversion because the plants have significant economics of scale. The thirteen largest coal mines in the United States are listed in Table 2.4. This provides a perspective on the location and relative size of the most concentrated resources. Twelve of the thirteen largest coal mines in the United States are located in the Powder River Basin.

Table 2.4: Thirteen Largest Coal Mines in the United States

Mine	State	2007 Production short tons
North Antelope Rochelle	Wyoming	91,523,280
Black Thunder	Wyoming	86,196,275
Cordero	Wyoming	40,467,627
Jacob's Ranch	Wyoming	38,101,560
Antelope	Wyoming	34,474,682
Caballo	Wyoming	31,172,396
Belle Ayr	Wyoming	26,608,765
Buckskin	Wyoming	25,268,145
Eagle Butte	Wyoming	24,985,991
Rawhide	Wyoming	17,144,361
Spring Creek	Montana	15,712,091
Freedom	North Dakota	14,955,989
Rosebud	Montana	12,583,084

Based on the above assessments, the most attractive area for CTL conversion is the Powder River Basin of Wyoming and Montana; it contains 12 of the 13 largest coal mines in the U.S. and large undeveloped resources remain. Another key issue is the availability of water.

Bituminous coal is mined underground in Colorado and Utah and production has been increasing, but the mines are distributed over a vast area and there is no surplus water in the Colorado River watershed. Although large coal reserves are attributed to Illinois and water is abundant there, coal production in Illinois has been steadily declining for at least 15 years, partly because Illinois coal is high in sulfur content. During that time, coal production from the Powder River Basin has grown more than that of the U.S. as a whole. One reason for this growth is that the very large surface mines that characterize coal production in the Powder River Basin have low labor costs. The EIA lists labor productivity in Wyoming surface mines in 2007 as 34.19 short tons per employee-hour. By comparison, underground mines in the Appalachian Basin average 2.91 short tons per employee-hour Anonymous [2008a], nearly 12 times less.

The Powder River Basin coals are found in the Tongue River member of the Fort Union Formation of Paleocene age. The depositional environment was a warm subtropical wooded swamp, similar to parts of southern Louisiana today. This was a very large swamp, and the Wyodak-Anderson Coal was deposited as a laterally-continuous unit over most of the basin. Clastic sediment input was overbank and crevasse-splay mudstone deposits associated with major floods.

The unique feature of this swamp was the combination of limited clastic sediment input with high biologic productivity; the Powder River Basin is known for unusually thick coal seams. In the central part of the Powder River Basin, the seams that make up the Wyodak-Anderson Coal merge into a single bed that ranges from 46 to 202 feet (15 – 62 m) in thickness and is present over 950 square miles (2,500 km^2) of the Powder River Basin in Wyoming and southernmost Montana Flores and Bader [1999]. This merged seam is at a depth of more than 1,000 feet (300 m), so it is considered underground mineable reserves.

The Rosebud and Knobloch Coals are present on the Montana side of the basin and extend north of the Wyodak-Anderson. Each of these units can be a single massive coal or may be divided into multiple separate coal beds, complicating nomenclature. The Wyodak-Anderson Coal is at its thickest in eastern Johnson County, Wyoming, in the central part of the Powder River Basin, but there are no coal mines in Johnson County because the overburden is too thick for surface mining. The Wyodak-Anderson Coal is subbituminous and has a fairly low heat yield, but it also has a lower-than-average sulfur content of about half a pound of sulfur per million btu (200 mg S/MJ). Table 2.5 gives mean compositional values for coals from current and proposed mines in the Powder River Basin.

The sediments on the eastern flank of the Powder River Basin dip 2 to 5 degrees, so the region of surface-mineable coal is a narrow strip in Campbell and Converse counties in Wyoming. The Montana side has lower dips and multiple coals, so surface-mineable coal exists over a broad area in Bighorn, Rosebud, Powder River, and Custer Counties. Except for the Rosebud Coal in one area, the other coals are not as thick as the Wyodak-Anderson, which is mostly in Bighorn County. The Wyoming side of the Powder River Basin has thicker coal seams and better rail access, so it has been developed more.

Table 2.5: Mean Composition of Powder River Basin Coal Stricker and Ellis [1999]

Ash content, % by weight	6.44
Moisture content, % by weight	27.66
Sulfur content, % by weight	0.48
Heating value, Btu/lb	8220
Heating value, MJ/kg	19.1

Coal development in Montana is characterized by a few large surface mines that have been in existence for some time. These are located on the thickest part of the Wyodak-Anderson and Rosebud coals. Although Montana has been described for decades as having the largest coal reserves in the U.S., Montana coal production has been relatively static for the past 15 years. Wyoming coal production has grown dramatically during the same time period. This pattern of development has been driven by the economics of surface mining; it is easier to mine one or two massive coals than three or more thinner ones. **Figure 2.4** shows a mine in the Wyodak-Anderson Coal in southernmost Montana.

Figure 2.4: Decker Coal Mine, Montana, showing split Wyodak-Anderson Coal. Image from Flores & Bader.

Clinker beds are present over large parts of the Powder River Basin. These have been caused by lightning strikes igniting exposed coal seams. Coal seam fires have substantially reduced the surface-mineable coal reserves of the Powder River Basin, especially on the Montana side of the Wyodak-Anderson coal. Surface coal mines are located between the clinker areas. The clinker beds themselves are nodular and resemble terra cotta. The clinker beds do not persist to great depths, so much more of the Wyodak-Anderson Coal remains in deeper areas, many of which are too deep for surface mining. At present there is no underground mining of coal in the Powder River Basin.

2.4 History of Coal Production in the U.S.

The past and future coal production in the U.S. is modeled here with the multi-Hubbert curve model described in detail in Patzek [2008]. The historical coal production data series are from Anonymous [2008b] for the years 1949 through 2007 and from Schurr and Netschert [1960] for the years 1850 through 1948. The annual production data are subdivided by coal rank.

Here suffices it to say that, theoretically, the Hubbert curve approach captures very well coal production from a multitude of independent mines in the U.S. For example, a single complete Hubbert curve models anthracite production in the U.S., see **Figure 2.5**.

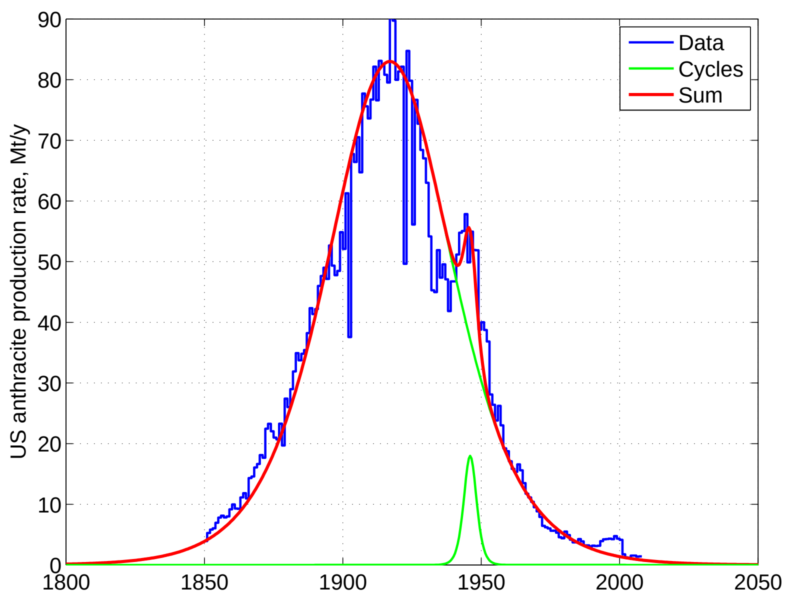

Figure 2.5: Almost all history of anthracite production in the U.S. is modeled with one fundamental Hubbert curve. The small second Hubbert curve reflects WWII production. Anthracite production data since 1850 has been obtained from EIA and Schurr & Netschert (1960).

Extending this approach to all anthracite and bituminous coal produced in the U.S. requires four Hubbert curves: (1) The fundamental Hubbert curve with the peak in 1988; (2) The early production curve with the peak in 1897; (3) The WWI curve with the peak in 1920; and (3) The WWII curve with the peak in 1946, see **Figure 2.6**. The historical data and the Hubbert curves in Figure 2.6 can be integrated in time to yield the cumulative coal production, see **Figure 2.7**. The most important conclusion is that the slope of the the cumulative production of bituminous coal (anthracite production is already irrelevant) remains comparable to the present one for only 20 more years and some 80% of U.S. bituminous coal has already been produced from the existing mines. This conclusion is consistent with the data in Table 2.3.

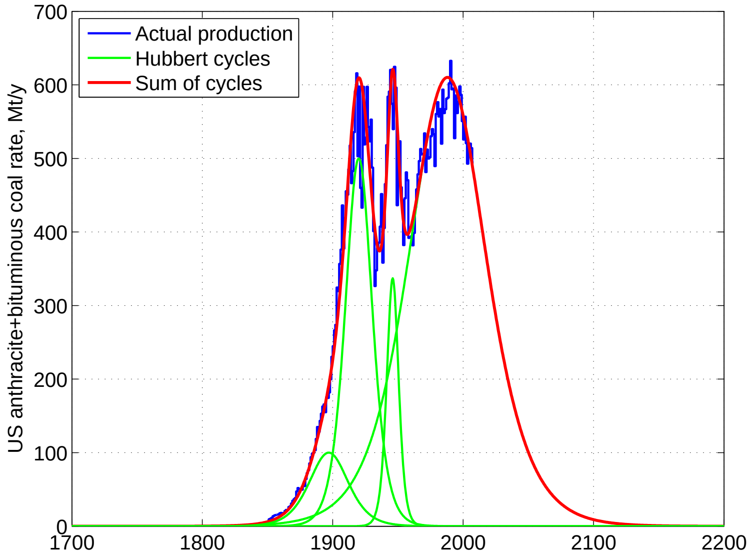

Figure 2.6: The production rates of anthracite and bituminous coal in the U.S. since 1850 can be modeled with four Hubbert curves, the fundamental curve and three smaller curves for the pre-1900 coal production, WWI, and WWII. The production data are from EIA and Schurr & Netschert (1960).

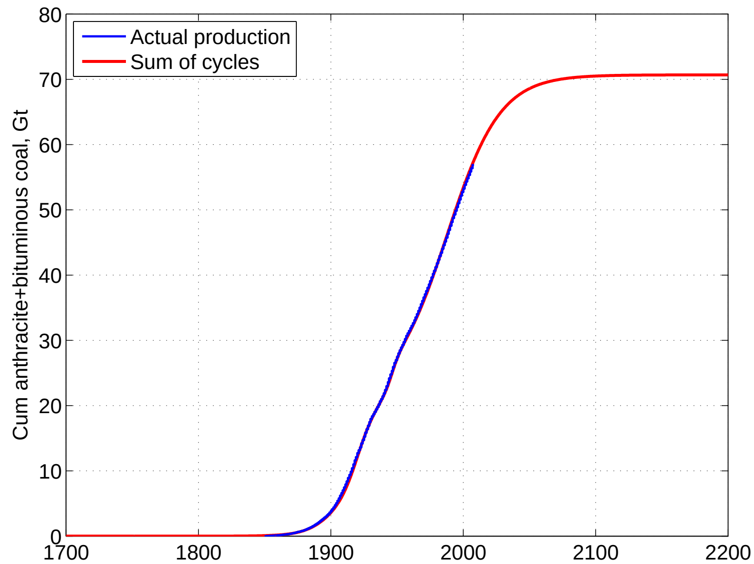

Figure 2.7: The cumulative production of anthracite and bituminous coal in the U.S. since 1850 shows that all mines have produced about 80% of their reserves and will be producing bituminous coal at rates comparable to the present one for another 20 years. Anthracite production is already negligible.

A similar analysis of all coal production in the U.S. is shown in **Figures 2.8** and **2.9**. The only difference is that the fundamental Hubbert curve now peaks near 2008, because of the inclusion of subbituminous coal. It appears that about 55% of coal producible from historical and current mines has been produced and production can be maintained at rates comparable to present for another 40 years.

2.4.1 Lignite

Lignite is the softest coal and is sometimes considered a separate category rather than a type of coal. Because of its high content of ash and sulfur and its low heat yield, lignite has not been mined on a large scale for power plant fuel in the US. The history of U.S. lignite production is not suitable for Hubbert analysis because it is dominated by a small number of projects, many of which were created with government financing. The largest U.S. lignite mine produces at a nearly constant rate to feed a coal gasification facility in North Dakota. Lignite accounted for 7.2 % of U.S. coal production in 2006 and 8.7 % of the U.S. demonstrated reserve base in the 1997 reserve study. Lignite is produced in Texas, North Dakota, Louisiana and Mississippi. To give an idea of the difficulty in analyzing lignite production history, the state with the largest demonstrated reserve base of lignite is Montana, yet it had no production in 2006.

The most important lignite deposits in the US, accounting for 62 % of 2007 lignite production, are found in Eocene-age sediments in the Gulf Coast area, especially the Wilcox Formation. An analysis of 52 samples of Wilcox Formation lignite by the Arkansas Geological Survey found average values of 35.7 % moisture, 17.6 % ash, 0.57 % sulfur and 5,759 Btu per pound on an as-received basis Prior et al [1985].

Lignite has more hydrogen than true coals, which is an advantage for Fischer-Tropsch synthesis, but the ash content presents a waste disposal problem. Because of the difficulty in analyzing the lignite production history, the conclusions of this paper apply to anthracite, bituminous and sub-bituminous coals, but not to lignite. Lignite resources are best evaluated by traditional volumetric methods, which indicate that the demonstrated reserve base of lignite in the entire U.S. is about a quarter of the reserve base of sub-bituminous coal in the Powder River Basin.

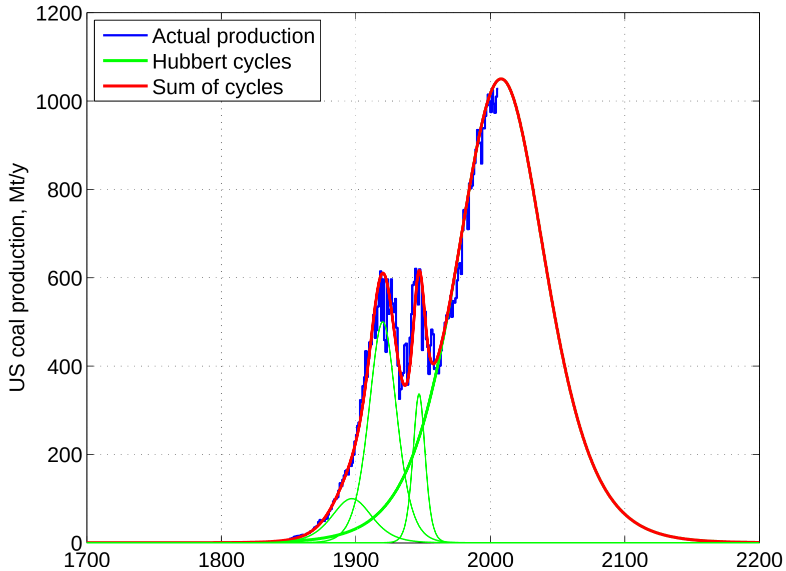

Figure 2.8: The production rate of coal of all ranks in the U.S. since 1850 can be modeled with four Hubbert curves, the fundamental curve and three smaller curves for the pre-1900 coal production, WWI, and WWII. The production data are from EIA and Schurr & Netschert (1960).

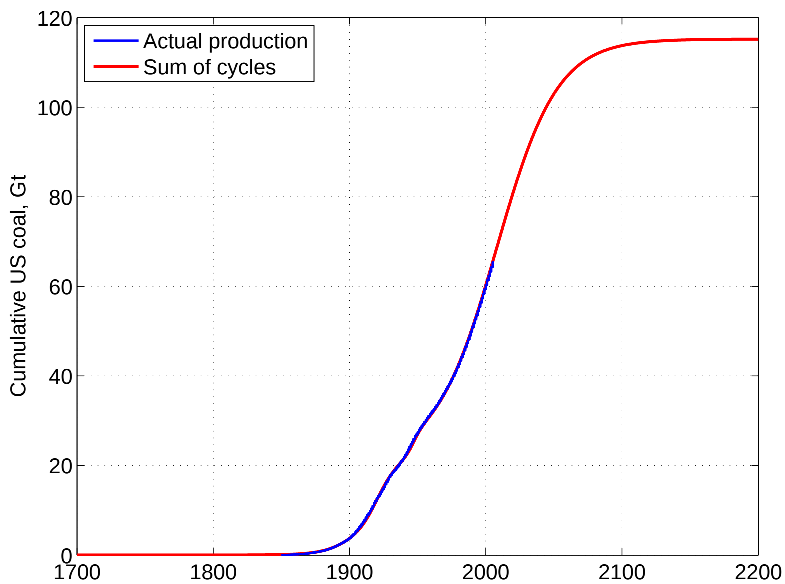

Figure 2.9: The cumulative production of coal in the U.S. since 1850 shows that all mines have produced about 55% of their reserves and will be producing mostly subbituminous coal at rates comparable to the present one for another 40 years.

2.5 Conclusions

The multi-Hubbert curve model of historical coal production in the U.S. leads us to the most important conclusion of this paper. Based on the existing coal production data from all mines in the U.S., it appears that the current mines will be largely exhausted 40 years from now. New giant mines in the Powder River basin, the only region of the country with a high upside potential for such mines, will have to be developed to replace the falling production, and this new coal may be already subscribed to by the current users, especially power utilities. Thus talk of a massive diversion of coal to production of liquid transportation fuels is likely to be just that, regardless of other serious environmental and technical reasons for abstaining from such a diversion. Some of these other reasons will be described in Part II of this paper. Because Wyoming is already the largest U.S. producer of coal, producing roughly 50% of all coal, the new mine extensions will have to be in southeastern Montana. The conclusions of this paper apply to anthracite, bituminous and sub-bituminous coals, but not to lignite, which has little production history in the areas where it is most abundant.

2.6 Acknowledgements

Greg Croft has been supported by 2 years of Jane Lewis Fellowship from U.C. Berkeley.

Bibliography

Anonymous 1999, *U.S. Coal Reserves: 1997 Update*, Coal Reserves Report DOE/EIA-0529(97), Energy Information Administration, Washington, DC.

Anonymous 2008a, *Annual Coal Report 2007*, Annual Coal Report DOE/EIA-0584(2007), Energy Information Administration, Washington, DC.

Anonymous 2008b, *Annual Energy Review 2007*, Annual Energy Review DOE/EIA-0384(2007), Energy Information Administration, Washington, DC.

Fettweiss, G. B. 1979, *World Coal Resources Methods of Assessment and Results*, Elsevier, Amsterdam.

Flores, R. and Bader, L. 1999, *Fort Union Coal in the Powder River Basin, Wyoming and Montana: a Synthesis*, Resource Assessment Professional Paper 1625-A, U.S. Geological Survey, Washington, DC.

Patzek, T. W. 2008, Exponential growth, energetic Hubbert cycles, and the advancement of technology, *Arch. Min. Sci.* v. 53, no. 2, p. 131 – 159.

Prior, W. L., Clardy, B. F., and Baber, Q. M., III, 1985, lignite investigations, Arkansas Geological Commission Information Circular 28-C, 214 p.

Schurr, S. H. and Netschert, B. C. 1960, *Energy in the American Economy, 1850-1975*, Chapt. Statistical Appendix to Part 1, pp 492 – 493, Johns Hopkins Press, Baltimore.

Stricker, G. and Ellis, M. 1999, *Coal Quality and Geochemistry, Powder River Basin, Wyoming and Montana*, Resource Assessment Professional Paper 1625-A, U.S. Geological Survey, Washington, DC.

Chapter 3

Potential for Coal-to-Liquids Conversion in the U.S., Part II – Fischer-Tropsch Synthesis

3.1 Abstract

The United States has the world's largest coal reserves, see Part I. Consequently, large-scale coal-to-liquids (CTL) conversion has been proposed as a major source of domestic transportation fuels. We calculate that the energy efficiency of the best existing Fischer-Tropsch (FT) process applied to an average coal in Montana is less than 1/2 of the corresponding efficiency of an average crude oil refining process. The resulting CO_2 emissions are 20 times higher for CTL than for conventional petroleum products. One barrel of the FT fuel requires roughly 800 kg of coal and 800 kg of water. The minimum energy cost of subsurface CO_2 sequestration would be at least 40% of the FT fuel energy, essentially halving energy efficiency of the process. We argue therefore that CTL conversion is not the most valuable use for the coal, nor will it be as long as it is economical to use natural gas for electric power generation. This finding results from the low efficiency inherent in FT synthesis, and is independent of the monumental FT plant construction costs, mine construction costs, and environmental considerations.

3.2 Introduction

In this paper we focus on Montana, because of her very large coal reserves discussed in Part I, and current designs on this coal. The CBS *60 minutes* reported on Feb. 26, 2006:

> America's dependence on foreign oil – President Bush called it "an addiction" in his State of the Union address – has become a threat to the country's economy and security. The governor of Montana, Brian Schweitzer, says there's something we can have up and running in the next five years. What he has in mind is using the coal, billions of tons of it, under the high plains of his home state. The governor tells correspondent Lesley Stahl he wants to use

> an existing process to turn that coal into a synthetic liquid fuel, or synfuel. The plan is controversial, but Gov. Schweitzer – half Renaissance man, half rodeo cowboy – seems ready for the challenge. In fact, he sounds like he's ready to take on the world. "Why wouldn't we create an economic engine that will take us into the next century, and let those sheiks and dictators and rats and crooks from all over the world boil in their own oil?" Schweitzer said at a press conference.

In Part II, we give a brief background of Fischer-Tropsch (FT) synthesis of liquid fuels. We analyze the energy efficiency of FT with average subbituminous coal from Montana as feedstock. We calculate the minimum emissions of CO_2 from the FT process, and compare them with the corresponding emissions of a conventional crude oil refinery. We then calculate the minimum energy costs of subsurface CO_2 sequestration for a FT plant in Montana. Finally, we compare the respective uses of coal and natural gas in electricity generation and automobile transportation, and arrive at the main conclusions of this paper.

3.3 Fischer-Tropsch Synthesis of Liquid Fuels

3.3.1 History

In 1925, Professor Franz Fischer, founding director of the Kaiser-Wilhelm Institute of Coal Research in Mülheim an der Ruhr, and his head of department, Dr. Hans Tropsch, see **Figure 3.1**, applied for a patent describing a process to produce liquid hydrocarbons from carbon monoxide gas and hydrogen using metal catalysts. The hydrocarbons synthesized in the process consisted primarily of liquid alkanes, also known as paraffins. Other by-products were alkenes (olefins), alcohols and solid paraffins (waxes). The required gas mixture of carbon monoxide and hydrogen was created through a reaction of coke or coal with steam and oxygen, at temperatures over 900 degrees Celsius. The raw product of the FT hydrocarbon synthesis is a liquid mixture similar to a waxy crude oil. This mixture is further refined to yield gasoline and diesel fuel, among others.

By the beginning of the 1940s, some 600,000 tonnes of liquid hydrocarbons were produced per year in German facilities, made from coal using Fischer-Tropsch (FT) Synthesis. Licensed by Ruhrchemie, four facilities in Japan, as well as a plant in France and in Manchuria, were in service. In 1944, Germany's annual synthetic fuel production reached more than 124,000 barrels per day from 25 plants, or ~6.5 million tons of fuel Agrawal et al [2007]. Almost all of this production was used to run the Nazi war machine. The results are well known[1].

After 1950, the only new FT production facilities were built for political reasons in South Africa in the town of Sasolburg. Currently, the two plants operated by SASOL Synfuels provide about 25 percent of South Africa's diesel and gasoline needs, processing 45 million tonnes of coal per year[2].

[1] After the war, captured German scientists continued to work on synthetic fuels in the United States in a U.S. Bureau of Mines program initiated by the Synthetic Liquid Fuels Act.

[2] Eight million tonnes more than Montana's annual coal production.

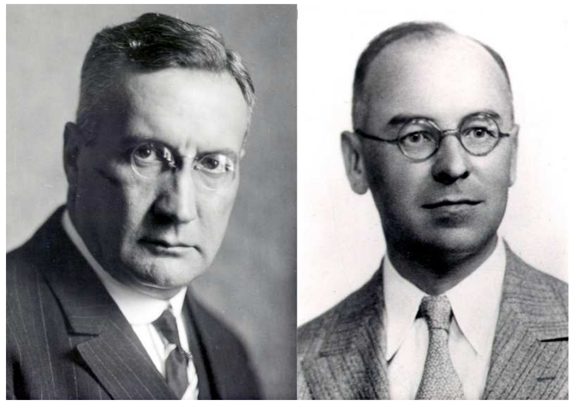

Figure 3.1: Professor Franz Fischer (left) and Dr. Hans Tropsch, the inventors of a process to create liquid hydrocarbons from carbon monoxide gas and hydrogen using metal catalysts. Image: Max Planck Institute of Coal Research.

Profligate coal production and use in South Africa give rise to a number of serious environmental problems Whyte [1995]. Vast stretches of land are affected by strip mining, coal discards and mines. A large amount of waste is created through beneficiation to improve coal quality. These discards have a high sulfur content (1 to 7.8 percent) and high ash values (24 to 63 percent), so the waste material is almost unmarketable and stockpiles grow at a rate of 40 to 50 million tonnes per year. The burning of these coal dumps contributes to acid precipitation in the Eastern Transvaal Highveld.

The SASOL plants are reported to have even greater environmental impacts than coal power stations of the same size Whyte [1995]. Aside from producing acid rain, they are voracious water users (five barrels of water per barrel of FT oil[3]) and produce a variety of toxic petrochemical wastes. Since the commissioning of its facilities at Secunda, SASOL has spent some 600 million rands[4] on environmental projects, including the recovery and reuse of waste streams, the development and testing of low-smoke fuels, research on industrial water use and reuse, and the toxicity and biodegradability of its products.

Currently, only a handful of other companies have commercialized their FT technology. For example, Shell in Bintulu, Malaysia, uses natural gas as a feedstock, and produces primarily low-sulfur diesel fuel and wax.

Recently, a U.S.-based company Syntroleum produced a whopping[5] 9500 barrels of diesel and jet fuel from the FT process at its demonstration plant near Tulsa, Oklahoma. Using natural gas as a feedstock, the synthetic FT fuel has been tested by the U.S. Department of Energy, the Department of Transportation, and most recently, the Department of Defense, which utilized the fuel in a flight test of a B-52 bomber at Edwards Air Force Base, CA, see **Figure 3.2**.

[3]Chapter 6 in Whyte [1995].

[4]In July 1995, 3.6 South African rand = 1 US dollar.

[5]This small practical joke on the U.S. taxpayers is consistent with the unrealistic and non-physical attitude towards biofuels and synthetic fuels.

Figure 3.2: A B-52 Stratofortress takes off from Runway 22 during a Fischer-Tropsch test flight from Edwards Air Force Base, Calif., on Sept. 19, 2006. During the flight, two of the aircraft's eight engines ran on the natural gas-based Fischer-Tropsch fuel blend. The bombers are from the 5th Bomb Wing at Minot Air Force Base, N.D. (U.S. Air Force photo/Chad Bellay).

3.3.2 The FT Process

The original Fischer-Tropsch process is described by the following chemical equation with $n = 1, 2, \ldots,$

$$n\mathrm{CO} + (2n+1)\mathrm{H_2} \rightarrow \mathrm{C}_n\mathrm{H}_{2n+2} + n\mathrm{H_2O} \tag{3.1}$$

The reactants in the reaction above, CO and H_2, are called the *synthesis gas* or *syngas*. They can be produced by other reactions such as the partial combustion of a hydrocarbon:

$$\mathrm{C}_m\mathrm{H}_{2m+2} + \frac{1}{2}m\mathrm{O_2} \rightarrow (m+1)\mathrm{H_2} + m\mathrm{CO}, \qquad m \ll n \tag{3.2}$$

For example, when $m = 1$, methane in the gas-to-liquids applications reacts as follows:

$$\mathrm{CH_4} + \frac{1}{2}\mathrm{O_2} \rightarrow 2\mathrm{H_2} + \mathrm{CO} \tag{3.3}$$

Alternatively, coal may be gasified in the water-shift reaction:

$$\mathrm{C} + \mathrm{H_2O} \rightarrow \mathrm{H_2} + \mathrm{CO} \tag{3.4}$$

Note that compared with coal gasification, methane gasification uses 1/2 of oxygen for the same amount of hydrogen.

The energy needed for the endothermic reaction of coal and steam is usually provided by exothermic combustion with air or oxygen. This leads to the following reactions:

$$\begin{aligned} \mathrm{C} + \frac{1}{2}\mathrm{O_2} &\rightarrow \mathrm{CO} \\ \mathrm{CO} + \frac{1}{2}\mathrm{O_2} &\rightarrow \mathrm{CO_2} \end{aligned} \tag{3.5}$$

Direct conversion of fossil fuels to hydrogen and carbon monoxide causes more CO_2 and other greenhouse gas emissions than burning of the same fuels outright. For example, burning coal, $\mathrm{C+O_2} \rightarrow \mathrm{CO_2}$ *produces* 35 MJ/kgC of heat. Coal gasification, $\mathrm{C+H_2O} \rightarrow \mathrm{CO+H_2}$, *consumes* 10 MJ/kgC of heat. This heat consumption is equivalent to the burning of up to extra 1/2 kilogram of raw coal per kilogram of gasified coal bobrownicki-justat-pawlikowski [1965].

Synthesis gas is generated at temperatures in excess of 900^0C, and processed at the pressure of about 60 bars and temperature of 250^0C over a suitable catalyst that may contain cobalt, nickel or ruthenium, in addition to iron.

3.4 Efficiency of Coal-Based FT Process in the Powder River Basin

According to Shell, Table 1 in Eilers et al [1990], the theoretical efficiency of the coal-based FT synthesis of liquid fuels is 60 percent. TU Delft calculates energy efficiency of the FT process of about 55 percent Hemelinck [2004]. Practically, a 50 percent energy efficiency of coal conversion to liquid fuels seems to be an upper limit. For example, the calculation in Steynberg and Nel [2004] yields 41.1 percent as the overall conversion efficiency of CTL fuels[6]. Also, according to Shell the cost of a coal-based FT plant is twice that using natural gas Eilers et al [1990], making the CTL process prohibitively expensive.

The product of FT synthesis is not diesel fuel but rather a high-wax crude oil similar to Indonesian Minas or Altamont-Bluebell (Utah). Other products are natural gas, LP gas and electricity from waste heat. The efficiencies quoted above include all of the hydrocarbon outputs and, in the Sasol estimates, the electricity as well.

For efficiency comparison, we use Sheehan *et al.*'s NREL [1998] estimate of primary energy spent on refining crude oil delivered to the refinery gate and processed to diesel fuel. This energy input is 12 percent of the calorific value of the diesel fuel product. In other words, converting petroleum to diesel fuel is 88 percent energy-efficient.

The low-rank western coals, such as those in Montana, usually[7] have a moisture content of 25–55%, sulfur content of 0.5–1.5%, and heating value of 5500–9000 Btu/lb. Table 1 in Part I shows the assumed Montana coal composition as received at the FT plant gate.

The higher heating value of the FT fuel is 45.9 MJ/kg Castorph, Kollera and Waas [1999]. Therefore

$$\frac{45.9}{19.1 \times 0.411} = 5.85 \text{ kilograms of Montana coal/kg of FT fuel} \tag{3.6}$$

is used to produce 1 kilogram of fuel. Since one barrel of the FT fuel weighs ~134 kilograms, 784 kg of coal is used to produce one barrel of this fuel.

The Sasol FT process currently uses 5 barrels (795 kilograms) of water per barrel of the FT fuel produced Whyte [1995], and this ratio is assumed in the current analysis.

[6] Counting all hydrocarbon products, liquid and gaseous and a small amount of extra electricity. Because we are not including the energy costs of coal mining and transport, we omit this electricity in the energy balance.

[7] Advanced coal conversion process demonstration. Progress report, January 1, 1992–March 31, 1992. Source: www.osti.gov/bridge/product.biblio.jsp?osti_id=106461, accessed May 12, 2007.

Assuming that 60% of Montana coal is carbon, see Table 1 in Part I, and that the typical FT fuel composition is $C_{12}H_{26}$, one may calculate that CO_2 produced in the FT liquid fuel plant is

$$\begin{aligned}&(1 - 0.14 - 0.25 - 0.01) \times \left(784 - 134 \times \frac{144}{144+26}\right) \times \frac{44}{12}\\&\approx 1460 \text{ kg of } CO_2/\text{bbl of FT fuel}\end{aligned} \tag{3.7}$$

This calculation is consistent with the EIA's estimate[8] of 213.4 lbm CO_2 per 1 million Btu in Montana's subbituminous coals that translates into $\sim$1200 kg of CO_2 per barrel of FT fuel.

In spite of the huge variety of chemical compounds they contain, all crude oils have carbon contents between 83 and 87 wt % Speight [1990]. The CO_2 emissions from crude oil are therefore constant across a wide variety of sources Hiete and Berner [2001]:

$$CO_2 \text{ emissions} = \frac{44}{12}(0.84 \pm 0.03)\frac{\text{kg } CO_2}{\text{kg crude oil}} \tag{3.8}$$

Since about 0.12 bbl of oil with the density of 840 kg m^{-3} is burned to produce 1 barrel of diesel fuel, the CO_2 emissions are

$$44/12 \times 0.84 \times 0.12 \times 42 \times 3.785/0.84 \approx 70\frac{\text{kg } CO_2}{\text{bbl of diesel fuel}} \tag{3.9}$$

Therefore CO_2 emissions from the production of coal-based FT fuel are approximately $1400/70 = 20$ times higher than those from the production of petroleum-based diesel fuel.

3.4.1 Scale-up of CTL Plants

With the assumptions above one may calculate the amounts of coal and water necessary to produce various quantities of FT fuels, as well as the respective amounts of waste streams. The results are listed in **Table 3.1**. Note that the single-plant capacity of 150,000 BPD is more than the total 124,000 BPD capacity of the 25 plants operated by Nazi Germany to supply its military.

It appears that even the smallest plant producing 22,000 BPD of FT fuel, would use 20% of the current coal production in Montana and impose significant environmental stresses on the state. The three larger plant designs extend into the realm of insanity. For example, the 300,000 BPD plant, sufficient to supply most of the U.S. military needs, would consume twice the current coal production in Montana, trice the current water use by Montana mines, and each year would produce 145 million tonnes of CO_2, 1.7 million tonnes of SO_2 and 11 million tonnes of ash. If Montanans wish to destroy their beautiful state, then large FT plants offer a quick and certain fulfilment of this wish.

[8] Hing and Slatick [1994], Table FE4. Average Carbon Dioxide Emission Factors for Coal by Rank and State of Origin.

Table 3.1: Production of coal-based FT fuel in Montana

FT fuel out, BPD[a]	22,000	150,000	300,000	1,000,000
Montana coal in, Mt/yr[b]	6.3	43	86	286
Ratio[c]	0.15	1.0	2.1	6.8
Water in, Billion gal/yr	2	11[d]	23	77[e]
CO_2 out, Mt/yr[b]	12	80	160	533[f]
Ash out, Mt/yr[b]	0.4	2.8	5.5	18
SO_2 out, Mt/yr[b]	0.06	0.4	0.8	2.7
Capital investment[g], \$ billion	1.2 – 4	7.2 – 24		48 – 160

[a] BPD = Barrels of fuel per day
[b] 1 Mt = 1 Million metric tonnes per year
[c] Ratio of plant input of coal to all coal mined in Montana in 2006
[d] 1/3 of all water currently used for mining in Montana
[e] As much as all personal and commercial water use in Montana
[f] Eight percent of current U.S. CO_2 emissions of 6 billion tonnes per year in 2005. Source: EIA, ftp.eia.doe.gov/pub/oiaf/1605/cdrom/pdf/ggrpt/057305.pdf
[g] **?**, Table 2 and the footnotes therein

3.5 CO_2 Sequestration

To calculate the decrease of energy efficiency of the coal-based FT process as a result of CO_2 sequestration, we make the following assumptions:

1. For efficiency, and to concentrate CO_2 in effluent gases, pure oxygen is used in coal combustion.
2. Because the hot compressed process gases are used for electricity cogeneration, the work of compressing CO_2 to the necessary injection pressure is external to the FT process.
3. Pressure losses in a pipeline from the plant to the aquifer are neglected.

As a reference, we use 1 barrel of FT fuel that contains 6.2 GJ of primary energy.

3.5.1 Work of Oxygen Separation

Because exhaust from combustion of coal with excess air contains only 10 - 14 % of carbon dioxide by volume (the rest is nitrogen, unused oxygen, etc.), the cost of separating this dilute carbon dioxide would be prohibitive. Therefore, pure oxygen (>99% by volume) must be used to combust coal if one wants to capture and sequester CO_2.

The production of 1 barrel of FT fuel requires $1300 \times 32/44 = 945$ kilograms of O_2; $26/170 \times 134 \times 32/2/2 = 164$ kg of oxygen is produced from steam, but the remaining

Table 3.2: Energy requirements for oxygen production

Method	^{a}kWh t^{-1}	^{b}MJ kg^{-1}
Cryogenic separation, 50% O_2	400	1.4
Cryogenic separation, > 99% O_2	1100[c]	4.0
Pressure swing adsorption, 90% O_2	550	2.0
Perm-selective membrane, 37.5% O_2	210	0.8
Perm-selective membrane, 44% O_2	300	1.1
Cryogenic Air Separation Unit[d], ??%[e] O_2	235	0.85

[a]Electricity required to produce equivalent pure O_2, Table 2 in Bisio et al [2002].
[b]Exergy required to produce 1 kg of equivalent pure O_2
[c]Liquid oxygen. Heat recovery from boiling off liquid gases lowers this energy cost by a factor of 2 – 2.5
[d]Gray literature presentation by Mr. Stiegel of NETL stiegel [2006], p. 11, quoting Air Products and Chemicals, Inc.
[e]Oxygen concentration was not listed

780 kg of oxygen must be separated from air. The 1300 kg of CO_2 generated per barrel of FT fuel is a mean of the two estimates in Section 3.4.

The minimum work of reversible separation ("unmixing") of air into oxygen and nitrogen at ambient conditions is, e.g., Gyftopoulos and Beretta [2005]:

$$\begin{aligned} W_1 &\approx RT_0 \left[y_{O_2} \ln(y_{O_2}) + y_{N_2} \ln(y_{N_2}) \right] \\ &= 1.27 \text{ MJ kmol}^{-1} \text{ air} = 0.19 \text{ MJ kg}^{-1} \text{ O}_2 \end{aligned} \tag{3.10}$$

where $R = 8.314$ J K^{-1} mol^{-1} is the universal gas constant, $T_0 = 298$ K is the ambient temperature, $y_{O_2} = 0.21$ is the mole fraction of oxygen in ambient air, and $y_{N_2} \approx 0.79$ is the mole fraction of nitrogen (and other gases).

The actual work of oxygen separation is about 4 – 20 times larger, depending on whether the final oxygen product is pure and/or liquid or gaseous, see **Table 3.2**. We choose the efficient cryogenic process with heat recovery[9]: $1.44 \times 780 = 1123$ MJ/bbl FT fuel or 1.1 GJ/bbl. As one can see, just the oxygen separation for the entire process costs $1.1/6.2 \times 100 = 18\%$ of the FT fuel energy. This energy is generated with steam turbines and has been included[10] in the energy analysis of the Sasol FT process in Steynberg and Nel [2004]. Of course the shaft work of a rotating turbine could be converted to electricity with an almost 100% efficiency, so roughly 1/5 of the FT fuel energy could be electricity, not oxygen.

[9] 400 kWh_e per tonne of O_2. The "best" reported energy use of 235 kWh_e per tonne of O_2, see Table 3.2, has not been verified yet. Sasol uses cryogenic separation.
[10] Dr. André Steynberg, private communication, May 18, 2007.

3.5.2 Work of CO_2 Compression

We assume that the CO_2 from the FT process ends up at ambient conditions after extracting all energy from the process gases to generate electricity. Therefore, this CO_2 must be compressed to a pressure allowing it to be injected. Suppose that the injection target, a sandstone rock formation filled with saline water and capable of storing the injected CO_2 indefinitely is initially at hydrostatic pressure and is pressured up to 0.8 of the overburden pressure[11]. The initial aquifer pressure might be 88 bars and this pressure might increase quickly to 144 bars. Suppose that the average injection pressure is 120 bars.

The actual CO_2 compression from 1 bar to 120 bars may be achieved as a 4-stage compression with 3 inter-coolers (at 15 ^{0}C) and compressor adiabatic efficiency decreasing from 85% (low pressure) to 75% (high pressure) Bolland and Undrum [1998]. The work of CO_2 compression is then about 0.415 MJ/kg or 0.54 GJ/bbl of FT fuel. Because this work is almost certainly delivered by electrical motors, the primary energy consumption is $0.54/0.36 = 1.5$ GJ thermal/bbl FT fuel, or $1.5/6.2 \times 100 = 24\%$ of the fuel energy.

3.5.3 Work of CO_2 Injection

The geothermal gradient in Montana is about 2 degrees Fahrenheit per 100 feet of depth[12]. Therefore the CO_2 temperature in the aquifer at 1000 m is 40 ^{0}C or 313 K and its density[13] about 820 kg m^{-3}. We assume that the temperature of the compressed CO_2 approximately matches the aquifer temperature with no extra work of compression.

On the other hand, if the CO_2 were to be injected into deeper, lower Cretaceous or upper Paleozoic aquifers, its temperature would be reaching 70 – 100 ^{0}C very quickly and the CO_2 density would decrease to 200 kg m^{-3}. This would mean increasing the volume of injection 4-fold, while compressing the CO_2 to substantially higher pressures.

The volume of CO_2 at our aquifer conditions would be $1300/820 = 1.6$ m^3 per barrel of FT fuel. Assuming a 20% porosity and 35% irreducible water saturation, the bulk aquifer rock volume would be $1.6/0.2/0.35 = 23$ m^3 bbl^{-1}.

If the average aquifer thickness filled with the injected CO_2 were 10 meters (33 ft), the aquifer areas necessary to store one year's production of the FT CO_2 would range from 5 to 226 hectares, see **Table 3.3**. Assuming a 20-year duration of the disposal, a pipeline infrastructure and wells would have to be build over several square kilometers. If the CO_2 disposal were significantly deeper, our current estimates may have to be multiplied by a factor of up to 4.

[11] *Overburden* or *lithostatic* pressure is the weight per unit area of all rock above the top of the aquifer. Once injection pressure reaches or exceeds the overburden pressure, the injected CO_2 may fracture and lift the rock above the aquifer and will leak creating mortal danger to all life on land surface above the leak.

[12] Ground Water Atlas of the U.S. – Montana, North Dakota, South Dakota, Wyoming HA 730 – I, USGS, capp.water.usgs.gov/gwa/ch_i/I-text3.html.

[13] See *Supercritical Fluid* in Wikipedia.

Table 3.3: Compression power and aquifer areas to dispose of FT CO_2

FT fuel BPD	Compression MW thermal	Volume[a] 1000 m^3 yr^{-1}	Area ha yr^{-1}	Cum area[b] ha
22000	1	498	5	100
150000	10	3397	34	679
300000	20	6794	68	1359
1000000	66	22648	226	4530

[a] At aquifer conditions
[b] Assuming a 20-year duration of CO_2 disposal

3.5.4 Energy Impact of CO_2 Sequestration

Provided that there are shallow aquifers large enough to hold the injected CO_2, and this is far from certain, some $18 + 24 \approx 40\%$ of the fuel energy will be diverted to CO_2 sequestration. In deep aquifers this energy estimate may grow by a factor of up to four.

3.6 Other Uses of Coal

Electric power generation is the dominant use of coal in the United States, accounting for 92.2 percent of U.S. coal usage in 2005. Other industrial use accounted for 5.4 percent and coke accounted for only 2.1 percent of U.S. coal consumption in 2005. For the purpose of this study, electric power generation is considered to be the alternate use for the marginal ton of coal.

The most efficient coal-fired electric power plants use pulverized coal and superheat the steam in order to increase the Carnot efficiency. These plants can have efficiencies as high as 39 percent, although typical values are 35 to 38 percent of low heating value. Further Improvements to efficiency can be obtained by using Integrated Gasification Combined Cycle (IGCC) plants. Depending on the design, these plants could have efficiencies as high as 52 percent of low heating value Johnston [2006]. Natural gas-fired combined cycle plants can be converted to coal-fired IGCC plants in some cases with the addition of a gasification unit and only minor changes on the turbines Gutierrez et al [2006]. In spite of the high efficiency of IGCC plants, only a few have been built due to their greater cost relative to conventional steam plants. One such plant that has an operating history is the Wabash River plant in Indiana. From completion in 1995 through 1999, that plant produced 3.91 million megawatt hours of power from 1.55 million tons of coal with a typical high heating value of 10,536 btu per poundAnonymous [2000], which works out to an efficiency of 40.8 percent of the high heating value.

3.7 Coal and Natural Gas

One can burn coal or natural gas to generate electricity, hot water, and greenhouse gases. One can also convert coal to a liquid fuel or compress natural gas, and power automobiles with either fuel. In both situations coal and natural gas compete against one another. The question is then, which one of the two sets of alternatives is better?

3.7.1 Fuel Competition in Electric Power Generation

Natural gas competes with coal as an electric power generation fuel. Natural gas-fired power plants come in two kinds; peak plants that can be turned on or off quickly, and more efficient combined-cycle plants. Combined cycle plants compete directly with coal-fired plants because both are baseload generation. The efficiency of actual natural gas-fired combined cycle power plants is about 48.5 percent of low heating value, as reported by Siemens for their SCC6-5000F Flex-Plant 10 McManus et al [2007].

Residual fuel oil is also used for electric power generation, but this is mostly a historical artifact, and very little oil-fired capacity is planned for the 2007-2011 timeframe. **Figure 3.3** shows planned electric power generation capacity increases in the United States during the 2007 to 2011 period, broken down by type of fuel. Note that natural gas-fired plants account for more than half of all capacity additions over that time period, 1/3 more than coal. The use of oil for new electricity generation is insignificant.

3.7.2 CTL versus CNG for Transportation Fuel

Coal can also be converted to liquid transportation fuels, and natural gas can be compressed and used as a transportation fuel. These processes can be thought of as arbitrage between the markets for electric power generation and transportation fuels. Besides the financial cost of such conversion, there is also an energy cost. The energy cost alone dooms Fischer-Tropsch conversion of coal to liquid hydrocarbons to be uneconomical, regardless of potential reductions in the large capital cost of CTL plants. This is true as long as it is economical to build natural gas-fired baseload electric power plants.

The work required to compress 1 mole of natural gas isothermally at 20^0 C to the $P_2 = 20$ MPa pressure used for CNG vehicles from an initial pressure of $P_1 = 0.3$ MPa is:

$$RT \ln \left(\frac{P_2}{P_1} \right) = 10.2 \text{ kilojoules} \tag{3.11}$$

This work is small; it is only 1.1 percent of the 891 kJ per mole liberated from burning the methane. It could be as small as 1.7 kJ if one is starting from the $P_1 = 1.5$ to 10 MPa pressures used in interstate natural gas pipelines. In practice, compressors are neither perfect nor isothermal, and some CNG stations will need a high degree of compression while others will be located along high-pressure lines, so a 98 percent compression efficiency is a reasonable estimate.

Let us assume a coal-fired power plant efficiency of 35 percent, a gas compression efficiency of 98 percent, and a natural gas-fired power plant efficiency of 48.5 percent. If gas and coal compete in power generation, the Fischer-Tropsch synthesis would have to

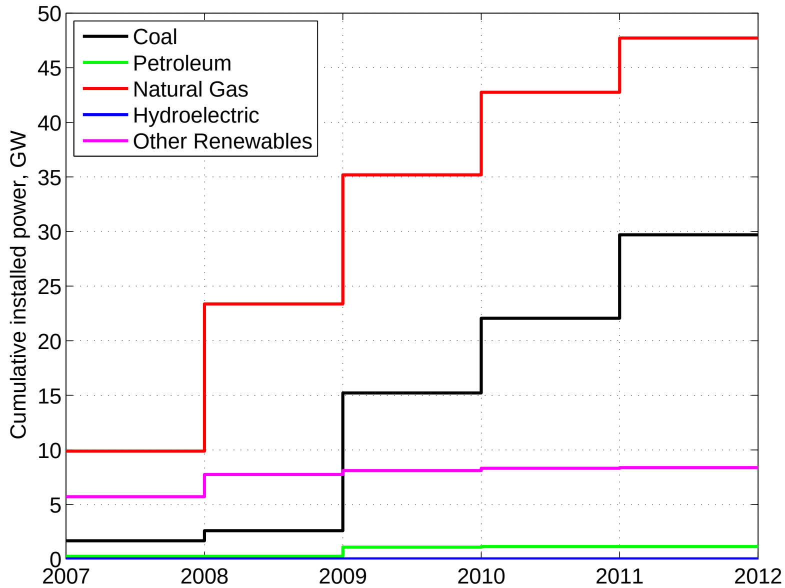

Figure 3.3: Cumulative planned additions of nameplate electrical generation capacity in the U.S., 2007-2011. Petroleum abbreviates distillate fuel oil (all diesel and No. 1, No. 2, and No. 4 fuel oils), residual fuel oil (No. 5 and No. 6 fuel oils and bunker C fuel oil), jet fuel, kerosene, petroleum coke (converted to liquid petroleum), and waste oil. Natural gas abbreviates natural gas, blast furnace gas, propane gas, and other manufactured and waste gases derived from fossil fuels. Other renewables are wood, black liquor, other wood waste, municipal solid waste, landfill gas, sludge waste, agriculture byproducts, other biomass, geothermal, solar thermal, photovoltaic energy, and wind. Data source: Form EIA-860, *Annual Electric Generator Report*.

have a conversion efficiency of $(0.98) \times (0.35/0.485) = 71$ percent, almost twice its actual efficiency, in order to produce a competitively priced transportation fuel.

3.7.3 Coal, Diesel Fuel, and Natural Gas Prices

Coal prices are more sensitive to location than oil prices. **Figure 3.4** below shows recent coal prices in the United States. Markets with access to ports saw dramatic price increases in 2008, but Wyoming did not. This suggests that Wyoming coal production is limited by transportation out of the area because otherwise competition between buyers would drive prices up to world levels. This is another reason that the Powder River Basin would be the most attractive area in the U.S. for FT plants, but it is likely that the coal transportation problem would be remedied during the life of the plant, so economics over the longer term depends on the differences between world coal prices and world oil prices.

These recent coal price increases are a result of major changes in Pacific Basin coal markets. China, formerly a major exporter, has become a major importer, and Vietnam is no longer approving coal export permits. The export price in the Australian port of Newcastle exceed USD 190 per metric ton in July 2008. Prices at this level render FT synthesis uneconomical. This observation raises the question of whether improved

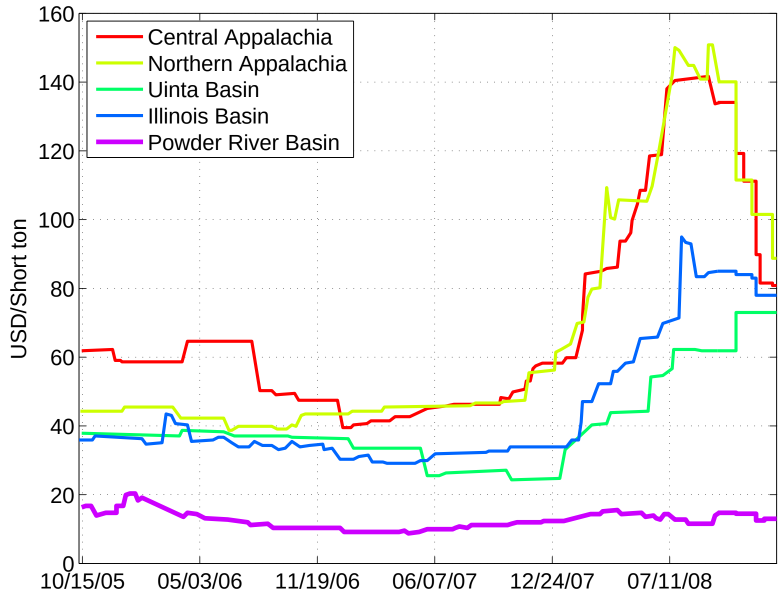

Figure 3.4: United States historical coal prices. Data source: EIA

transportation of coal out of the Powder River Basin might add more value than a larger investment in FT plants.

3.8 Conclusions

The following are the main conclusions of this paper:

1. The large volumes of coal required for CTL suggest that the Powder River Basin of Wyoming and Montana is likely to be the coal source.

2. Because of the different energy contents of subbituminous coal and the FT fuel, and a low energy efficiency of the conversion, 784 kilograms of the average Powder River Basin coal will be needed to produce 1 barrel of the fuel.

3. Although coal reserves are large, recent coal price increases suggest that there is no global coal surplus in the short term.

4. The energy efficiency of an optimal coal-based FT process that produces liquid fuels is 41 percent Steynberg and Nel [2004]. This means that for every 1 unit of fuel energy out, one needs to put in 2.4 units of coal energy.

5. Per unit energy in a liquid transportation fuel, carbon dioxide emissions from a CT plant are about 20 times higher than those from a petroleum refinery.

6. Subsurface disposal of carbon dioxide produced by the FT plants, costs at least 40% of the thermal energy in FT fuels. If this disposal were deeper than assumed here, the current estimate might increase by a factor of up to 4.

7. Montana does *not* have the ca. 800 kilograms of clean water necessary to produce each barrel of FT fuel.

8. Natural gas can be compressed and used for transportation fuel with an efficiency of 98%, so CTL will be an uneconomic source of transportation fuel as long as natural gas competes with coal for power generation. This is true even if the gas-fired plants are more efficient combined cycle designs and the coal plants are conventional.

9. Judging by the recent financing of corn ethanol refineries, the huge construction costs of coal-based FT plants might be borne by the U.S. taxpayers through a massive new subsidy program.

10. The societal costs of the subsidies required to render CTL economical, and the environmental costs of fuel production would be borne by the people of Montana, the surrounding states, and the Earth.

Bibliography

Agrawal, R., Singh, N. R., Ribeiro, F. H., and Delgass, W. N. 2007, *Sustainable Fuel for the Transportation Sector*, PNAS v. 104, no. 12, p. 4828 4833.

Anonymous 2000, *The Wabash River Coal Gasification Repowering Project*, Clean Coal Topical Report Number 20, U.S. Department of Energy, Washington,

Anonymous 2005, *Montanas Energy Future And Why a Proposed Fisher-Tropsch Coal-to-Diesel Plant in Southeastern Montana Should Not Be a Part of It*, Report, Northern Plains Research Council, Billings, Montana.

Bisio, G., Bosio, A., and Rubattoa, G. 2002, Thermodynamics Applied to Oxygen Enrichment of Combustion Air, *Energy Conversion and Management* v. 43, no. 18, p. 2589 2600.

Bobrownicki, W., Justat, A., and Pawlikowski, S. 1965, *Inorganic Chemical Technology*, Wydawnictwa Naukowo-Techniczne, Warsaw.

Bolland, O. and Undrum, H. 1998, *Removal of CO2 from Gas Turbine Power Plants Evaluation of pre- and postcombustion methods*, in Greenhouse Gas Control Technologies, Vol. 4, SINTEF, Switzerland.

Castorph, D., Kollera, M., and Waas, P. 1999, *Brennwert und Heizwert* (The High and Low Heating Values), Technical report, Fachhochschule Munchen, FB 03, Dachauer Strae 98 b, 80335 Munchen, http://www.fm.fh-muenchen.de/labore/waas/skripten/kap11.pdf.

Eilers, J., Posthuma, S. A., and Sie, S. T. 1990, The Shell middle distillate synthesis process, *Catalysis Letters* v. 7, no. 1 4, p. 253 269.

Gutierrez, Juan Pablo Sullivan, T. B. and Geller, G. J. 2006, *Turning ngcc into igcc: Cycle Retrofitting Issues*, in ASME Power Conference, Atlanta.

Gyftopoulos, E. P. and Beretta, G. P. 2005, *Thermodynamics Foundations and Applications*, Dover Publications, Inc., New York.

Hamelinck, C. N. 2004, *Ph.D. thesis*, Utrecht University, Faculteit Scheikunde.

Hiete, M. and Berner, U. 2001,Calculation of global carbon dioxide emissions: Review of emission factors and a new approach taking fuel quality into consideration, *Global Biogeochemical Cycles* v. 15, no. 1, p. 169 182.

Hing, B. D. and Slatick, E. R. 2005,*Carbon Dioxide Emission Factors for Coal*, Quarterly Coal Report DOE/EIA-0121(94/Q1), Energy Information Administration, Washington, DC.

Johnston, R. P. 2006,*Evaluation of the effect of firing temperature, cycle, engine configuration, components and bottoming cycle on the overall thermal efficiency of an indirectly coal-fired gas turbine based power plant*, in ASME Power Conference, Atlanta.

Mcmanus, M., Boyce, D., and Baumgartner, R. 2007,*Integrated technologies that enhance power plant operating flexibility*, in Power-Gen International, New Orleans.

Sheehan, J., Camobreco, V., Duffield, J., Graboski, M., and Shapouri, H. 1998,*Life Cycle Inventory of Biodiesel and Petroleum Diesel for Use in an Urban Bus*, Final Report NREL/SR-580-24089, National Renewable Energy Laboratory, Golden, Colorado 80401, www.nrel.gov/docs/legosti/fy98/24089.pdf.

Speight, J. G. (ed.) 1990, *Fuel Science and Technology Handbook*, Chapt. Petroleum, composition and properties, pp 71 121, Marcel Dekker, New York.

Steynberg, A. P. and Nel, H. G. 2004, Clean coal conversion options using Fischer-Tropsch technology, *Fuel* v. 83, no. 6, p. 765 770.

Stiegel, G. J. 2006, *Gasification Technologies Advanced Technology Options for FutureGen*, Presentation National Energy Technology Laboratory, www.netl.doe.gov/technologies/- coalpower/gasification/pubs/pdf/Gasification-March%2003%202006.pdf.

Whyte, A. V. (ed.) 1995, *Building a new South Africa: Environment, Reconstruction, and Develop- ment*, Vol. 4, International Development Research

Chapter 4

A Global Coal Production Forecast with Multi-Hubbert Cycle Analysis

4.1 Abstract

Based on economic and policy considerations that appear to be unconstrained by geophysics, the Intergovernmental Panel on Climate Change (IPCC) generated forty carbon production and emissions scenarios. In this paper, we develop a base-case scenario for global coal production based on the physical multi-cycle Hubbert analysis of historical production data. Areas with large resources but little production history, such as Alaska and the Russian Far East, are treated as sensitivities on top of this base case, producing an additional 125 Gt of coal. The value of this approach is that it provides a reality check on the magnitude of carbon emissions in a business-as-usual (BAU) scenario. The resulting base-case is significantly below 36 of the 40 carbon emission scenarios from the IPCC. The global peak of coal production from existing coalfields is predicted to occur close to the year 2011. The peak coal production rate is 160 EJ/y, and the peak carbon emissions from coal burning are 4.0 Gt C (15 Gt CO_2) per year. After 2011, the production rates of coal and CO_2 decline, reaching 1990 levels by the year 2037, and reaching 50% of the peak value in the year 2047. It is unlikely that future mines will reverse the trend predicted in this BAU scenario.

4.2 Introduction

A quick check of press reports on July 8, 2009, yielded the following three stories:

> (INDIA) Coal shortage is set to hit Nalco's aluminium production this year. A 110 MW unit of Nalco's captive power plant was shut down this week due to a shortage of coal. The drop in power generation has affected aluminium production, prompting company officials to discuss the coal supply issue with MCL (Mahanadi Coalfields

> Limited) authorities.[1]
>
> (AUSTRALIA) Coal exports from Australia's Newcastle port, the world's largest coal export terminal, rose 9.5 percent in the latest week, while the number of vessels queuing off the port rose to the highest in 18 months. Trade sources said on Wednesday ship queues had risen for a second week due to unplanned maintenance at the port and as wet weather slowed production at some mines leaving some vessels short of cargo. Exports from the eastern coast port, which ships mostly thermal coal used in power generation, rose to 1.85 million tonnes in the week to July 6, port data showed. Ship queues stood at 49 as of Tuesday, according to data from the Web site of the Hunter Valley Coal Chain Logistics Team (HVCCLT), which coordinates coal movements from mines to the port. Of the 49 vessels waiting to load coal, 13 had coal availability issues while an additional seven did not have coal available when they arrived, HVCCLT said. The number of coal ship arrivals, a key indicator of demand, also rose by four to 24, while waiting time for vessels scheduled to load coal fell to 11.7 days.[2]
>
> (SOUTH AFRICA) Coal volumes railed to South Africa's Richards Bay Coal Terminal are continuing to fall far short of the corridor's nameplate yearly capacity of 70 million tonnes, coming in at closer to an annualized 60 million tonnes. Mr Chris Wells acting CEO of Transnet said that South Africa will do well to achieve volumes of between 64 million tonnes and 65 million tonnes for the year as a whole. At the start of its 2009 financial year in April, the State-owned group's rail division said it had budgeted to handle 69-million tons up until March 31, 2010, but undersupply from the mines had all but put paid to that ambition. Rail volumes last year fell to a very disappointing 61.9 million tonnes, capping a three year trend of underperformance, with volumes having fallen consistently since 2006, when 68.8 million tons was railed. There has been a concerted Transnet effort to improve rail's performance since September, but now the mines are running short of supply. Both sides need to reach a deal that optimizes South Africa's foreign exchange potential.[3]

Is it possible that global demand for coal is outstripping supply? Is production in some of the major coal-exporting countries falling? Can it be that peak of global coal production is near?

Our answer to these three questions is yes.

Faced with the imminent global peaks of oil and coal production, economists, scientists, and policy makers have been taking radically different positions. One prominent group claims that there can be no peak of production because society's ability to find new fossil fuel deposits and exploit them is practically infinite, see, e.g., Anonymous [2007].[4] Besides, some add, many of the oil and gas reservoirs are recharged with hydrocarbons

[1] *ANGUL (Orissa): Coal crisis hits Nalco's aluminium production*, 2009-07-08 14:50:00, Commodity Online, www.commodityonline.com.

[2] *Australia Newcastle coal exports up 9.5 pct*, 2009-07-08, 10:59:02 AM, PERTH, Reuters.

[3] *RBCT coal exports to remain below capacity in 2009*, steelguru.com, 2009-07-07 (from Miningweekly.com).

[4] In the 2008 version, however, the perpetual growth predictions of 2007 were toned down, see www.worldenergyoutlook.org/docs/weo2008/WEO20084_es_english.pdf.

in real time, e.g. Holland et al. [1980]. This group sees an uninterrupted increase in the demand and production of fossil fuels in the foreseeable future, depicted in **Figure 4.1** from Anonymous [2007].

As a reaction to such claims, a powerful social movement has sprung up to demonize fossil fuels as the root of all pain and suffering on the planet. A central belief in this camp is that fossil fuels cause most if not all of the recent climate change.

Remarkably, both sides apparently assume an infinite capacity of the Earth to yield fossil fuels at arbitrary rates. They only differ when it comes to dealing with the effects of this ever-increasing production. In short, the action and reaction described here are merely two aspects of the same dialectic process described by Chalybäus Chalybäus [1837] beautifully, see Section 4.6.

An opposite view was best summarized by William Stanley Jevons Jevons [1866]:

> The expression "exhaustion of our coal mines," states the subject in the briefest form, but is sure to convey erroneous notions to those who do not reflect upon the long series of changes in our industrial condition which must result from the gradual deepening of our coal mines and the increased price of fuel. Many persons perhaps entertain a vague notion that some day our coal seams will be found emptied to the bottom, and swept clean like a coal-cellar.

Those who adhere to this line of thinking lump coal, petroleum, and natural gas together, alleging that the cellars filled with these respective resources will be emptied soon, so they should be shut tight. Holders of this view, make parallel demands to abruptly curtail fossil fuel consumption ("energy security") and emissions ("global warming"). These demands lack consistency, for one cannot curtail that which one does not have.

An old Jew in Galicia once made an observation: "When someone is honestly 55% right, that's very good and there's no use wrangling. And if someone is 60% right, it's wonderful, it's great luck, and let them thank God. But what's to be said about 75% right? Wise people say this is suspicious. Well, and what about 100% right? Whoever says he's 100% right is a fanatic, a thug, and the worst kind of rascal." Miłosz [1981]. Which brings us to the last group of scientists, who do not mind being 55% right and generally disparaged. These people conceive of a spherical Earth with finite resources (M. King Hubbert and Paul R. Ehrlich) and interconnected fragile ecosystems (James Lovelock and Vaclav Smil). They also quantify how woefully inadequate and nonphysical the governing economic models are in addressing the society's future and present needs (Nicolas Georgescu-Roegen, Herman Daly, Charles Hall, and Philip Mirowski).

The authors intend to stay within the wise Jew's estimate of maximum tolerable correctness[5], and set out to estimate the future of coal production in the world through the actual production data and Central Limit Theorem. We build on the three earlier papers Patzek [2008]; Croft and Patzek [2009]; Patzek and Croft [2009], and use the coal production data from the Supplemental Materials to Mohr and Evans Mohr and Evans [2009], who have gathered and made public a global data set that agrees with our

[5]This paper is falsifiable in parts and as a whole. If we are wrong, stricter controls on the increase of coal production and use will have to be applied. If we are right, major restructuring and shrinking of the global economy will follow. Because the second alternative is so much more far-reaching, prudent policy makers ought to perhaps consider it.

earlier sources for China and USA. However, we have not been able to replicate several of the coal reserves estimates published by Mohr and Evans Mohr and Evans [2009]; the discrepancies are listed in 4.13.

The base-case global coal production forecast in this paper is compared with forty IPCC scenarios in the SRES Report Nakicenovic et al. [2000]. Most of the IPCC scenario writers accepted the common myth of 200 – 400 years of coal supply, and now their "eternal" (100 years plus) growth of carbon dioxide emissions in turn is a part of the commonly accepted social myth. It seems, therefore, that the present attempt to inject some geophysics into the debate will be an uphill battle.

4.3 A Multi Hubbert-Cycle Approach

Ever since M. King Hubbert's seminal work Hubbert [1949, 1956, 1962, 1969, 1971], there has been an ongoing controversy about the very existence of "Hubbert cycles," and their ability to predict the future rate of mining an earth resource. This controversy seems to have been more ideological than scientific. Emergence of Hubbert cycles that approximate time evolution of the total production rates from populations of coal mines, oil reservoirs, ore deposits, etc. was put to rest in the notes to a course offered at Berkeley by Patzek Patzek [2007a]. These arguments are summarized here as **Appendices 4.9** and **4.10**.

The emergence of Hubbert cycles is assured by the Central Limit Theorem[6], provided that the coal mines in the population are numerous, independent of each other, and there are few artificial regulatory constraints on mine production. The total coal production in a country or worldwide can be treated as a sum of many independent random variables that in turn describe production from individual coalfields and/or mines. By the Central Limit Theorem, the distribution of the sum tends to be normal or Gaussian. Thus, the fundamental Hubbert curve or "cycle" is approximately symmetric and bell-shaped. The story does not end there, however. Expansions of existing mines or additions of new mines result in an oscillatory, damped deviation of true production from the fundamental Hubbert cycle. This deviation can be modeled with a Fourier series or, simply, with a few secondary Hubbert curves that capture depletion of these expansions or additions.

The authors have maintained that coal production data series are independent of reserve numbers, and tell a very different story Croft and Patzek [2009]; Patzek and Croft [2009]. One other way checking the maturity of underground coal mining is to look at mine depth, but that is a more qualitative approach. That said, in China 2 out of 3 approaches suggest a near-term peak in coal production. Coal-producing areas have two sets of numbers: (1) reserves at existing mines that are supported by engineering studies and (2) proved coal reserves that are a much broader category than proven oil reserves. Over time, these two sets of numbers trend in opposite directions. For example, in Illinois, the number two proven coal reserve holder in the U.S., coal production has declined by almost half from what it was twenty years ago. By playing such numbers

[6]Proposed by Abraham de Moivre who, in an article published in 1733, used the normal distribution to approximate the distribution of the number of heads resulting from many tosses of a fair coin. This finding was far ahead of its time, and was nearly forgotten until Pierre-Simon Laplace rescued it from obscurity in his *Théorie Analytique des Probabilités* published in 1812.

games governments worldwide get the big reserves they want, while mine operators do not promise more than they can deliver. It is clever politics, but it leaves us analysts with the question of how to reconcile two dramatically different sets of reserve estimates. We do not put much stock in the proved reserves, but the existing mine numbers are good and should always be below (or equal to) the Hubbert curve approximations. The proved reserve numbers are the source of the myth of a 200 – 400 year supply of coal worldwide at the rate of production of roughly 6.5 billion tons per year.

There are distinct advantages to using the Hubbert curves as models of large populations of mines:

1. A single Hubbert curve is the natural approximating function for the time evolution of the total coal production rate from each fixed population of coalfields.

2. New curves can be added to describe mine expansions in any of the coalfields or production from new coalfields.

3. The Hubbert curves are based on coal production, and not on ill-defined and subjective coal "reserves."

4. Historical production trends reflect the prevailing economics prior to the time of production.

The advantages of Hubbert curves in large-scale models of resource production make them a valuable tool in policy-making.

At a given time, a collection of Hubbert curves that fully describes the existing populations of coal mines in the known coalfields carries no information about the possible future mine populations in new coalfields. Thus, the Hubbert cycle predictions almost always underpredict the true future production rate of a resource. The underprediction of production in immature coal provinces, such as Alaska, Kazakhstan, East Siberia, Australia and Mongolia, may be substantial, but it may take decades to produce very large quantities of coal from future mines. In the meantime, production from the existing mine populations may decline so much that no future production increases can reverse the current global trend. Because the world is only 2 – 5 years away from the peak of coal production, numerous major new mines would have to be brought online within half a decade to arrest the predicted decline of global coal production. This may be difficult because of the remoteness of Mongolia, or environmental and water supply concerns in India, Australia, and the United States.

To convert the mass of coal of different ranks to the corresponding higher heating values (HHV), the following averages of the HHV are used: 30 MJ/kg of anthracite, 27 MJ/kg of bituminous coal, 21 MJ/kg of subbituminous coal, and 15 MJ/kg of lignite. These averages are then multiplied by the annual production of coal reported by rank. The mass of all coals is converted to the corresponding carbon dioxide emissions with a procedure described in **Appendix 4.11**. The nearly-constant ratio of carbon emissions to energy content of coal is based on the results of exhaustive sampling of U.S. coals by Hing and Slatick [1994]. This result is surprisingly consistent across U.S. coals, regardless of locality or geologic age. The authors contend that the average carbon emissions values by rank from this large and diverse U.S. dataset should be representative of global coals.

The best fits (or "matches") of historic coal production are carried out by minimizing the sum of squares of the deviations between the sum of Hubbert curves and the data. As the figures below demonstrate, these matches can be quite accurate. The "linearized Hubbert cycle" approach, i.e., a linear fit of the ratio of coal production rate divided by cumulative coal production versus the cumulative coal production is avoided. This fit is unstable and often does not intercept zero to yield an estimate of ultimate coal recovery. Where stable estimates exist, the multi-cycle fits presented here yield values similar to those published by Mohr and Evans Mohr and Evans [2009]. Otherwise, there can be significant differences between our ultimate coal recoveries and those by Mohr and Evans.

4.4 Global Coal Production and CO_2 Emissions

The key coal-producing countries are discussed in the Online Supporting Material to this paper, temporarily referred to in the manuscript as **Appendix 4.13**. The ultimate coal production, peak production rate, ultimate CO_2 emissions and peak emissions rate by country are listed in **Table 4.1**. The Hubbert cycles represent mining districts (populations of mines), rather than individual mines. In the case of Mongolia, the 2105 peak production will come from mines that were not producing in 2005 – 2007, but these future mines are assumed to follow the early production trend. In most other cases, the mining districts operated in earnest in 2005 – 2007, and their predicted future development is consistent with historical records.

The findings of this report are illustrated in **Figures 4.2** – **4.6** and summarized here:

1. The higher heating value (HHV) of global coal production is likely to peak in the year 2011 at 160 exajoules per year, see Figure 4.2.

2. The global CO_2 emissions from coal will also peak in 2011 at 15 Gt/year, see Figure 4.3.

3. The estimated CO_2 emissions from global coal production will decrease by 50 percent by the year 2050, see Figure 4.3.

4. Between the years 2011 and 2050, the average rate of decline of CO_2 emissions from the peak is 2 % per year, and this decline increases to 4% per year thereafter, see Figure 4.6.

5. It may make sense to have carbon capture and sequestration (CCS) to alleviate the highest CO_2 emissions between now and the year 2020 or so.

6. Given the imminence of the global coal production peak, a better alternative would be to gradually replace the existing electrical power generation blocks with the new ultra supercritical steam blocks (steam temperatures of 620 – 700^0C, and pressures of 220 – 250 bars), whose electrical efficiency is close to 50%, compared with the $\sim$35% efficiency currently realized. This replacement might ultimately lower current CO_2 emissions from coal-fired power stations by $15/35 \approx 40\%$ for the same amount of electricity.

4.5 Error Analysis

As shown in Appendix 4.9, matching cumulative production of a distributed resource with multiple Hubbert curves captures most of the variance of data. A typical example for the U.S. coal production is shown in **Figure 4.7**. The statistics of linear fits of cumulative coal production by all major producers are summarized in **Table 4.2**. It is seen that the mean square errors of the fits are negligible and the R^2 statistics are close 1.

4.6 The IPCC Coal Production Scenarios

Here is a brief summary of the process used by the Intergovernmental Panel on Climate Change (IPCC) to arrive at their fossil fuel production and greenhouse gas emissions scenarios Nakicenovic et al. [2000]:

> The Special Report on Emissions Scenarios (SRES) writing team included more than 50 members from 18 countries who represent a broad range of scientific disciplines, regional backgrounds, and non-governmental organizations. The team, led by Nebojsa Nakicenovic of the International Institute for Applied Systems Analysis (IIASA) in Austria, included representatives of six scenario modeling groups and lead authors from all three earlier IPCC scenario activities - the 1990 and 1992 scenarios and the 1994 scenario evaluation. The SRES preparation included six major steps:
>
> - analysis of existing scenarios in the literature;
> - analysis of major scenario characteristics, driving forces, and their relationships;
> - formulation of four narrative scenario "storylines" to describe alternative futures;
> - quantification of each storyline using a variety of modeling approaches;
> - an "open" review process of the resultant emission scenarios and their assumptions; and
> - three revisions of the scenarios and the report subsequent to the open review process, i.e., the formal IPCC Expert Review and the final combined IPCC Expert and Government Review.
>
> As required by the Terms of Reference, the SRES preparation process was open with no single "official" model and no exclusive "expert teams." To this end, in 1997 the IPCC advertised in relevant scientific journals and other publications to solicit wide participation in the process. A web site documenting the SRES process and intermediate results was created to facilitate outside input. Members of the writing team also published much of their background research in the peer-reviewed literature and on web sites.

Our best production-based predictions of coal energy and carbon emissions produced worldwide are compared with the 40 IPCC scenarios released online.[7] The comparison is shown in **Figures 4.8** and **4.9**. Between the years 1990 and 2011 all but two of the IPCC scenarios are at or below the actual world coal production and emissions. In contrast, after 2011, most of the IPCC predictions increase unrealistically in a variety of exponential ways. Thirty six out of 40 of these scenarios deviate significantly upwards from our base-case, up to a factor of 100; see **Figure 4.10**. In particular, 2 IPCC scenarios peak in the year 1990, 3 in 2020, 3 in 2030, 3 in 2040, 13 in 2050, while in the 16 remaining scenarios coal production simply grows exponentially until the year 2100. Because IPCC did not rank its forty scenarios on purpose, the 16 nonphysical outliers, and 4 other scenarios,[8] were given *de facto* a weight equal to the more realistic lowest scenarios. The policy makers tend to focus on the most extreme outcomes, and the outliers have gained prominence as inputs to the subsequent climate models. The real problem 40 years from 2009 will be an insufficient supply of fossil energy, not its overabundance, as the IPCC economists would have it.

4.7 Sensitivity Analysis and Future Work

Because this study is a multi-cyclic Hubbert analysis, the possibility of future cycles that are not reflected in the historical data must be considered. The base-case in this study includes all coal-producing regions with any significant production history. New mines in existing coalfields should be part of existing Hubbert cycles and thus are part of the base-case. New cycles could occur if a technological breakthrough allowed mining of coal from very thin seams or at much greater depths, or if non-producing coal districts become important producers. Since we do not extract all of any mineral resource, the technology argument will always be there. Looking at recent trends, improvements in coal mining technology have increased the proportion of coal that is extracted, but safety considerations have limited depth. Gradual improvements in recovery percentage should fall within the base-case; only a technology that allows access to a new population of coal seams should create a new fundamental Hubbert cycle, such as in unconventional natural gas recovery in the U.S. Patzek [2008].

Unlike oil or natural gas, discovery of new fields plays only a minor role in coal resources. Of the major coal districts described in [Appendix 4.13], only one (Lublin, in Poland) was discovered in the last 50 years. For this reason, the authors contend that the most important quantifiable sensitivities are known, undeveloped resources. Because Alaska's North Slope and Siberia have very large, known, undeveloped coal reserves and because climate change increases access to at least some of these resources, these two areas are likely to dominate any sensitivity analysis of non-producing districts.

Siberia is divided into three political regions; West Siberia, East Siberia and Russian Far East. West Siberia includes the Kuzbass region, described in [Appendix 4.13], which

[7] In Appendix SRES Version 1.1, published at www.grida.no/publications/other/ipcc_sr/?src=/-climate/ipcc/ -emission/101.htm, and accessed on July 4, 2009.

[8] Twenty out of the 40 IPCC scenarios result in carbon emissions in the year 2100 that are 20 – 100 times the base-case here, see Figure 4.10.

is Russia's most important coal-producing region. East Siberia includes the important Kansk-Achinsk soft coal region. Both of these areas have established production and are included in the base-case. The coal resources of the Lena River Valley and part of the Tunguska Basin lie within Russian Far East. According to Takaishvili and Sokolov [2006], the Russian Far East contains 1244 Gt of coal resources, which is 28% of the coal resources of the Russian Federation. The same authors suggest that it would be reasonable to project the ratio of reserves to resources of the entire Russian Federation onto the Russian Far East. For the purpose of this analysis, we will go one step further and project the ratio of reserves to resources from the remainder of the Russian Federation on the Russian Far East. This results in an estimate of 70 Gt for the Russian Far East. While there is some production in this area already, we assume an entirely new Hubbert cycle with an area of 70 Gt and a peak in the year 2100 at the rate of 1240 million tons of coal per year. Applying the ratio of hard coal to soft coal in the A+B+C1 reserves to our 70 Gt estimate gives 28 Gt of hard coal and 42 Gt of soft coal. For the purpose of carbon calculations, it is assumed that the soft coal is sub-bituminous and the hard coal is bituminous in this case.

The strongest case for a major new coal Hubbert cycle anywhere in the world lies within the United States. The Cretaceous Nanushak Group of Alaska's National Petroleum Reserve (NPR-A) is estimated to contain resources of 1.49 trillion short tons (1350 Gt) of bituminous coal and 1.24 trillion short tons (1120 Gt) of sub-bituminous coal Sable and Stricker [1987]. The reason that the North Slope coal must be a sensitivity case is there is no recent production history, but this resource could represent up to 10% of the economically recoverable coal in the world Thomas [2002]. Alaska's National Petroleum Reserve area is underlain by permafrost, but so is about 85 % of Russia's Pechora Basin Walker [1993], which has been an important coal-producing area for decades. The Alaska North Slope coal is low in ash and sulfur content and low in content of elements of environmental concern, such as As, Be, Hg, Mo, Sb and Se Affolter and Stricker [1987].

Alaska's coal resources may be undeveloped, but they are not newly-discovered; they were mined for use by whaling ships as early as 1879 Flores et al. [2004]. Recent exploration activity has been concentrated in three areas west of the NPR-A, near the Chukchi Sea coast: Cape Beaufort, Deadfall Syncline and Kukpowruk River. Coal beds outcrop around the rims of these three synclines, and extrapolating them across gives total hypothetical resources of 7.9 billion short tons (7.2 Gt) of coal averaging 28 – 32 MJ/kg (12,300 to 13,800 btu per pound) for the three synclines Anonymous [1993]. This area is currently being explored by a joint venture of BHP-Billiton and the Arctic Slope Regional Corporation that drilled 29 coreholes in the coal fields north of Cape Lisburne in 2007-2008, but the corehole results are confidential Szumigala and Hughes [2008]; Szumigala et al. [2009].

In their abstract, Sable and Stricker Sable and Stricker [1987] state that the NPR-A may contain as much as one-third of the United States coal resource potential. Since most of the coal is high-quality bituminous, 55 Gt would be a coal resource about half the size of that of the entire U.S. lower-48. As the sensitivity case here, we assume that 55 Gt of the Alaskan coal is produced starting immediately, and the peak of production is in the year 2100. The results of the Alaska sensitivity case are shown in **Figures 4.35**

– **4.38**.

Figure 4.11 shows the coal production base-case with these two additional sensitivity cycles superimposed. Note that production of an additional 125 Gt of coal slows down, but cannot reverse the decline of global CO_2 emissions from coal.

The authors have chosen to include Mongolia in the base-case, but admit that a region with such limited production history represents a test of the Hubbert approach. The question in this case is whether the hard coal mines of the South Gobi Desert represent a separate Hubbert cycle from the soft coal mines of northern Mongolia and, if so, how well the former cycle can be modeled from only four years of production history.

Future work should include a similar analysis of liquid petroleum and natural gas. As long as the heavy oil deposits of Canada and Venezuela are treated as sensitivities, a liquid petroleum base-case can be developed with the Hubbert approach. In the case of natural gas, a major challenge will be how to model unconventional gas production from shales, which has been shown to be significant in the USA, but has no production history elsewhere.

4.8 Summary and Conclusions

Paraphrasing the words of Chalybäus Chalybäus [1837]: "We have discovered here, in the individual as in the general, a law at work, a blind internal necessity, which, however, appears as necessity only because we look at it from without and as objective appearance (phenomenon)." That "objective phenomenon" is the fundamental behavior of large populations of coal mines worldwide and the emerging peak of coal production and CO_2 emissions.

The most important conclusion of this paper is that the peak of global coal production from the existing coalfields is imminent, and coal production from these areas will fall by 50 percent in the next 40 years. The CO_2 emissions from burning this coal will also decline by 50 percent. Thus, current focus on carbon capture and geological sequestration may be misplaced. Instead, the global community should be devoting its attention to conservation and increasing efficiency of electrical power generation from coal.

The current paradigms of a highly-integrated global economy and seamless resource substitution will fail in a severely energy-constrained world. A new territory is being charted by all, thus close attention must be paid to what the physical world reveals about energy conservation and production.

Soft coal has a problem akin to that of electric car batteries: it takes a lot of its own energy to move it. Energy content per unit mass of mine-run lignite is about a third that of anthracite. This doesn't matter in the case of lignite production in Poland or Germany because the markets are local power plants. In the U.S., soft coal can be shipped from Powder River Basin because markets are not that far away and the trip is largely downhill (Gillette, Wyoming, is 4,800 feet above sea level). Soft coal from Xinjiang has hills to traverse in order to get to markets in China, so it is being developed slowly. Inner Mongolia has better coal, the path from there to markets is downhill and there is large rail capacity from neighboring Shanxi. Siberia is flat and vast so, while hard coal from Kuzbass is shipped by rail, soft coal from Kansk-Achinsk is burned locally in power plants and delivered to markets as electricity.

Carbon dioxide captured from industrial operations can drive new enhanced oil recovery projects and might be injected into coal seams to displace methane. In view of the imminent difficulties with the coal supply, a lasting increase of natural gas production in the United States is of utmost importance. We repeat again that immediate upgrades of the *existing* electrical coal-fired power stations to new, ultra supercritical steam turbines that deliver electrical efficiencies of ca. 50 percent are urgently needed. The authors do *not* suggest that new coal-fired power plants be constructed, unless they are to replace less-efficient existing coal-fired plants.[9] The goal should be to increase efficiency rather than capacity.

Scarce coal will make it difficult to justify the energy penalty of CCS Apps [2006]; reforestation projects are more useful because they remove CO_2 quickly from the atmosphere, where concentrations will increase for several years after peak carbon emissions.[10] Destruction of tropical forest for biofuel production adds carbon emissions near the peak Patzek [2007b], maximizing damage. Emphasis of a thoughtful greenhouse gas mitigation policy should be on maximizing sequestration rate in the years 2009 – 2040. Cap-and-trade policies for carbon dioxide emissions will not be effective if the cap is set near peak emission levels, and may allow the natural decline of coal production to effectively subsidize a lack of effort on the part of energy industry.

Acknowledgements

Greg Croft has been supported for 2 years by the Jane Lewis Fellowship from U.C. Berkeley. We would like to thank Drs. Mohr and Evans for publishing their coal database. We have received critical feedback from Drs. Larry Lake, John Butler, William Spencer, and Sheridan Titman of UT Austin; Richard Norgaard, John Newman and John Prausnitz of UC Berkeley; Sally Benson of Stanford; and Mr. Lucas Patzek, a Ph.D. student at Washington State. Most of their criticisms and suggestions have been incorporated and significantly benefited the paper. We would like to extend special thanks to Dr. Lake for his critique of the initial discussion of emergence of Hubbert cycles. Lucas has edited this paper considerably. Upon reading the paper, Mr. Robert Bryce of Austin has pointed out the remarkable Excel spreadsheet and presentation, *Hubbert's Peak, the Coal Question, and Climate Change*, by Dr. David Rutledge of Caltech. Most of Dr. Rutledge's calculations and conclusions related to coal are very similar to those in this paper. The remaining errors and omissions are the sole responsibility of the authors.

[9] "Around 920 U.S. coal plants – 78 percent of the total – are small (generating less than half a gigawatt), antiquated and horrendously inefficient. Their average age is 45 years, with many over 75. They tend to be located amidst dense populations and in poor neighborhoods to lethal effect. These ancient plants burn 20 percent more coal per megawatt hour than modern large coal units and are 60 to 75 per cent less fuel-efficient than combined cycle gas plants. They account for only 21 per cent of America's electric power but almost half the sector's emissions." *How to End America's Deadly Coal Addiction*, by Robert F. Kennedy, Jr. Published in the Financial Times, July 19, 2009.

[10] The mean residence time of CO_2 in the atmosphere seems to be 20 years Levin and Hesshaimer [2000].

4.9 Why Do Hubbert Cycles Exist?

All quantities whose distributions are considered here are dimensionless.

Soon, in will become obvious that Hubbert cycles are theoretically related to the normal distribution and the error function. However, it is much easier to approximate them with the logistic S-shaped curve and its derivative. The logistic growth curve of human population was first proposed by the Belgian mathematician Pierre François Verhulst after he had read Thomas Malthus' second, expanded edition of the *Essay on the Principle of Population or, a View of its Past and Present Effects on Human Happiness; with an enquiry into our Prospects respecting the Future Removal or Mitigation of the Evils which it occasions*, published in 1803. Malthus was a rare scoundrel Chase [1980], but he correctly predicted the ultimate predicament of humanity: too many people competing for insufficient resources on the finite Earth. He also deeply influenced the thinking of David Ricardo, Karl Marx, Charles Darwin, and many other famous economists and scientists, M. King Hubbert being one of them.

4.9.1 Logistic Growth

The cumulative mass production or yield in logistic growth depends on time as follows Verhulst [1838]:

$$m(t) = \frac{m_{\max}}{1 + e^{-r(t-t^*)}} \tag{4.1}$$

where $m_{\max}$ is the ultimate production or carrying capacity, r is the fractional rate of growth; t is time, and t^* is the time of maximum production rate:

$$t^* = \frac{1}{r} \ln\left(\frac{m_{\max}}{m(0)} - 1\right) \tag{4.2}$$

Note that $m(0) > 0$.

The production rate can be obtained by differentiation of the cumulative production $m(t)$:

$$\dot{m} = \frac{dm}{dt} = \frac{2\dot{m}^*}{1 + \cosh[r(t - t^*)]} \tag{4.3}$$

where $\dot{m}^*$ is the peak production rate.

It may be easily shown that

$$m_{\max} = 4\dot{m}^*/r \tag{4.4}$$

4.9.2 Logistic vs. Gaussian Distribution

The logistic equation (4.1) and its derivative, Eq. (4.2), are close (*but not identical*) to the Gaussian distribution centered at t^*, and having the standard deviation, σ, related to r as follows:

$$\sigma \approx \frac{1.76275}{r\sqrt{2\ln 2}} \qquad \text{Matched half-widths} \tag{4.5}$$

or, better,

$$\sigma \approx \frac{4}{r\sqrt{2\pi}} \qquad \text{Matched peaks} \tag{4.6}$$

See **Appendix 4.10** for the derivations.

The cumulative logistic growth and its rate then approximate the following equations, theoretically more appropriate for the Hubbert curve models:

$$m(t) \approx \frac{\mathbf{m}_{\max}}{\mathbf{2}} \left[1 + \operatorname{erf}\left((t - t^*)/\sqrt{2}\sigma\right)\right] \tag{4.7}$$

where $\operatorname{erf}(x) = 2/\sqrt{\pi} \int_0^x e^{-t^2} dt$ is the error function

$$\dot{m} = \mathbf{m}_{\max} \frac{1}{\sqrt{2\pi}\sigma} \exp\left[-\frac{(t - t^*)^2}{2\sigma^2}\right] \tag{4.8}$$

The two coefficients in bold rescale the normal distribution to the actual production history.

4.9.3 Oilfield Examples

An argument advanced against Hubbert has been that the depletion histories of oil reservoirs are distinctly skewed towards longer times. This is true separately for the rate of oil production in every field in a sample, but not so for the sum of these rates. The first example from the Middle East is not perfect because of the complications with data reporting and gradual switching from primary recovery to waterflood. We remind the reader that during the time period considered in this paper, the Middle East went through three major wars, oil embargo, and the Iranian revolution. We have decided to use the Middle East example – warts-and-all – to illustrate the all too real difficulties in predicting the future.

Here we illustrate the emergence of a Hubbert curve with production data from 23 lower Jurassic limestone oilfields in the Middle East, reported in Anonymous [1982], Appendix A. These are: Awali, Damman, Abu Hadriyah, Abqaiq, Qatif, Ghawar, Fadhili, Khursaniyah, Khurais, Harmaliyah, Manifa, Abu Safah, Berri, Sassan, Rostam, Rakhsh, Umm Shaif, Abu al Bakoosh, Dukhan, Idd el Shargi, Maydan Mahzan, Bul Hanine and El Bunduq. The public reporting of most of individual field production stopped by 1982, but the total continued to be reported. We have excluded Ghawar, the largest oilfield on the Earth, because it dominates production from all other fields. However, including Ghawar in the analysis leads to the same conclusions, with the production peak in 1977.

The available historical production of the 23 fields included in the analysis peaked in 1974, and waterfloods were implemented in some of them, resulting in a subsequent total production increase. Abqaiq was waterflooded starting in the late fifties and Ghawar's three northern culminations were waterflooded starting in the late sixties. Other big waterflood expansions occurred at the two southern culminations of Ghawar (1996), Abu Safah (2004), Qatif (2004), Khursaniyah (2008), and Khurais (2009). The data through 1982 are shown in **Figure 4.12**. Beyond 1982, all we know is that the total production from several of the fields, including Ghawar, started to increase again due to the waterfloods.

We assert that a Hubbert cycle represents a normal process, see e.g, Ott [1995]; Grinstead and Snell [1998]. Many variables found in nature result from the summing of numerous unrelated components. When the individual components are sufficiently unrelated, the resulting sum tends towards normality as the number of components comprising the sum becomes increasingly large. Two important conditions for a normal process are: (1) the summation of many discrete (or continuous) random variables, and (2) the independence of these random variables. A normal process is also called a random-sum process ($\mathcal{R}-\mathcal{S}$-process).

The Central Limit Theorem of statistics states Grinstead and Snell [1998] that if S_n is the sum of n mutually independent random variables, then the distribution function of S_n is well-approximated by a continuous normal density function, which is given by the formula

$$f(t;\mu,\sigma) = \frac{1}{\sqrt{2\pi}\sigma}\exp\left(\frac{(t-\mu)^2}{2\sigma^2}\right)$$

where μ and σ^2 are the finite mean and variance of the sum. Each variable is sampled at discrete times $t_j, j = 1, 2, \ldots, N$.

> The total *dimensional* production from $n = 22$ oilfields shown in Figure 4.12 should be close to a single Hubbert cycle, described by Eq. (4.8), or its logistic curve approximation, Eq. (4.3).

The fitting of the Hubbert cycle to data is done more stably through the cumulative production shown in **Figure 4.13**, but the total rate of production is also fit well, see **Figure 4.14**.

When the Hubbert curve in Figure 4.13 is plotted versus the actual production data, **Figure 4.15**, it explains 99 percent of the variance of the data. However, the residuals of the best Hubbert fit, defined as the cumulative production data minus the Hubbert fit, are correlated, see **Figure 4.16**.

The power spectrum of the numerical Fast Fourier Transform (FFT) of the residuals reveals two dominant frequencies at 1/23 and 1/32 years^{-1}, see **Figure 4.17**. One may conclude that the characteristic time of oil production from new developments in the same fields is about 27 years. These secondary developments are new random variables, whose sum can be handled with FFT or secondary Hubbert curves, which is the approach chosen in this paper. Either way, importance of the secondary field developments decreases with time, see **Figure 4.18**, and the fundamental Hubbert curve predicts most of oil (or coal or gas) production from a fixed population of deposits.

The multi-Hubbert curve approach in this paper does a good job of capturing the temporary and decaying deviations from the fundamental Hubbert peak, see **Figures 4.19** – **4.20**. Therefore:

> By matching both the cumulative production as well as the rate of production, a multi-Hubbert curve approach may provide a better estimate of the future recovery than a single fundamental Hubbert curve fit of the cumulative

production data. In the particular example of the lower Jurassic limestone fields in the Middle East, the ensuing waterflood projects would have to be matched with a separate Hubbert curve peaking much later. We do not have the field-specific data beyond 1982 to quantify this assertion.

The second example consists of 65 offshore oil fields in Norway, whose production rates are shown in **Figure 4.21**. Out of the tangled spaghetti of individual field production curves, there emerges a picture-perfect normal distribution in **Figure 4.22**. The cumulative production is matched perfectly and the predicted ultimate oil recovery is 26 billion barrels. A two-curve approximation is marginally better, see **Figure 4.23**, but it does not matter. The dominant frequencies of the new field projects or project expansions are about 1/13 and 1/30 years^{-1}.

Norway has been a unique human experiment; it had no wars, revolutions, nor Great Depressions over the time period of the North Sea development. What did vary, and wildly, was the price of oil. That variation apparently had no effect on curtailing oil production and distorting the Hubbert cycle. Mixing Norwegian Sea and North Sea production also was not a problem; these are two different areas, but similar geology and operating conditions caused them to act as a single cycle. The most serious deviation between the oil production and the Hubbert cycle was caused by the very low oil prices between 1995 and 2000.

4.10 Matching the Logistic and Normal Distributions

To approximate the Gaussian distribution (rate) curve,

$$f_1(t;\sigma,t^*,m_{\max}) = m_{\max}\frac{1}{\sqrt{2\pi}\sigma}\ \exp\left[-\frac{(t-t^*)^2}{2\sigma^2}\right] \tag{4.9}$$

with the logistic curve,

$$f_2(t;r,t^*,m_{\max}) = \frac{m_{\max}r}{2}\ \frac{1}{1+\cosh[r(t-t^*)]} \tag{4.10}$$

we will first attempt to match their full widths at 1/2 heights.

For the Gaussian distribution

$$\begin{aligned}
&f_1(t_0;\sigma,t^*,m_{\max}) = \frac{1}{2}f_1(t^*;\sigma,t^*,m_{\max})\\
&\frac{1}{\sqrt{2\pi}\sigma}\exp\left[-\frac{(t_0-t^*)^2}{2\sigma^2}\right] = \frac{1}{2}\ \frac{1}{\sqrt{2\pi}\sigma}\\
&\exp\left[-\frac{(t_0-t^*)^2}{2\sigma^2}\right] = \frac{1}{2}
\end{aligned} \tag{4.11}$$

and

$$\begin{aligned} \frac{(t_0 - t^*)^2}{2\sigma^2} &= \ln 2 \\ t_0 &= \pm\sigma\sqrt{2\ln 2} + t^* \end{aligned} \tag{4.12}$$

The full width at half maximum is therefore

$$2\sigma\sqrt{2\ln 2}$$

for the Gaussian distribution.

For the logistic distribution

$$\begin{aligned} & f_2(t_0; r, t^*, m_{\max}) = \frac{1}{2} f_2(t^*; r, t^*, m_{\max}) \\ & \frac{m_{\max} r}{2} \; \frac{1}{1 + \cosh[r(t_0 - t^*)]} = \frac{m_{\max} r}{8} \\ & \frac{1}{1 + \cosh[r(t_0 - t^*)]} = \frac{1}{4} \\ & \cosh[r(t_0 - t^*)] = 3 \end{aligned} \tag{4.13}$$

An approximate solution to this transcendental equation is $r(t_0 - t^*) \approx 1.76275$. The full width at half maximum is therefore

$$\frac{3.5255}{r}$$

for the logistic distribution.

To match the respective full widths, we require that

$$\begin{aligned} 2\sigma\sqrt{2\ln 2} &= \frac{3.5255}{r} \\ \sigma &= \frac{1.76275}{r\sqrt{2\ln 2}} \end{aligned} \tag{4.14}$$

To match the peaks, we require that

$$\begin{aligned} \frac{m_{max}}{\sqrt{2\pi}\sigma} &= \frac{r m_{max}}{4} \\ \sigma &= \frac{4}{r\sqrt{2\pi}} \end{aligned} \tag{4.15}$$

Since heights of the two distributions are somewhat different for equal half-widths (the t_0 in Eq. $(4.13)_4$ is in fact different than that in Eq. $(4.11)_3$), the half-width match is approximate, see **Figure 4.24**. The peak matching is also approximate, see **Figure 4.25**, but seems to be better.

4.11 Heating Values and CO_2 Emissions for Coal

The coal heating value data, expressed as the higher heating values (HHV) of coals of different ranks, are listed in **Tables 4.3** and **4.4**. The weighted averages of the data rounded off to 2 significant digits are shown in column 1 of **Table 4.5**.

The average HHVs of coals of different ranks and the corresponding the specific CO_2 emissions from these coals, are listed in Table 4.5.

It turns out that the mass of CO_2 emitted by burning a coal correlates very well with the ratio of the coal's HHV to the enthalpy of oxidation of the solid carbon, 32.8 MJ/kg, Table 5-76 in Lide [1994], adjusted upwards for the heating effects of hydrogen in the coal:

$$\frac{\text{kg CO}_2}{\text{kg coal}} \approx \frac{\text{HHV of coal}}{32.8 \times 1.22} \tag{4.16}$$

The measured CO_2 emissions from coals of different ranks, reported in Hong and Slatick [1994] and listed in Table 4.5, are well-approximated by Eq. (4.16), see **Figure 4.26**. Equation (4.16) allows for an alternative conversion of coal mass to CO_2 emissions.

Bibliography

R. H. Affolter, G. D. Stricker, Alaska Coal Geology, vol. 50, special publication Geochemistry of Coal from the Cretaceous Corwin and Chandler Formations, National Petroleum Reserve in Alaska, Society of Economic Paleontologists and Mineralogists, Pacific Section, Bakersfield CA, 217 – 224, 1987.

Anonymous, The Petroleum Resources of the Middle East, Publication, US DOE EIA, Washington, D. C., 1982.

Anonymous, Alaska's High Rank Coals, Information Circular 33, Alaska Department of Geological and Geophysical Surveys, Alaska, 1993.

Anonymous, World Energy Outlook, 2007, China and India Insights, Report, International Energy Agency (IEA), 9 rue de la Fédération, 75739 Paris Cedex 15, France, 2007.

Anonymous, Polish Geological Institute, www.pgi.gov.pl/mineral_resources/-hard_coal.htm. Accessed July 11, 2009, 2009d.

Anonymous, Polish Geological Institute, www.pgi.gov.pl/mineral_resources/lignite.htm. Accessed July 11, 2009, 2009e.

Anonymous, South Africa Department of Minerals and Energy, www.dme.gov.za/-energy/coal.stm. Accessed July 10, 2009, hard Coal Mining, Germany, 2009f.

Anonymous, Borneo Coal Indonesia, www.bcindonesia.com/steam_coal.html. Accessed July 11, 2009, 2009g.

Anonymous, Tavan Tolgoi Mine, www.tavantolgoi.mn/?lang=english#132517MetawiseCMS. Accessed July 11, 2009, 2009h.

Anonymous, Inner Mongolia produces 268 million tonnes of coal in H1, www.steelguru.com. Accessed July 15, 2009, 2009a.

Anonymous, Deutsche Steinkohle, www.mining-technology.com/projects/germany/. Accessed June 17, 2009, hard Coal Mining, Germany, 2009b.

Anonymous, Energy in Australia, Australia Department of Resources, Energy and Tourism, abare.gov.au. Accessed June 17, 2009, iSBN 978-1-921448-3, 104 p, 2009c.

J. A. Apps, A Review of Hazardous Chemical Species Associated with CO_2 Capture from Coal-Fired Power Plants and their Potential Fate during CO_2 Geologic Storage, Report LBL-59731, Ernest Orlando Lawrence Berkeley National Laboratory, Earth Sciences Division, 1 Cyclotron Road, Berkeley, California 94720, USA, 2006.

R. Boyd, Performance Improvement at a Chinese Coal Fired Power Plant, www.iea.org/work/-2004/zets/apec/presentations/boyd.pdf, 2004.

M. H. Chalybäus, Historische Entwicklung der spekulativen Philosophie von Kant bis Hegel (Historical Development of Speculative Philosophy from Kant to Hegel), 18 Lectures, Leipzig, 5th, 1860 edn., 1837.

A. Chase, The Legacy of Malthus – The Social Costs of the New Scientific Racism, University if Illinois Press, Urbana, IL, 1980.

A. P. Chikkatur, A. D. Sagar, T. L. Sankar, Sustainable development of the Indian coal sector, ENERGY, vol 34, 2009, 942 to 953.

A. Copeland, Minerals and Energy, Major Development Projects, Report ABARE project 2681, Australia Department of Resources, Energy and Tourism, Australia, iSBN 978-1-921448-46-1, 17 p, 2009.

G. D. Croft, T. W. Patzek, Potential for Coal-to-Liquids Conversion in the U.S. – Resource Base, Natural Resources Research J. 18 (3) (2009) 173 – 180, dOI: 10.1007/s11053-009-9097-x.

A. Dokukin, Further development of Donbass mines urged (in Russian), Trud 10 (June), corresponding member, USSR Academy of Sciences.

R. M. Flores, G. D. Stricker, S. A. Kinney, Alaska Coal Geology, Resources and Coalbed Methane Potential, Report DDS-77, United States Geological Survey, Reston, VA, 2004.

C. M. Grinstead, J. L. Snell, Introduction to Probability, Americal Mathematical Society, New York, available at www.dartmouth.edu/∼chance, 1998.

D. S. Holland, W. E. Nunan, D. R. Lammein, R. L. Woodhams, Eugene Island Block 330 Field, Offshore Louisiana, Giant Oil and Gas Fields of Decade: 1968 – 1978, AAPG Memoir 30 (1980) 253 – 280, www.searchanddiscovery.net/documents/2003/sorenson02/index.htm.

B. D. Hong, E. R. Slatick, Carbon Dioxide Emission Factors for Coal, Quarterly Coal Report DOE/EIA-0121(94/Q1), Energy Information Administration, Washington, DC, 1994.

M. K. Hubbert, Energy from Fossil Fuels, Science 109 (2823) (1949) 103–109.

M. K. Hubbert, Nuclear Energy and the Fossil Fuels, Presentation at the Spring Meeting of the Southern District Division of the American Petroleum Institute, Shell Development Company, San Antonio, TX, http://www.hubbertpeak.com/hubbert/1956/-1956.pdf, 1956.

M. K. Hubbert, Energy resources, Report 1000-D, National Academy of Sciences-National Research Council, Washington, DC, 1962.

M. K. Hubbert, Resources and Man, chap. 8, National Academy of Sciences and National Research Council, Freeman, San Francisco, 1969.

M. K. Hubbert, Energy Resources of the Earth, Scienific American 225 (3) (1971) 60–70, reprinted as book (Freeman, San Francisco, 1971).

W. S. Jevons, The Coal Question: An Inquiry Concerning the Progress of the Nation, and the Probable Exhaustion of Our Coal-Mines, Macmillan and Co., London, 2, revised edn., www.eoearth.org/article/The_Coal_Question%3A_Preface, 1866.

W. R. Kaiser, W. B. J. Ayers, L. W. LaBrie, Lignite Resources in Texas, Report of Investigations 104, Texas Bureau of Economic Geology, Austin, TX, 1980.

I. Levin, V. Hesshaimer, Radiocarbon – a unique tracer of global carbon cycle dynamics, Radiocarbon 42 (1) (2000) 69 – 80, ecology.botany.ufl.edu/radiocarbon08/Downloads/-Reprints,%20Lecture/Levin&Hessheimer%202000.pdf.

R. L. Lide (Editor), CRC Handbook of Chemistry and Physics, CRC Press, Boca Raton, 75th edition, 1994.

G. Liu, L. Zheng, L. Gao, H. Zhang, Z. Peng, The characterization of coal quality from the Jining coalfield, ENERGY vol 30, 2005, pp 1903 to 1914.

G. Liu, P. Yang, Z. Peng, G. Wang, W. Zhang, Comparative study of the quality of some coals from the Zibo coal field, ENERGY vol 28, 2003, pp 969 to 978.

C. Miłosz, The Captive Mind, Vintage International, New York, english translation edn., 1981.

S. H. Mohr, G. M. Evans, Forecasting Coal Production until 2100, Fuel - (-), dOI:10.106/j.fuel.2009.01.032.

E. S. Moore, Coal, It's Properties, Analysis, Classification, Geology, Extraction, Uses and Distribution, John Wiley and Sons, New York, 1922.

N. Nakicenovic, et al., Special Report on Emissions Scenarios, Report, Intergovernmental Panel on Climate Change (IPCC), 7bis Avenue de la Paix, C.P. 2300, CH-1211 Geneva 2, Switzerland, 2000.

W. R. Ott, Environmental Statistics and Data analysis, Lewis Publishers, Boca Raton, 1995.

K. Pan, The Depth Distribution of Chinese Coal Resource, gcep.stanford.edu/pdfs/-wR5MezrJ2SJ6NfFl5sb5Jg/10_china_pankexi.pdf. Accessed July 9, 2009, Fudan University, School of Social Development and Public Policy, 2005.

T. W. Patzek, Earth, Humans and Energy, CE170 Class Reader, University of Califonia, Berkeley, 2007a.

T. W. Patzek, How Can We Outlive Our Way of Life?, in: 20th Round Table on Sustainable Development of Biofuels: Is the Cure Worse than the Disease?, OECD, Paris, www.oecd.org/dataoecd/2/61/40225820.pdf, 2007b.

T. W. Patzek, Exponential growth, energetic Hubbert cycles, and the advancement of technology, Arch. Min. Sci. 53 (2) (2008) 131 – 159.

T. W. Patzek, G. D. Croft, Potential for Coal-to-Liquids Conversion in the U.S. – Fischer-Tropsch Synthesis, Natural Resources Research J. 18 (3) (2009) 181 – 191, dOI: 10.1007/s11053-009-9098-9.

C. R. Platt, Coal, Methodology and Specifications Guide Platts, Austin, TX, 2009.

E. G. Sable, G. D. Stricker, Alaska Coal Geology, vol. 50, special publication Coal in the National Petroleum Reserve in Alaska, Society of Economic Paleontologists and Mineralogists, Pacific Section, Bakersfield CA, 195 – 215, 1987.

D. J. Szumigala, R. A. Hughes, Alaskas Mineral Industry 2007: A Summary, Information Circular 57, Alaska Department of Geological and Geophysical Surveys, Alaska, 1993.

D. J. Szumigala, R. A. Hughes, L. A. Harbo, Alaskas Mineral Industry 2008: A Summary, Information Circular 57, Alaska Department of Geological and Geophysical Surveys, Alaska, 1993.

L. N. Takaishvili, D. A. Sokolov, Coal in Energy Balance of Far East of Russia, www.sei.irk.ru/aec/proc2006/11.pdf. Accessed July 30, 2009, 2006.

L. Thomas, Coal Geology, John Wiley and Sons, New York, 2002.

P. F. Verhulst, Notice sur la loi que la population suit dans son accroissement, Corr. Math. et Phys. publ. par A. Quetelet T. X. (also numbered T. II of the third series) (1838) 113–121.

G. Volkmer, Coal deposits of Poland, including discussion about the degree of peat consolidation during lignite formation, www.geo.tu-freiberg.de/oberseminar/os07_08/-Gerald_Volkmer.pdf. Accessed July 11, 2009, 2009.

S. Walker, Major Coalfields of the World, Report IEACR/51, IEA Coal Research, London, 1993.

W. Wei, Current Issues of China's Coal Industry: The Case of Shanxi, in: Proceedings of the 15th Annual Conference of the Association for Chinese Economics Studies, Australia, 2003.

4.12 Figure Captions

1. World primary energy demand in the Reference Scenario by the International Energy Agency (IEA) is often equated with the energy providers' ability to deliver. "Coal sees the biggest increase in demand among all primary energy sources in absolute terms between 2005 and 2030, closely followed by natural gas and oil. Coal demand jumps by 38% between 2005 and 2015 and 73% by 2030 a faster increase than in previous editions of the Outlook." (Anonymous, 2007).

2. The best multi-Hubbert cycle match of the historical rate of production of energy in coal of all ranks worldwide. The year of peak production is 2011, and peak coal energy production (higher heating value) is 160 EJ/y. Data sources: US DOE EIA, IEA, and Supplemental Materials to (Mohr and Evans, 2009).

3. The best multi-Hubbert cycle match of the historical CO_2 emissions from coal burning worldwide. The year of peak emissions is 2011, and the peak rate of emissions is 15 Gt/yr. Data sources: US DOE EIA, IEA, and Supplemental Materials to Mohr and Evans (2009).

4. The best multi-Hubbert cycle match of the historical cumulative production of coal of all ranks worldwide. The ultimate higher heating value of global coal production is 13,200 EJ. Data sources: US DOE EIA, IEA, and Supplemental Materials to Mohr and Evans (2009).

5. The best multi-Hubbert cycle match of the historical rate of CO_2 emissions worldwide. The predicted cumulative emissions are 1,200 Gt CO_2. Data sources: US DOE EIA, IEA, and Supplemental Materials to Mohr and Evans (2009).

6. A semi-logarithmic plot of carbon emissions from coal burning worldwide. The year of peak emissions is 2011, and the peak rate of emissions is 4.0 Gt C/yr. In 1990, a benchmark year for IPCC, the calculated rate of emissions was 2.4 Gt C/y. The rates of decline from the peak are 1.9% per year until 2046, and 3.6% thereafter. Data sources: US DOE EIA, IEA, and Supplemental Materials to Mohr and Evans (2009).

7. A cross-plot of cumulative coal production in the U.S. predicted with multiple Hubbert curves, versus historical data. Points along the diagonal denote perfect fit. The broken lines are 95 percent confidence intervals for the linear fit of the data. The R^2 statistic is 0.9998, and the mean squared error (average squared residual) is 0.0694 Gt^2.

8. The best multi-Hubbert cycle match of the historical rate of production of energy in coal of all ranks worldwide (thick black line). The 40 IPCC coal energy production scenarios are the thin color curves. Note that most of the IPCC scenarios seem to have little to do with reality predicted by the actual coal production data. In the year 2100, the physical Earth will not be producing 5-7 times more than at the peak in 2011. Data sources: US DOE EIA, IEA, Supplemental Materials to Mohr and Evans (2009), and IPCC (2000).

9. The best multi-Hubbert cycle match of the historical rate of carbon emissions from coal of all ranks worldwide (thick black line). The 40 IPCC coal emissions scenarios are the thin color curves. Data sources US DOE EIA, IEA, Supplemental Materials to Mohr and Evans (2009), and IPCC (2000).

10. Comparison of carbon emission predictions in the year 2100. The final predictions of the forty IPCC scenarios are divided by our base-case scenario. For 35/40 scenarios the ratios are above 2, and for 10/40 above 30.

11. Figure 4.9 with an additional recovery of 70 Gt of Siberian coal and 55 Gt of Alaskan coal, both peaking in the year 2100, added in as a sensitivity case.

12. Production from each of the lower Jurassic limestone oilfields in the Middle East can be treated as independent random variable. The total production is then a random-sum ($\mathcal{R} - \mathcal{S}$) process that should be a fragment of a normal distribution or a fundamental Hubbert cycle. Data Source: EIA (1982).

13. The total cumulative production from the fields shown in Figure 4.12 is fit well with a single Hubbert curve. The ultimate recovery is 15 billion barrels of oil.

14. The total rate of production from the fields shown in Figure 4.12 is also fit reasonably well with a single Hubbert curve. The peak production is predicted for 1979, at 500 million barrels of oil per year.

15. The cumulative Hubbert curve versus the total cumulative production from the fields shown in Figure 4.12. The Hubbert curve explains 99 % of the variance of the data.

16. The Hubbert curve fit residuals (step curve) and their inverse Fast Fourier Transform (FFT) fit (continuous curve).

17. The power spectrum of the Hubbert curve fit residuals. The dominant frequencies are the inverses of 23 and 32 years. One may conclude that there are ~27-year disturbances that correspond to new field developments. These developments can be handled by adding an inverse FFT-fit of the residuals or by creating separate Hubbert curves.

18. The Hubbert peak residuals (new projects) divided by the elapsed cumulative production are strongly damped. They do not follow a single frequency, but damping is approximately exponential. This means that in the long run a fundamental Hubbert peak predicts most of oil production from a population of oil fields it tracks.

19. The multi-Hubbert curve approach used in this paper predicts oil production peak in 1976 at 545 million BO per year.

20. The multi-Hubbert curve approach fits cumulative oil production very well, predicting 10.4 billion barrels of ultimate recovery from primary production and early waterfloods, 70% of the ultimate recovery predicted in Figure 4.13. As far as we

can tell, this prediction happens to be closer to the actual production history prior to the full waterflood implementation. The waterfloods would have to be modeled with a separate Hubbert curve.

21. Production from each of the 65 North Sea and Norwegian Sea oilfields in Norway can be treated as an independent random variable. The total production is then a random-sum ($\mathcal{R} - \mathcal{S}$) process and it should yield a Gaussian distribution. Data Source: OG&J (2009).

22. The total rate of production from the fields shown in Figure 4.21 is an almost perfect Hubbert curve. The peak production is predicted for the year 1999, at 1170 million barrels of oil per year.

23. The multi-Hubbert curve approach used in this paper predicts oil production peak in 2000.5 at 1180 million BO per year.

24. Logistic vs. normal distribution with matched half-widths, for $r = 1$, $t^* = 0$, $\dot{m}^* = 1/4$.

25. Logistic vs. normal distribution with matched peaks, for $r = 1$, $t^* = 0$, $\dot{m}^* = 1/4$.

26. A fit of the measured CO_2 emissions with Eq. (4.16). The fit is least good for anthracite, but very little of anthracite is produced worldwide nowadays.

Table 4.1: Summary of coal production and CO_2 emissions by largest coal-producing countries on the Earth.

Country	EJ Peak[a] Year	Ultimate coal production EJ	Peak coal rate EJ/y	Ultimate CO_2 emissions, Gt	Peak CO_2 rate Gt/y
China	2011	4015.6	75.8	365.0	6.9
USA	2015	2756.7	26.8	250.5	2.4
Australia	2042	1714.5	23.5	155.8	2.1
Germany/Poland	1987	1104.4	14.9	100.4	1.4
FSU	1990	1070.3	20.3	97.3	1.8
India	2011	862.6	13.6	78.4	1.2
UK	1912	753.0	7.7	68.4	0.7
S. Africa	2007	478.6	6.8	43.5	0.6
Mongolia	2105	279.2	3.2	25.4	0.3
Indonesia	2012	135.5	5.8	12.3	0.5
Global ultimate/peak	2011	13170.5	160	1197.0	15.0

[a] Note that sometimes the peaks of produced coal tons and exajoules do not coincide.
[b]Excluding Alaskan coal.
[c]The Former Soviet Union, excluding the Russian Far East coal.

Table 4.2: Summary of fit statistics of the cumulative coal production by country with multiple Hubbert curves.

Country	R^2	MSE[a], Gt^2
China	0.9983	0.1777
USA	0.9998	0.0694
FSU	0.9996	0.0504
Australia	0.9989	0.0052
Former German Empire	0.9999	0.0157
South Africa	0.9998	0.0008
India	0.9992	0.0047
Indonesia	0.9889	0.0005
Mongolia	0.9884	0.0000

[a] MSE = Mean Squared Error = $\frac{1}{n}\sum_{i=1}^{n} R_i^2$, where R_i is the i$^{\text{th}}$-residual.

Table 4.3: Heating values of world coals.

Coal name	HHV Btu/lb	HHV kcal/kg	HHV MJ/kg	Source
Anthracite				
Pennsylvania #4 premium	13200		32.0	Lehigh Coal
Pennsylvania #4 standard	12500		30.3	Lehigh Coal
China Shenrong 1	7000		29.3	Shenrong Carbon Ltd.
China Shenrong 2	7100		29.7	Shenrong Carbon Ltd.
Bituminous Coal				
N. Appalachian	13000		31.5	EIA
C. Appalachian	12500		30.3	EIA
Illinois Basin	11800		28.6	EIA
Uinta Basin	11700		28.3	EIA
Penn Keystone low ash	12700		30.8	Penn Keystone Coal Co.
Penn Keystone High Vol.	11500		27.8	Penn Keystone Coal Co.
Penn Keystone Low Vol.	12000		29.1	Penn Keystone Coal Co.
China Jining 3-1			27.6	Liu et al [2005]
China Jining 3-2			26.7	Liu et al [2005]
China Zibo average			25.8	Liu et al [2003]
China Banshan			23.4	Boyd [2004]
China Datong			28.5	Walker [1993]
China Huabei			27.8	Walker [1993]
China Antaibao			27.6	Walker [1993]
Indonesia BCI 5300		5300	22.2	Borneo Coal Indonesia
Indonesia BCI 5500		5500	23.0	Borneo Coal Indonesia
Indonesia BCI 5800		5800	24.3	Borneo Coal Indonesia
Indonesia BCI 6000		6000	25.1	Borneo Coal Indonesia
Indonesia BCI 6200B		6200	26.0	Borneo Coal Indonesia
Indonesia steam		5800	24.3	Daryalal Trading
South Africa steam		6700	28.1	Daryalal Trading
Australia thermal		6700	28.1	Centennial Coal
Subbituminous Coal				
PRB Wyodak		8220	19.9	Stricker and Ellis [1999]
Lignite Coal				
Texas Wilcox		6500	15.7[a]	Kaiser et al [1980]

[a] Presumably dry lignite. Lignite at the power station gate will be moist and have a lower heating value.

Table 4.4: Platt's Coal Specifications Platt [2009].

Coal name	HHV Btu/lb	HHV MJ/kg
Pittsburg Seam[a]	13000	31.5
Upper Ohio River	12500	30.3
NYMEX look-alike	12000	29.1
Big Sandy River	12500	30.3
Thacker/Kenova	12500	30.3
Big Sandy/Ohio River	12000	29.1
Illinois Basin 1	11800	28.6
Illinois Basin 2	11500	27.8
Illinois Basin 3	11000	26.6
Illinois Basin 4	10500	25.4
Powder River Basin 1	8800	21.3
Powder River Basin 2	8400	20.3
Colorado 1	11700	28.3
Colorado 2	11000	26.6
Utah	11500	27.8
Colombia Bolivar 1[b]	11600	28.1
Colombia Bolivar 2	11300	27.4
Venezuela Maracaibo	12600	30.5
Poland Baltic	11300	27.4
Russia Baltic	11500	27.8
S. Africa Richards Bay	11200	27.1
Australia Gladstone	11700	28.3
Australia Newcastle	11340	27.5
China Qinhuangdao	11200	27.1
Indonesia Kalimantan	10600	25.7
Indonesia Kalimantan	9000	21.8
Russia Pacific	11300	27.4

[a]Source: Platt's Weekly U.S. Price Survey
[b]Source: Platt's International Coal Report

Table 4.5: Summary of coal heating values and specific CO_2 emissions.

Rank	HHV[a] MJ/kg	lb CO_2/MBtu[b]	g CO_2/MJ	kg CO_2/kg coal
Anthracite	30	227.4	97.9	2.936
Bituminous	27	203.7	87.7	2.367
Subbituminous	21	212.7	91.5	1.922
Lignite	15	213.5	91.9	1.378

[a]HHV = High Heating Value
[b]From Hong and Slatick [1994]

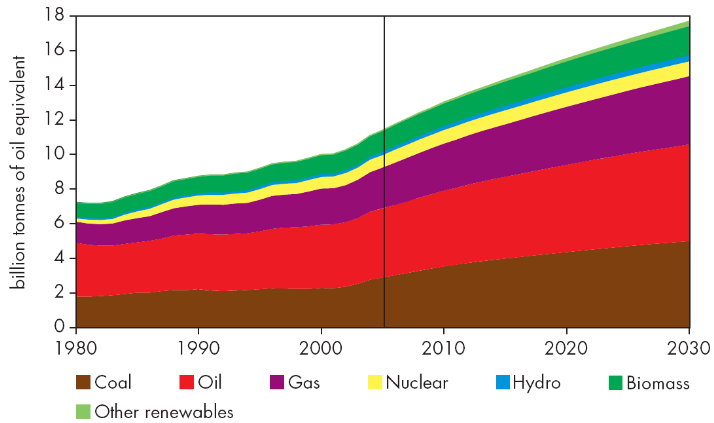

Figure 4.1: World primary energy demand in the Reference Scenario by the International Energy Agency (IEA) is often equated with the energy providers' ability to deliver. "Coal sees the biggest increase in demand among all primary energy sources in absolute terms between 2005 and 2030, closely followed by natural gas and oil. Coal demand jumps by 38% between 2005 and 2015 and 73% by 2030 a faster increase than in previous editions of the Outlook." (Anonymous, 2007).

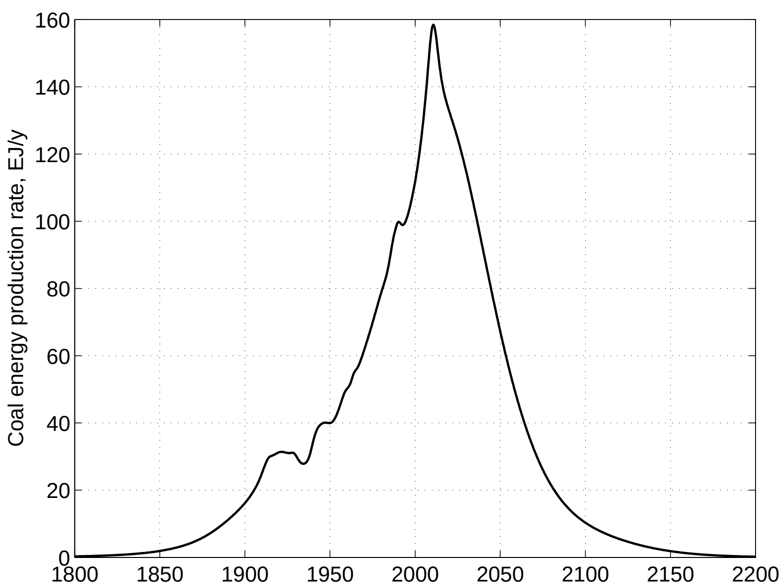

Figure 4.2: The best multi-Hubbert cycle match of the historical rate of production of energy in coal of all ranks worldwide. The year of peak production is 2011, and peak coal energy production (higher heating value) is 160 EJ/y. Data sources: US DOE EIA, IEA, and Supplemental Materials to (Mohr and Evans, 2009).

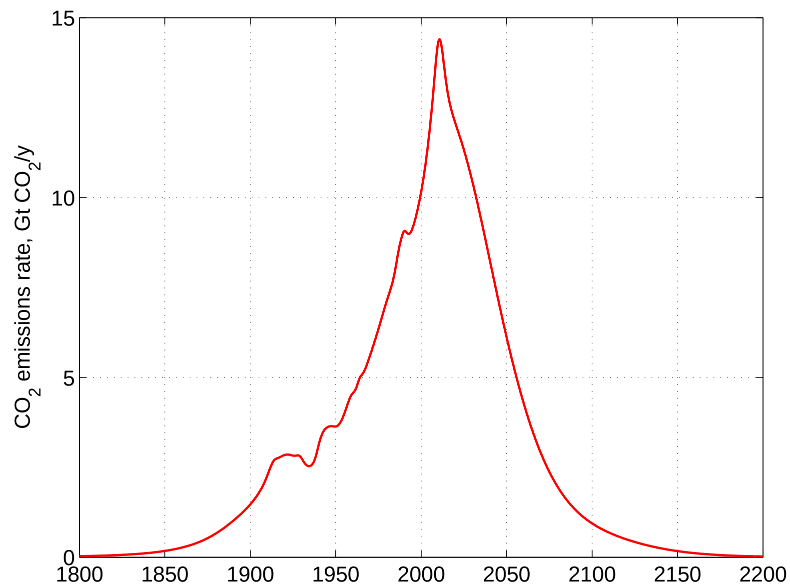

Figure 4.3: The best multi-Hubbert cycle match of the historical CO_2 emissions from coal burning worldwide. The year of peak emissions is 2011, and the peak rate of emissions is 15 Gt/yr. Data sources: US DOE EIA, IEA, and Supplemental Materials to Mohr and Evans (2009).

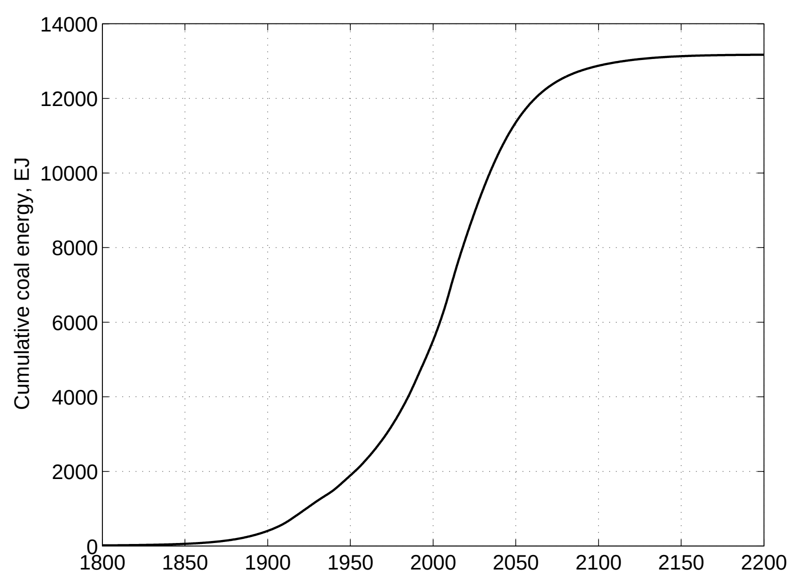

Figure 4.4: The best multi-Hubbert cycle match of the historical cumulative production of coal of all ranks worldwide. The ultimate higher heating value of global coal production is 13,200 EJ. Data sources: US DOE EIA, IEA, and Supplemental Materials to Mohr and Evans (2009).

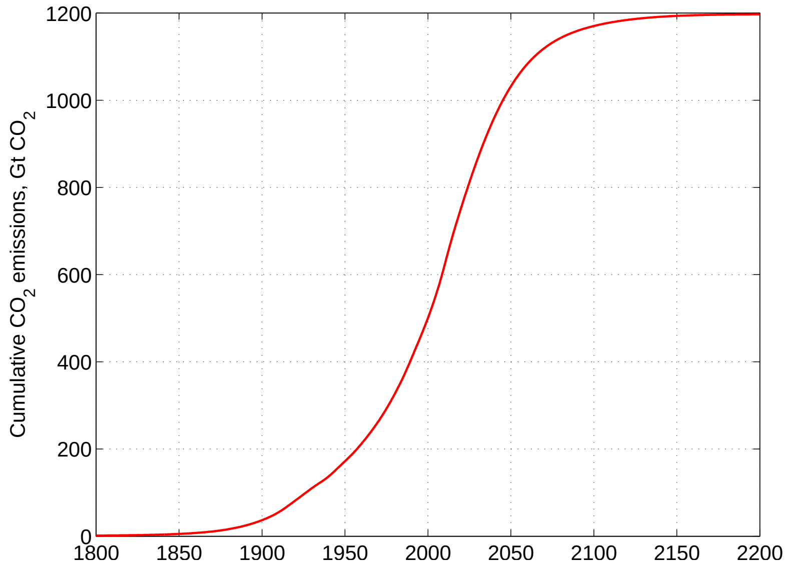

Figure 4.5: The best multi-Hubbert cycle match of the historical rate of CO_2 emissions worldwide. The predicted cumulative emissions are 1,200 Gt CO_2. Data sources: US DOE EIA, IEA, and Supplemental Materials to Mohr and Evans (2009).

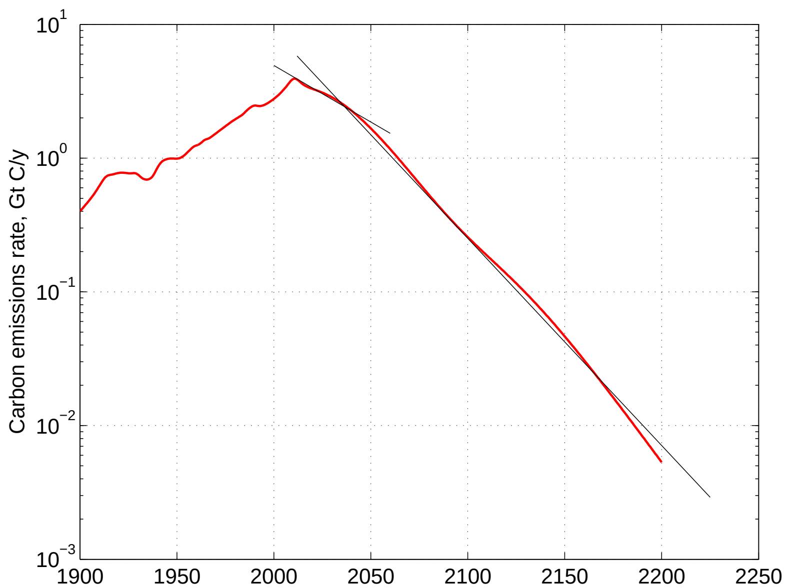

Figure 4.6: A semi-logarithmic plot of carbon emissions from coal burning worldwide. The year of peak emissions is 2011, and the peak rate of emissions is 4.0 Gt C/yr. In 1990, a benchmark year for IPCC, the calculated rate of emissions was 2.4 Gt C/y. The rates of decline from the peak are 1.9% per year until 2046, and 3.6% thereafter. Data sources: US DOE EIA, IEA, and Supplemental Materials to Mohr and Evans (2009).

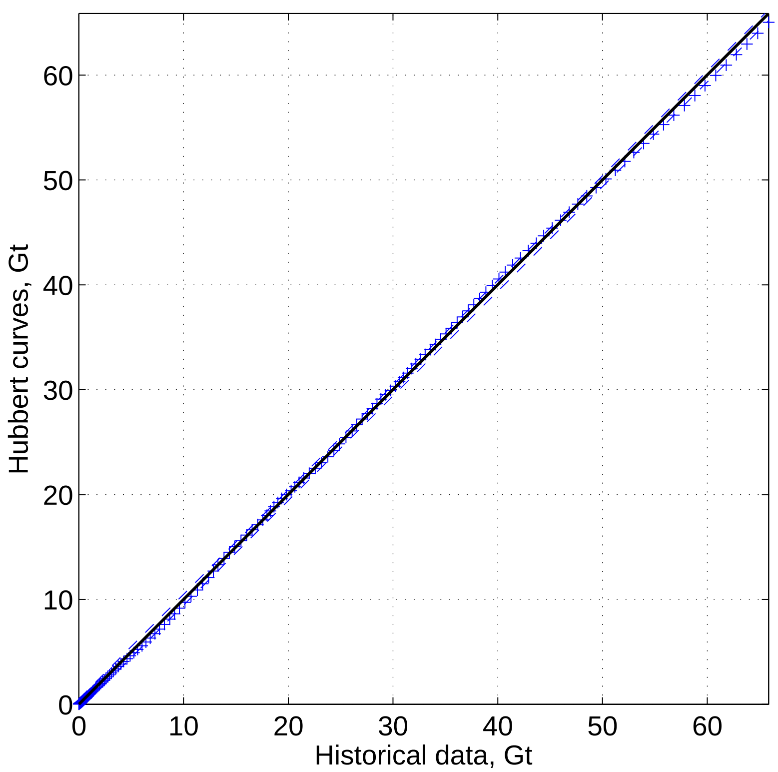

Figure 4.7: A cross-plot of cumulative coal production in the U.S. predicted with multiple Hubbert curves, versus historical data. Points along the diagonal denote perfect fit. The broken lines are 95 percent confidence intervals for the linear fit of the data. The R^2 statistic is 0.9998, and the mean squared error (average squared residual) is 0.0694 Gt^2.

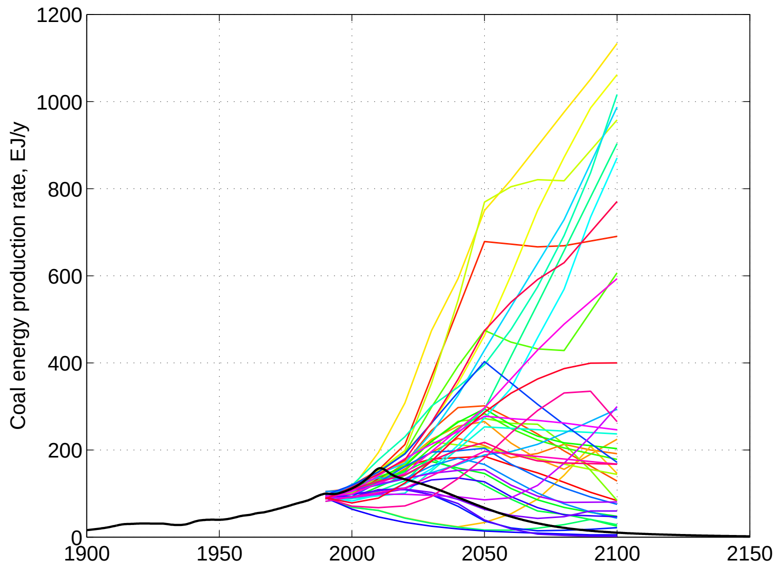

Figure 4.8: The best multi-Hubbert cycle match of the historical rate of production of energy in coal of all ranks worldwide (thick black line). The 40 IPCC coal energy production scenarios are the thin color curves. Note that most of the IPCC scenarios seem to have little to do with reality predicted by the actual coal production data. In the year 2100, the physical Earth will not be producing 5-7 times more than at the peak in 2011. Data sources: US DOE EIA, IEA, Supplemental Materials to Mohr and Evans (2009), and IPCC (2000).

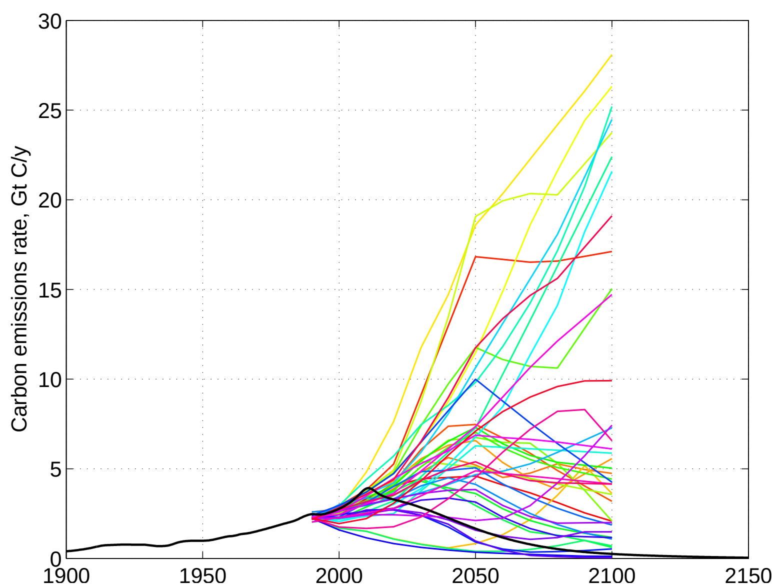

Figure 4.9: The best multi-Hubbert cycle match of the historical rate of carbon emissions from coal of all ranks worldwide (thick black line). The 40 IPCC coal emissions scenarios are the thin color curves. Data sources US DOE EIA, IEA, Supplemental Materials to Mohr and Evans (2009), and IPCC (2000).

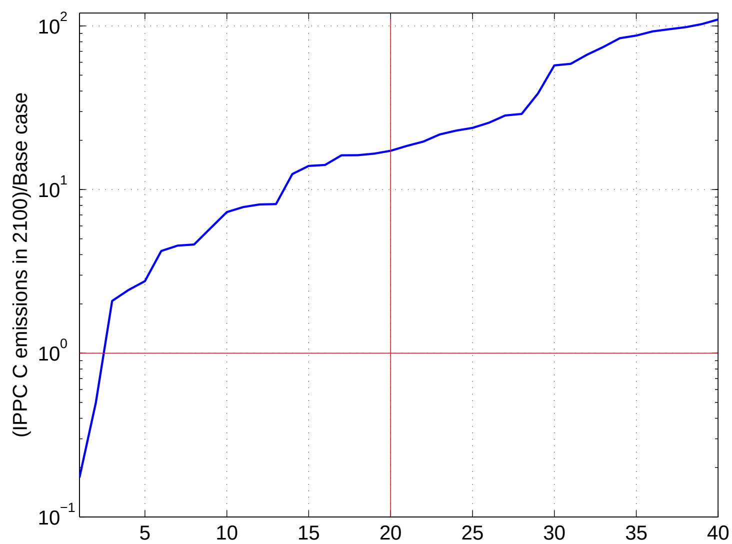

Figure 4.10: Comparison of carbon emission predictions in the year 2100. The final predictions of the forty IPCC scenarios are divided by our base-case scenario. For 35/40 scenarios the ratios are above 2, and for 10/40 above 30.

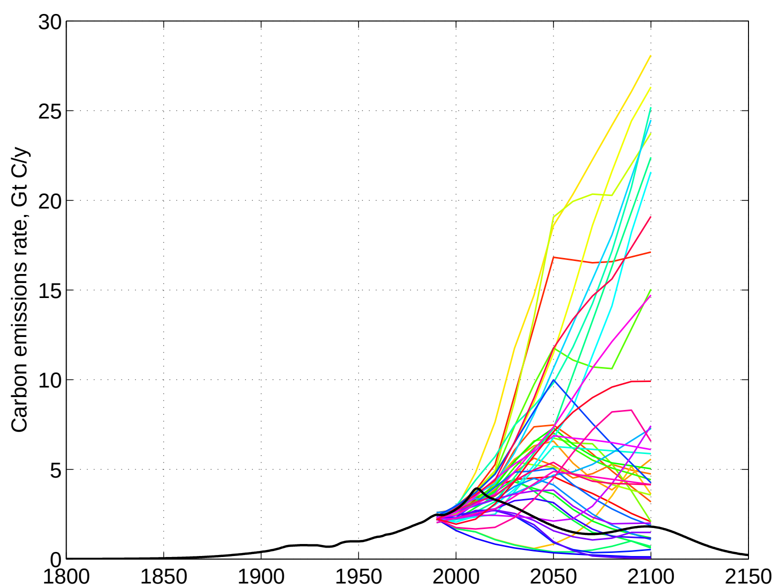

Figure 4.11: Figure 4.9 with an additional recovery of 70 Gt of Siberian coal and 55 Gt of Alaskan coal, both peaking in the year 2100, added in as a sensitivity case.

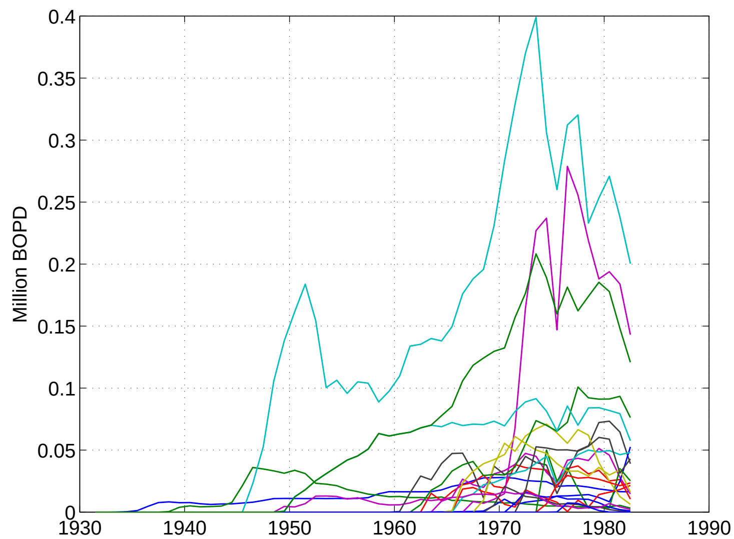

Figure 4.12: Production from each of the lower Jurassic limestone oilfields in the Middle East can be treated as independent random variable. The total production is then a random-sum ($\mathcal{R} - \mathcal{S}$) process that should be a fragment of a normal distribution or a fundamental Hubbert cycle. Data Source: EIA (1982).

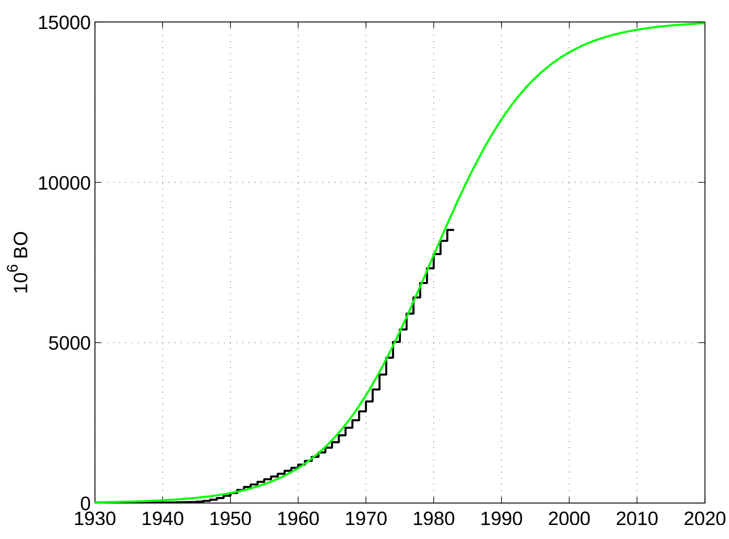

Figure 4.13: The total cumulative production from the fields shown in Figure 4.12 is fit well with a single Hubbert curve. The ultimate recovery is 15 billion barrels of oil.

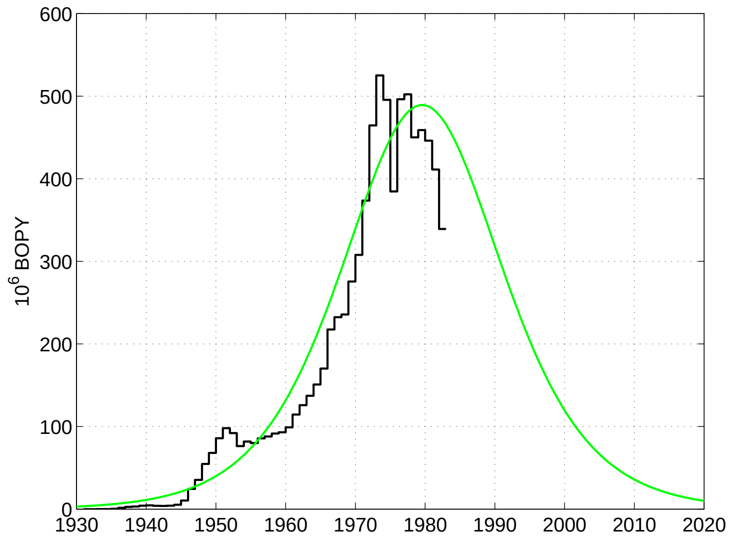

Figure 4.14: The total rate of production from the fields shown in Figure 4.12 is also fit reasonably well with a single Hubbert curve. The peak production is predicted for 1979, at 500 million barrels of oil per year.

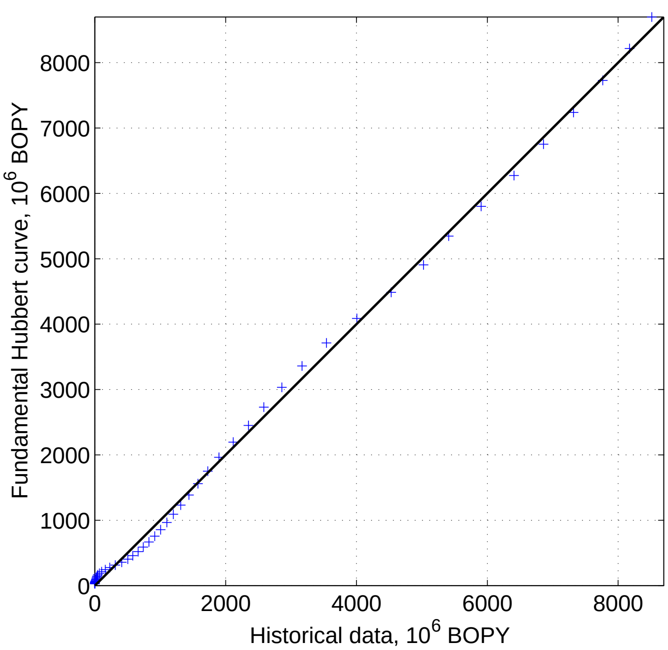

Figure 4.15: The cumulative Hubbert curve versus the total cumulative production from the fields shown in Figure 4.12. The Hubbert curve explains 99 % of the variance of the data.

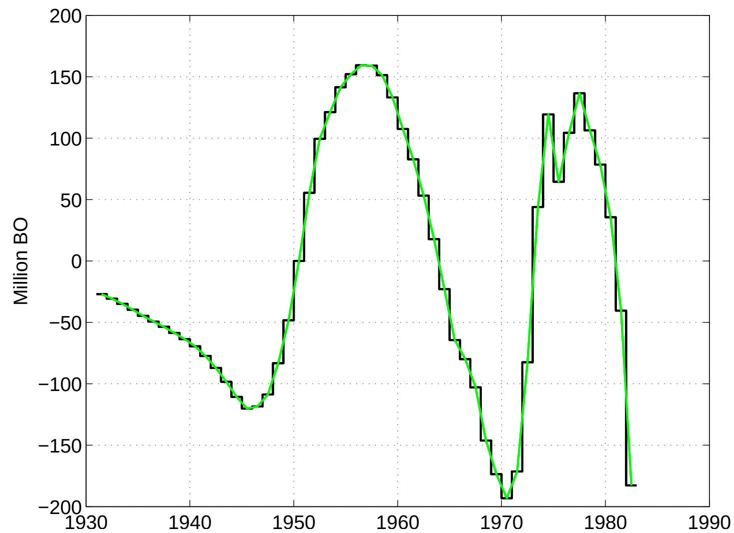

Figure 4.16: The Hubbert curve fit residuals (step curve) and their inverse Fast Fourier Transform (FFT) fit (continuous curve).

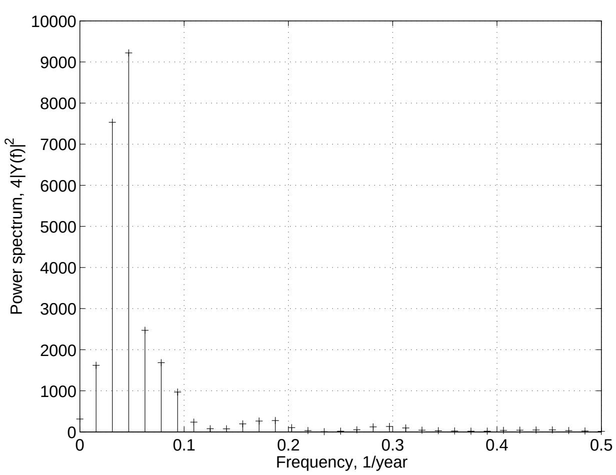

Figure 4.17: The power spectrum of the Hubbert curve fit residuals. The dominant frequencies are the inverses of 23 and 32 years. One may conclude that there are ∼27-year disturbances that correspond to new field developments. These developments can be handled by adding an inverse FFT-fit of the residuals or by creating separate Hubbert curves.

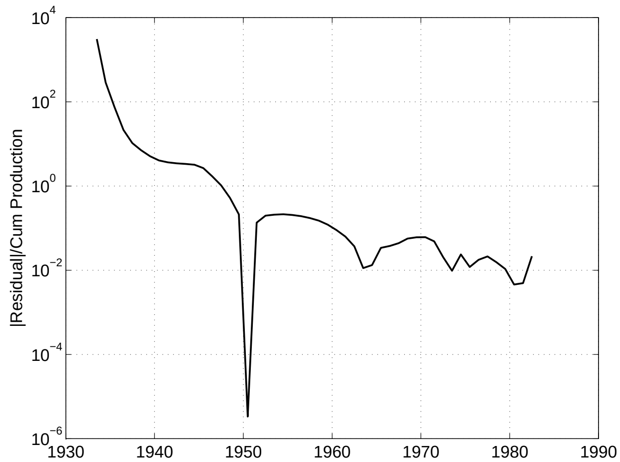

Figure 4.18: The Hubbert peak residuals (new projects) divided by the elapsed cumulative production are strongly damped. They do not follow a single frequency, but damping is approximately exponential. This means that in the long run a fundamental Hubbert peak predicts most of oil production from a population of oil fields it tracks.

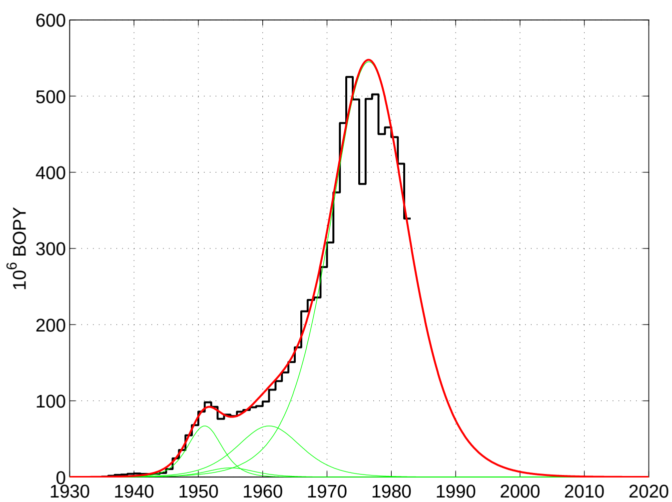

Figure 4.19: The multi-Hubbert curve approach used in this paper predicts oil production peak in 1976 at 545 million BO per year.

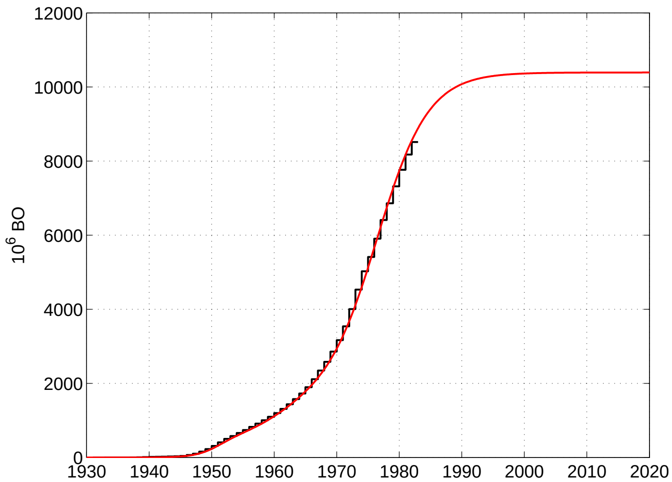

Figure 4.20: The multi-Hubbert curve approach fits cumulative oil production very well, predicting 10.4 billion barrels of ultimate recovery from primary production and early waterfloods, 70% of the ultimate recovery predicted in Figure 4.13. As far as we can tell, this prediction happens to be closer to the actual production history prior to the full waterflood implementation. The waterfloods would have to be modeled with a separate Hubbert curve.

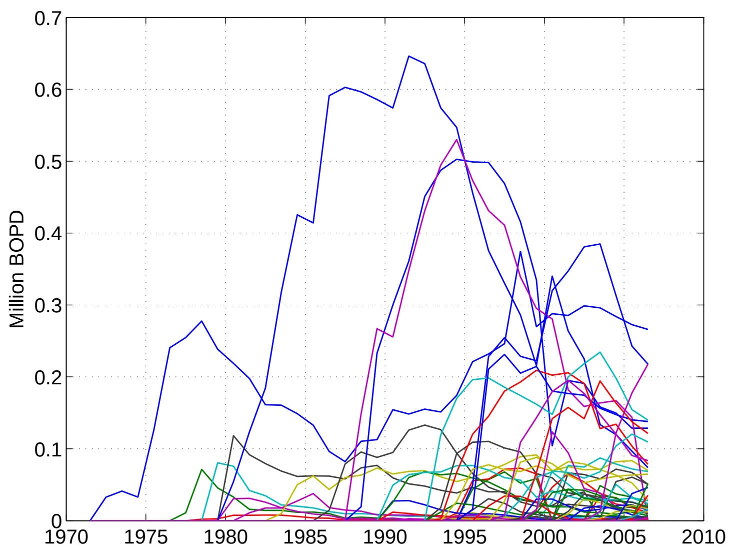

Figure 4.21: Production from each of the 65 North Sea and Norwegian Sea oilfields in Norway can be treated as an independent random variable. The total production is then a random-sum ($\mathcal{R} - \mathcal{S}$) process and it should yield a Gaussian distribution. Data Source: OG&J (2009).

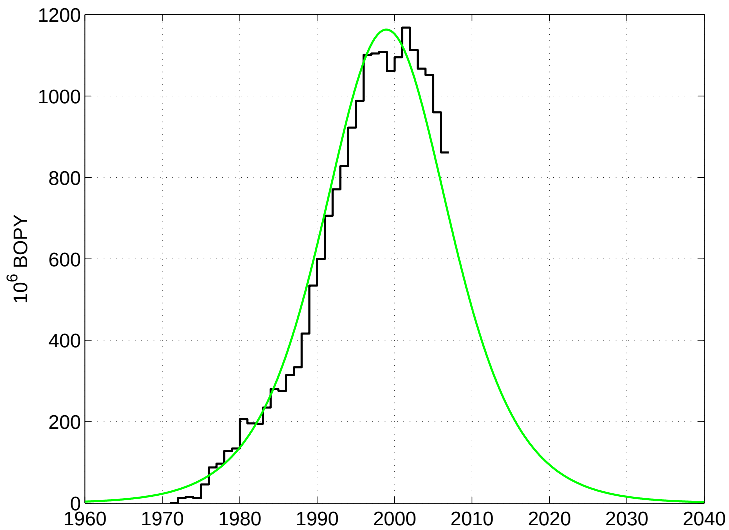

Figure 4.22: The total rate of production from the fields shown in Figure 4.21 is an almost perfect Hubbert curve. The peak production is predicted for the year 1999, at 1170 million barrels of oil per year.

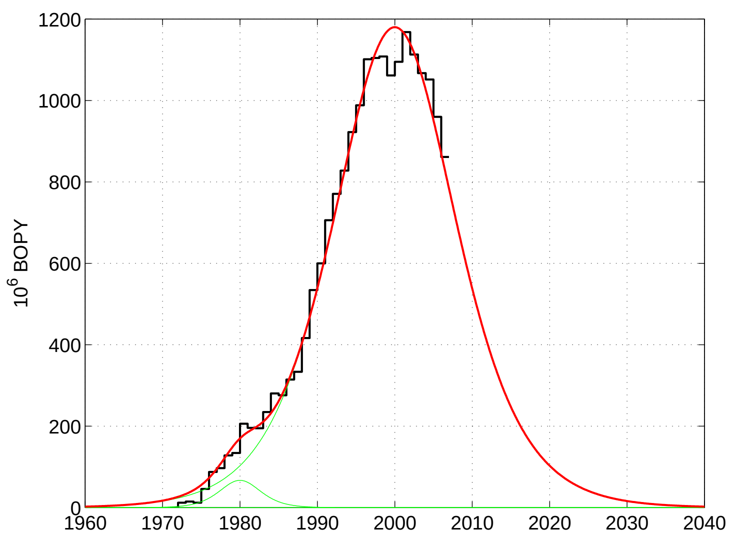

Figure 4.23: The multi-Hubbert curve approach used in this paper predicts oil production peak in 2000.5 at 1180 million BO per year.

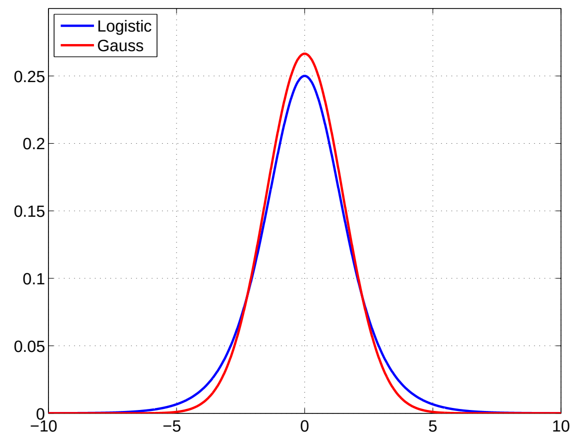

Figure 4.24: Logistic vs. normal distribution with matched half-widths, for $r = 1$, $t^* = 0$, $\dot{m}^* = 1/4$.

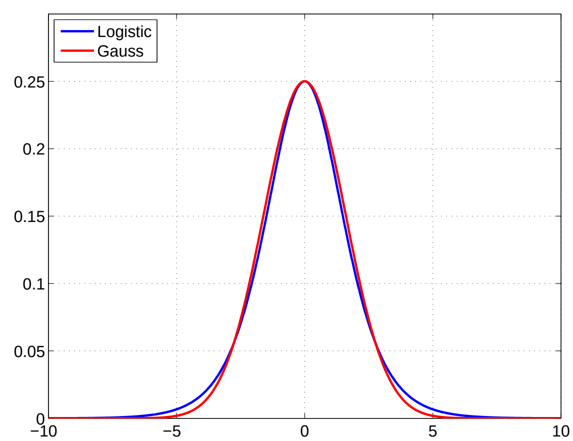

Figure 4.25: Logistic vs. normal distribution with matched peaks, for $r = 1$, $t^* = 0$, $\dot{m}^* = 1/4$.

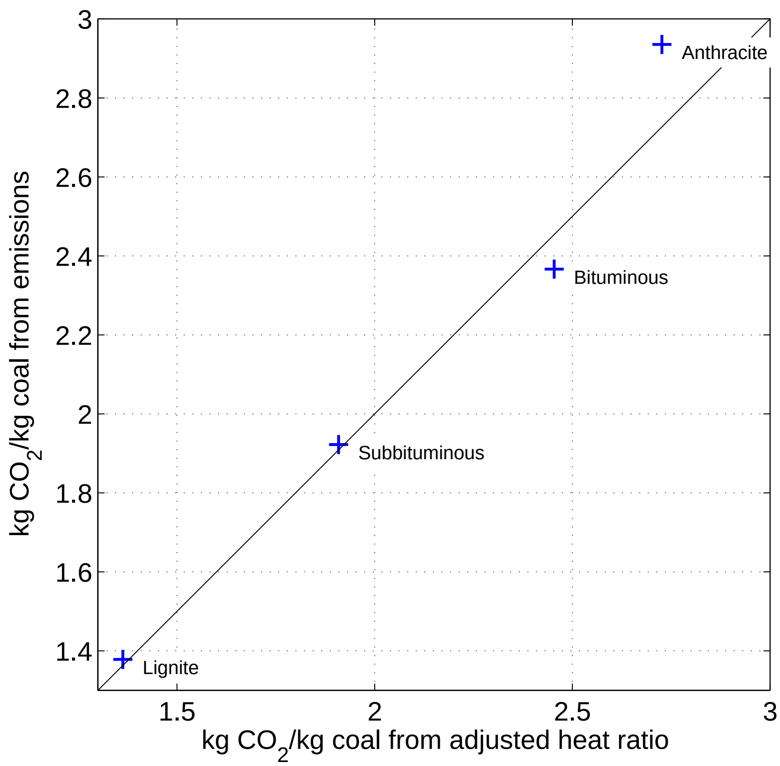

Figure 4.26: A fit of the measured CO_2 emissions with Eq. (4.16). The fit is least good for anthracite, but very little of anthracite is produced worldwide nowadays.

4.13 ONLINE SUPPORTING MATERIALS: The Key Coal Producers

4.13.1 China

The world's most important coal-producing area is North-Central China. The provinces of Inner Mongolia, Ningxia, Shaanxi and Shanxi together accounted for 83 percent of China's proven coal reserves in 2000, and Shanxi alone accounted for 25 percent of production Wei [2003]. Coal production from Inner Mongolia exceeded that from Shanxi for the first time during the first half of 2009 Anonymous [2009a]. Coals in these provinces are Carboniferous, Permian and Jurassic in age and coals of all three ages often occur in the same area Walker [1993]. The older coal deposits are often structurally complex, but the Jurassic Shenmu-Dongfeng coal field, located on the border between Inner Mongolia and Shaanxi, contains undisturbed coal seams up to 10 meters thick Thomas [2002]. The Jining and Zibo coalfields of Shandong province are an eastern extension of the North-Central China coal province. These are described in Liu et al [2003] and Liu et al [2005] as high-volatile bituminous coal of upper Carboniferous to lower Permian in age.

More than 90 percent of China's coal production comes from underground mines, as compared to about 40 percent in the U.S. According to Pan Pan [2005], the average depth of coal mine production in China is 456 meters. In in Shanxi, Hebei and Inner Mongolia, the average producing depth is more than 600 meters and the deepest mine is 1300 meters. By comparison, the average depth of hard coal production in Germany's very mature Ruhr Basin is 920 meters and coal deeper than 1200 meters is not considered reserves Anonymous [2009b]. Of China's forecasted coal reserves, a broader category than proven reserves, only 27 percent in East China are less than 1000 meters deep. Shallow coal deposits and some surface mines exist in parts of Inner Mongolia and Xinjiang, in remote areas that will require additional transportation infrastructure.

In 2008, China reported coal production that was almost 3 times higher than that in the United States. The best multi-Hubbert cycle fit of China's total coal production is shown in **Figures 4.27** and **4.28**. The production data for anthracite, bituminous and lignite coals are from the Supplemental Materials to Mohr and Evans [2009]. We predict the peak of production in 2011, and the ultimate coal recovery of 146.5 Gt. The peak of the fundamental Hubbert cycle is in the year 2019. Our estimate is an arithmetic average of “Reserves + Cumulative Production” ($R + C = 156.1$ Gt) and “Best Guess” ($BG = 136.1$ Gt) in Table B.1 in Mohr and Evans [2009].

Note that the area of the small cycle is very small. This cycle may well be an artifact of production overreporting (1958 – 1960), followed by a more recent period of production underreporting (1998 – 2002). The dramatic, 55 percent annual rate of increase of coal production in the small cycle in Figure 4.28 may also be the result of a short-lived, all out effort by China to fuel its 2000-2008 runaway economic growth. Over-reporting of coal production was standard in the communist Poland and the Soviet Union. Simply a part of mined rock waste mixed with coal was counted as coal.

On July 24, 2009, the Shanghai Securities News reported:

> Chinese net coal imports in H1 surge 8 times to 36.6 million tonnes, www.steelguru.com Friday, 24 Jul 2009. Statistics indicate that China's coal imports in H1 of the year

> remained at 48.27 million tonnes exceeding the total volume of the whole last year and surging by 126%YoY. In H1 coal exports stayed at 11.67 million tonnes sliding by 54%YoY. The net import volume stayed 36.6 million tonnes increasing by over 8 times YoY.
>
> As per report, from January to April, China's net coal import volume remained at 13.43 million tonnes and the figure for January to May was 21.67 million tonnes.
>
> Last year China's coal imports were about 40 million tonnes, 1.5% of the volume of China's raw coal production, which remained at over 2.7 billion tonnes. In the first six months of this year, China's raw coal production stayed at 1.35 million tonnes and overseas resource China bought took up over 3.55% of the volume.

The corresponding match of the rate and cumulative emissions of CO_2 in China is shown in **Figures 4.29** and **4.30**. The peak emissions of CO_2 of 7 Gt/y are predicted in the year 2011, and the ultimate emissions are 360 Gt of CO_2.

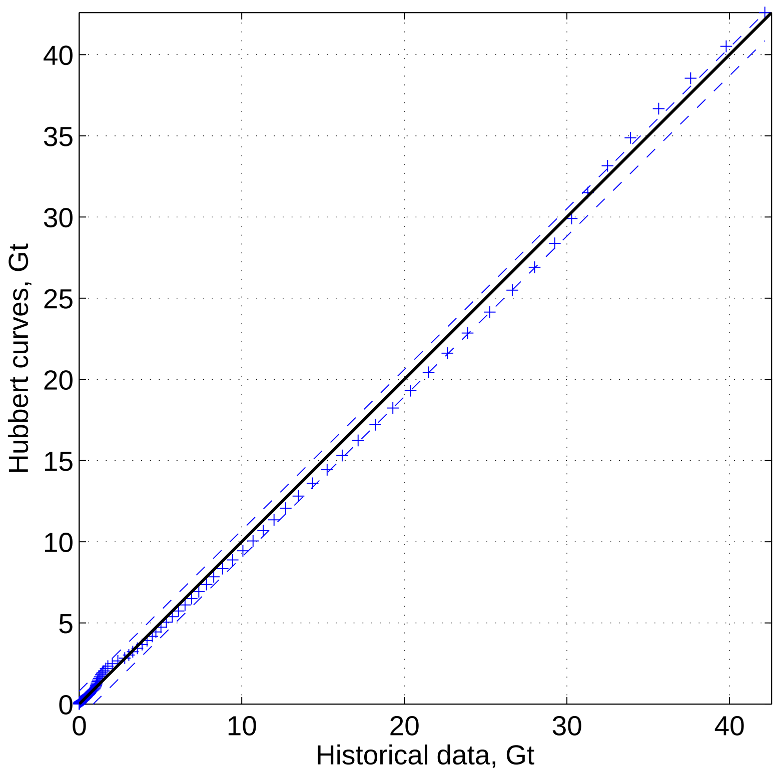

Figure 4.27: The best multi-Hubbert cycle match of the historical cumulative production of anthracite, bituminous, and lignite coal in China. The year of peak production is 2011, and the ultimate coal production is 146.5 Gt. The broad base peak is in the year 2019. Data source: Supplemental Materials to Mohr and Evans (2009).

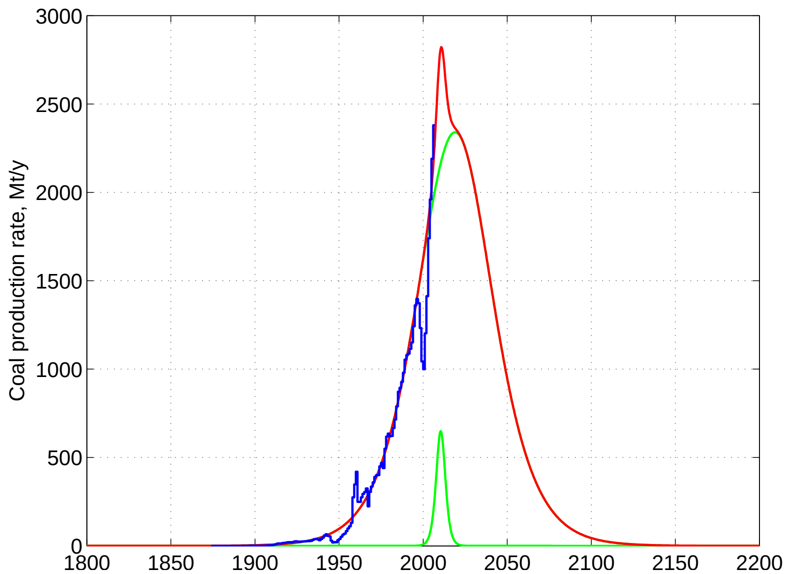

Figure 4.28: The best multi-Hubbert cycle match of the historical rate of production of anthracite, bituminous, and lignite coal in China. Data source: Supplemental Materials to Mohr and Evans (2009).

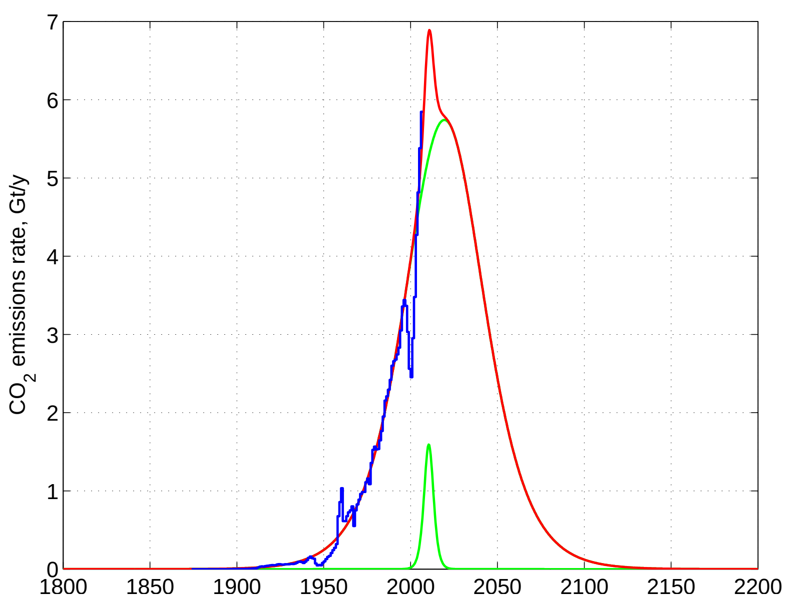

Figure 4.29: The best multi-Hubbert cycle match of the historical rate of CO_2 emissions in China. The predicted emission peak in the year 2011 is 7 Gt CO_2/y. Data source: Supplemental Materials to Mohr and Evans (2009).

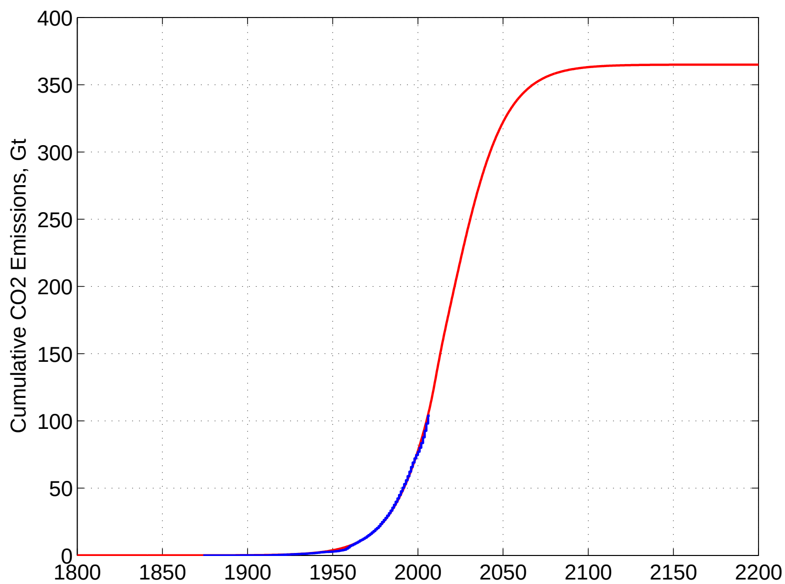

Figure 4.30: The best multi-Hubbert cycle match of the historical cumulative CO_2 emissions in China. The year of peak emissions is 2011, and the ultimate emissions are 360 Gt of CO_2. Data source: Supplemental Materials to Mohr and Evans (2009).

4.13.2 USA

The U.S. coal resources have been summarized in Croft and Patzek [2009]. The best multi-Hubbert cycle fit of total coal production in the United States is shown in **Figures 4.31** and **4.32**. The production data for anthracite, bituminous, subbituminous, and lignite coals are from the Supplemental Materials to Mohr and Evans [2009]. We predict the peak of production from the existing mines in 2016, and the ultimate coal recovery of 110 Gt. Our estimate is 50 percent lower that the "Linearized Hubbert" ($LH = 172$) Gt, and roughly 1/3 of the "Reserves + Cumulative Production" ($R + C = 308$ Gt) and the "Best Guess" ($BG = 308$ Gt) in Table B.1 in Mohr and Evans [2009]. There is no doubt that the USA has vast coal resources and the subbituminous (and, perhaps, lignite) coal mines *could* be greatly expanded. However, the current production data do not warrant such high ultimate recovery estimates; for more details see Croft and Patzek [2009]; Patzek and Croft [2009]. How the U.S. coal resources will continue be produced, we simply do not know. What we do know is that the new mines will be environmentally and technically ever more challenging, and may not be constructed in the foreseeable future.

The corresponding match of the rate and cumulative emissions of CO_2 in USA is shown in **Figures 4.33** and **4.34**. The peak emissions of CO_2 of 2.5 Gt/y are predicted in the year 2015, and the ultimate emissions are 250 Gt of CO_2.

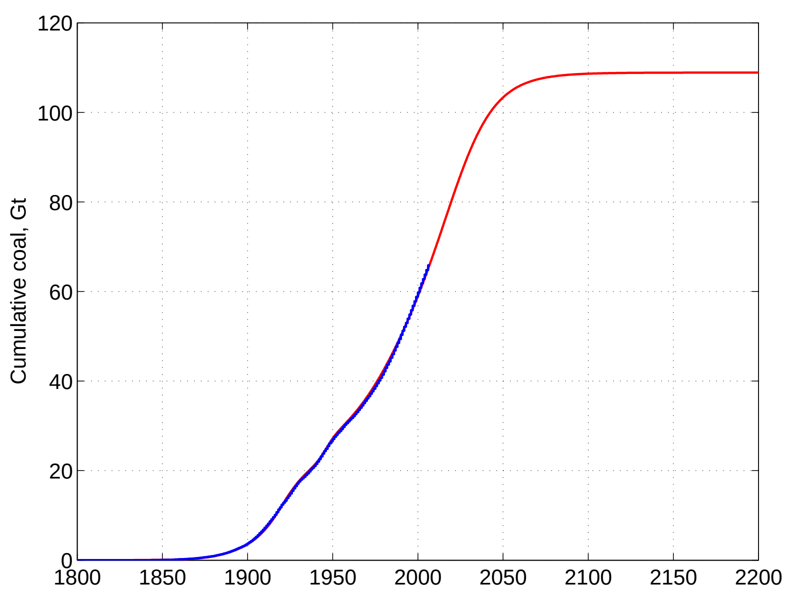

Figure 4.31: The best multi-Hubbert cycle match of the historical cumulative production of anthracite, bituminous, subbituminous, and lignite coal in the United States. The year of peak production is 2016, and the ultimate coal production is 110 Gt. Data sources: EIA (Croft and Patzek, 2009), Supplemental Materials to Mohr and Evans (2009).

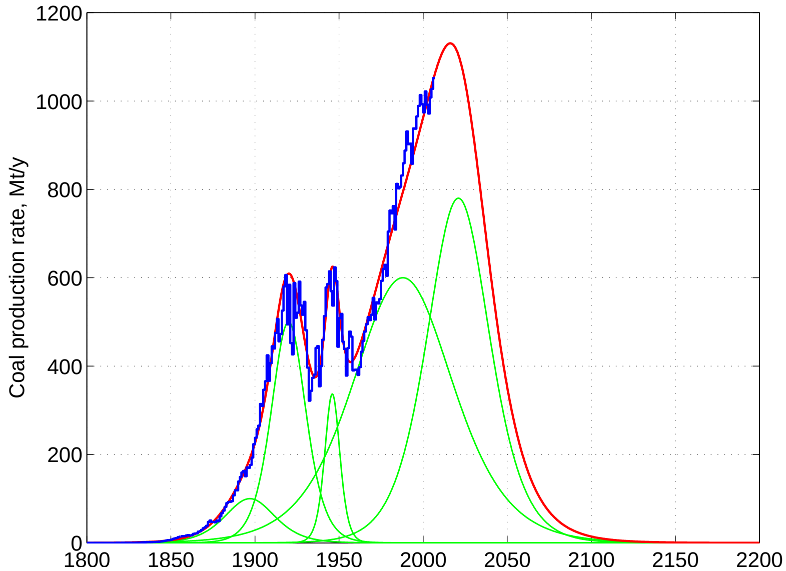

Figure 4.32: The best multi-Hubbert cycle match of the historical rate of production of anthracite, bituminous, subbituminous, and lignite coal in USA. The individual peaks are in the years 1897 (anthracite), 1920 (world War I), 1946 (World War II), 1988 (bituminous coal), and 2021 (subbituminous coal). The peak production is predicted to occur in the year 2015. Data sources: EIA (Croft and Patzek, 2009), Supplemental Materials to Mohr and Evans (2009).

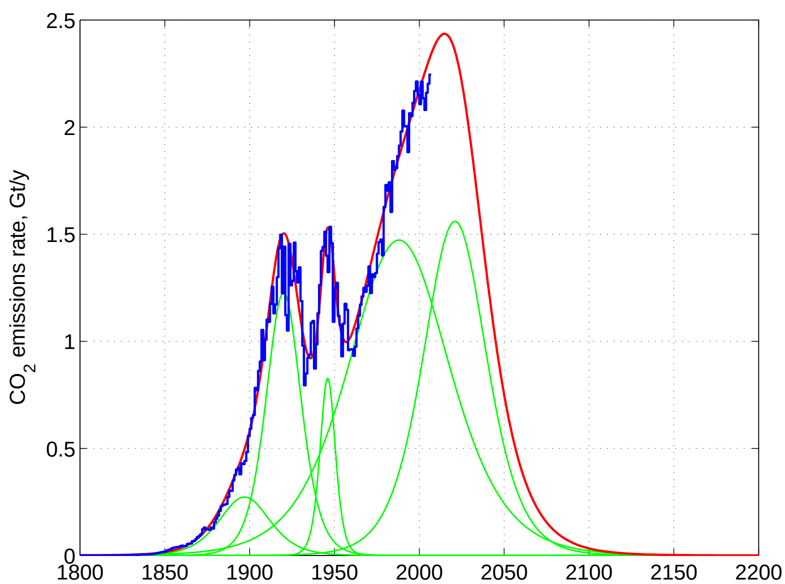

Figure 4.33: The best multi-Hubbert cycle match of the historical rate of CO_2 emissions in USA. The predicted emission peak in the year 2015 is 2.5 Gt CO_2/y. Data sources: EIA (Croft and Patzek, 2009), Supplemental Materials to Mohr and Evans (2009).

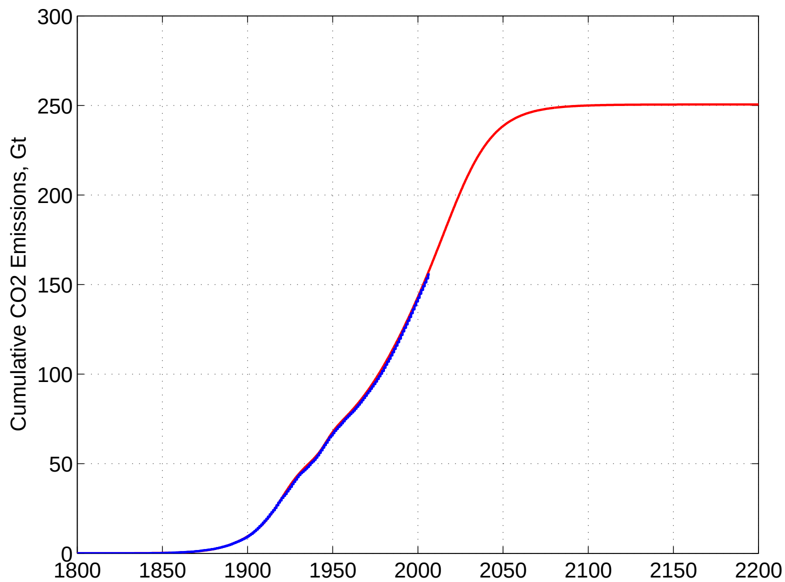

Figure 4.34: The best multi-Hubbert cycle match of the historical cumulative CO_2 emissions in USA. The year of peak emissions is 2015, and the ultimate emissions are 250 Gt of CO_2. Data sources: EIA (Croft and Patzek, 2009), Supplemental Materials to Mohr and Evans (2009).

Alaska Coal

As a sensitivity case, we assume that 55 Gt of bituminous coal (1/2 of the current ultimate recovery from the lower 48 states) equivalent will be recovered in Alaska in the next 200 years. The results are shown in **Figures 4.35 – 4.38**. Unlike oil, coal cannot be transported by pipeline over long distances in a harsh climate. Transport of 1Gt per year (2.7 million tons per day) of coal by ship and train is a rather difficult logistic task, requiring, e.g., thirty 100,000 ton coal ships to be loaded each day, 365 days a year. This task might be accomplished by building an equivalent of eleven copies of Australia's Newcastle port, the world's largest coal export terminal, that will work around the clock in the harsh Arctic environment. One train can transport about 9,000 tons of coal, so one would also need to load/unload 300 train loads of coal each day. We doubt that such a high rate of coal production will ever be achieved in Alaska.

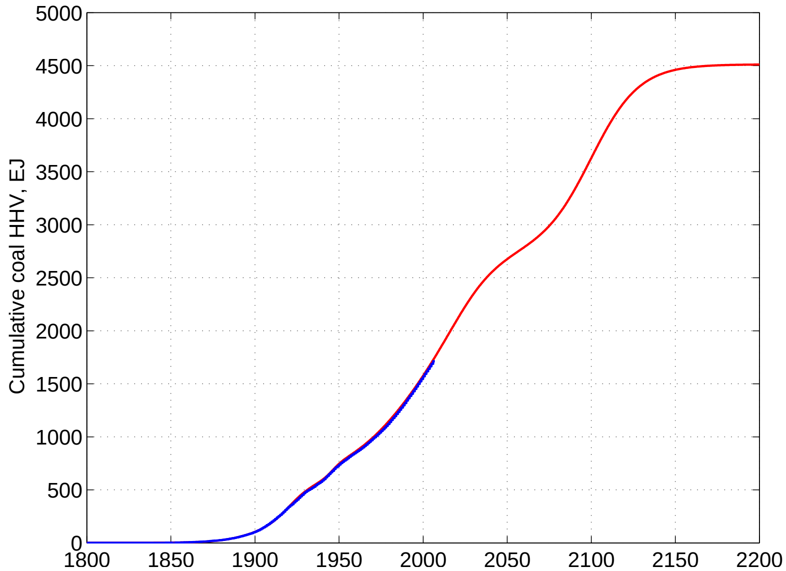

Figure 4.35: Figure 4.31 with 55 Gt of Alaska North Slope coal added in. The new ultimate recovery is 160 Gt.

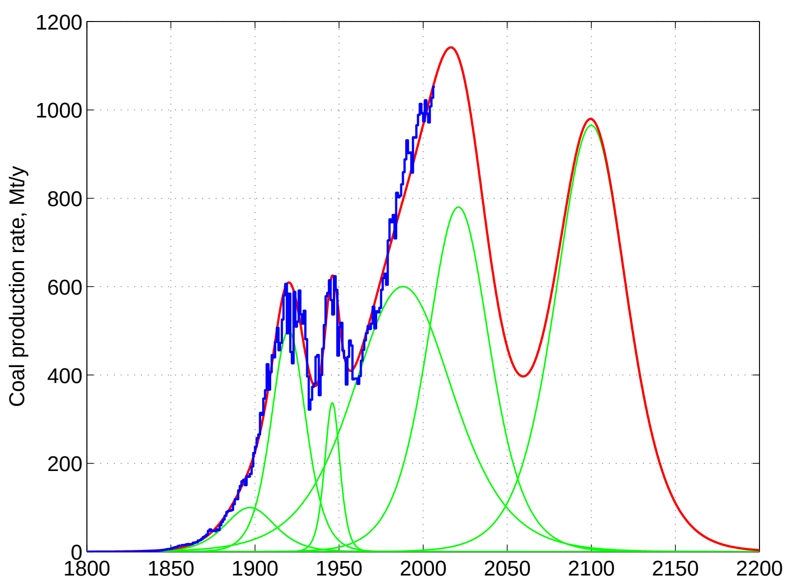

Figure 4.36: Figure 4.32 with 55 Gt of Alaska North Slope coal added in. The second production peak in the year 2100 is 1000 million tons of coal per year.

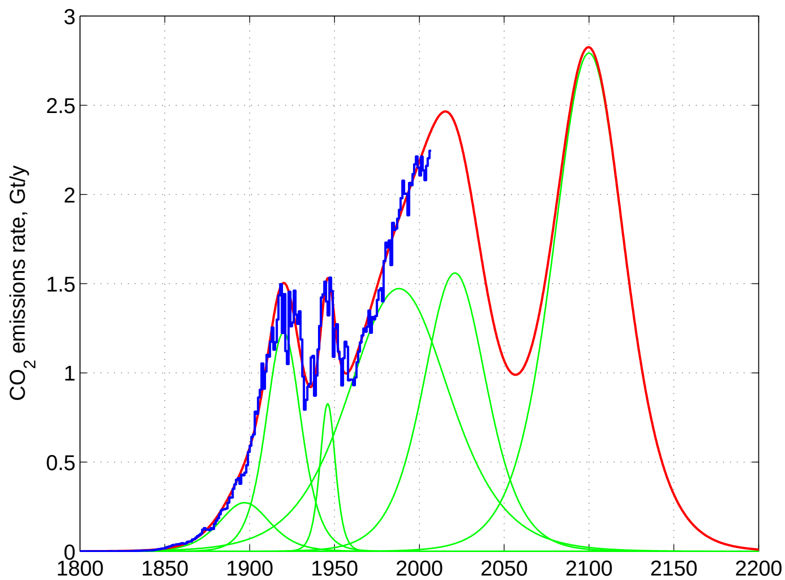

Figure 4.37: Figure 4.33 with 55 Gt of Alaska North Slope coal added in. The second production emissions peak in the year 2100 is 2.8 Gt of CO_2 per year. The second peak is slightly higher than the first one because the Alaskan coal is of higher quality.

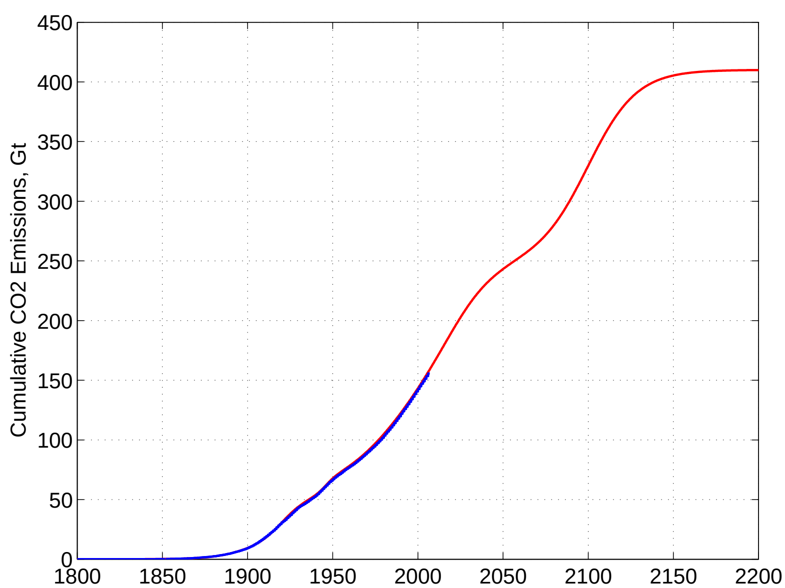

Figure 4.38: Figure 4.34 with 55 Gt of Alaska North Slope coal added in. The ultimate CO_2 emissions are 410 Gt.

4.13.3 FSU

The most important hard coal-producing areas in the Former Soviet Union are the Donbass region of Ukraine and Russia, the Kuzbass region of Siberia, the Pechora Basin of Russia and the Karaganda Basin of Kazakhstan. Important soft coal resources are present in the Kansk-Achinsk area of Eastern Siberia and the Ekibastuz Basin of Kazakhstan. All of these areas have enough production history to be well-quantified by the Hubbert method. Lena and Tunguska are lower quality deposits spread over vast areas. These deposits are discussed the Sensitivity Analysis and Future Work Section.

The Donetsk Basin (Donbass) coal fields produce bituminous coal and some anthracite from underground mines in Ukraine and Russia. The seams are typically less than 1.2 meters thick, but the coal quality and yield are high. Donbass was historically the most important coal-producing region in the Soviet Union. The production peaked at 223.7 million metric tons per year in 1976 and has been declining since Dokukin [1984]. Many of the mines have been developed to depths of 800 meters or more. The coals are Carboniferous age and numerous folds and faults render mining difficult in places Moore [1922]

The Kuznetsk Basin (Kuzbass) region is located around the city of Tomsk in the southeastern part of Western Siberia. This is the most important area in terms of coal reserves, with over 100 feet of coal in 17 seems Moore [1922]. Coals here are of Permian age Thomas [2002]. The Trans-Siberian railroad traverses the area, but long shipping distances to markets have hindered development.

The Kazakh coals are Carboniferous and, in the Karaganda Basin, multiple seams range from 1 to 3.5 meters thick. Coals in the area range from bituminous to anthracite. In the Ekibastuz Basin, a number of seams of sub-bituminous coal have coalesced to form a single seam 130 to 200 meters thick Thomas [2002].

The best multi-Hubbert cycle fit of the Former Soviet Unions's total coal production is shown in **Figures 4.39** and **4.40**. The production data for anthracite, bituminous, subbituminous, and lignite coals are from the Supplemental Materials to Mohr and Evans [2009]. The peak of production occurred in 1990, and the ultimate coal recovery of 43 Gt. Our estimate is 1/3 of the "Reserves + Cumulative Production" ($R + C = 120.7$ Gt) and the "Best Guess" ($BG = 127$ Gt) in Table B.1 in Mohr and Evans [2009]. There is no doubt that the FSU has vast coal resources. How these resources will be produced, and what has been the effect of 70 years of communist mismanagement is unknown.

The corresponding match of the rate and cumulative emissions of CO_2 in FSU is shown in **Figures 4.41** and **4.42**. The peak emissions of CO_2 of 1.8 Gt/y occurred in the year 1990, and the ultimate emissions are 97 Gt of CO_2.

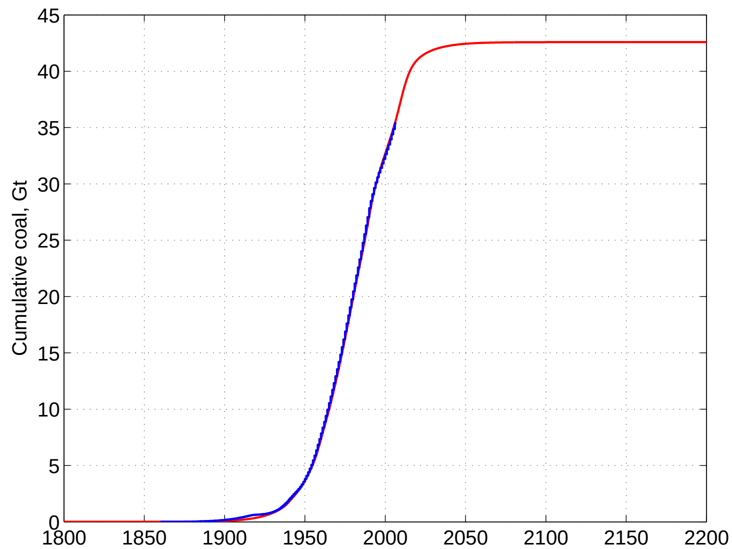

Figure 4.39: The best multi-Hubbert cycle match of the historical cumulative production of anthracite, bituminous, subbituminous, and lignite coal in the Former Soviet Union (FSU). The year of peak production was 1990, and the ultimate coal production is 43 Gt. Data source: Supplemental Materials to Mohr and Evans (2009).

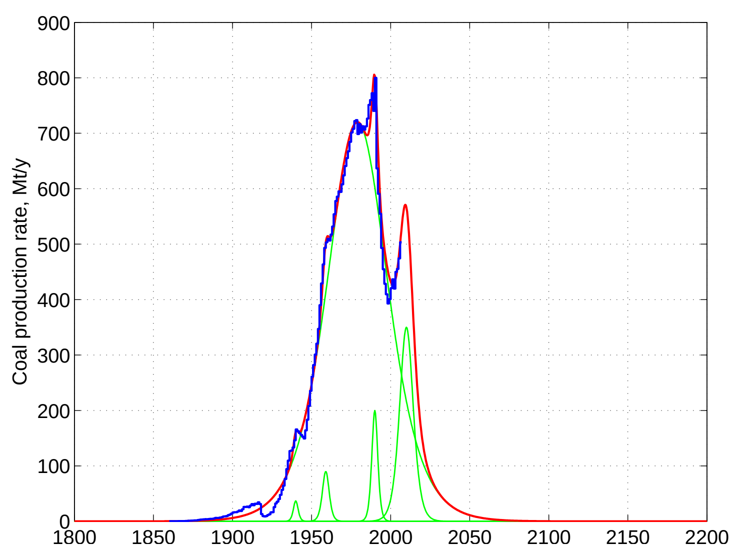

Figure 4.40: The best multi-Hubbert cycle match of the historical rate of production of anthracite, bituminous, subbituminous, and lignite coal in FSU. The smaller peaks are in the years 1940, 1959, 1970, and 2010. The size of the last peak is questionable. Data source: Supplemental Materials to Mohr and Evans (2009).

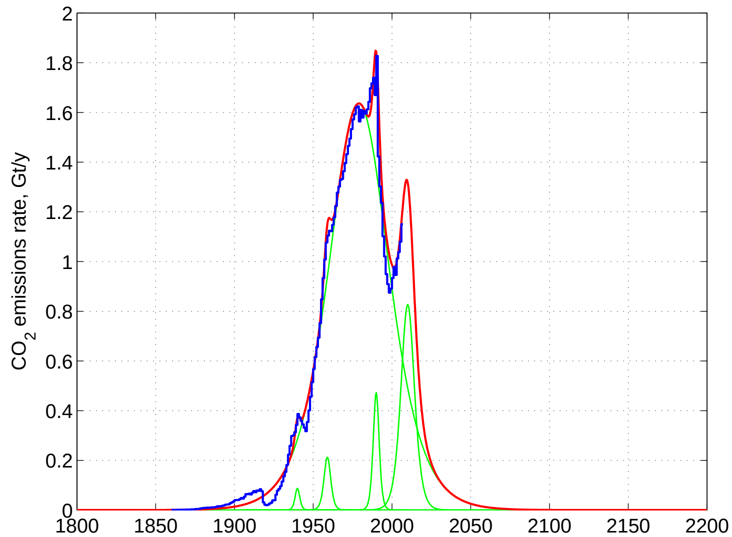

Figure 4.41: The best multi-Hubbert cycle match of the historical rate of CO_2 emissions in FSU. The emissions peak was the year 1990, at 1.8 Gt CO_2/y. Data source: Supplemental Materials to Mohr and Evans (2009).

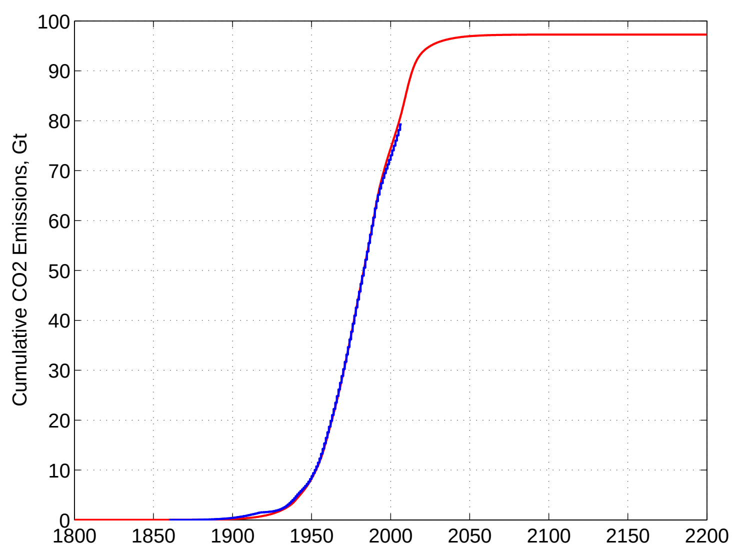

Figure 4.42: The best multi-Hubbert cycle match of the historical cumulative CO_2 emissions in FSU. The year of peak emissions was 1990, and the ultimate emissions are 97 Gt of CO_2. Data source: Supplemental Materials to Mohr and Evans (2009).

4.13.4 Australia

The Bowen Hard Coal Basin in Queensland is the most important coal-producing area in Australia, followed by the Sydney Hard Coal basin in New South Wales, and by the Clarence-Moreton Hard Coal Basin in Queensland and New South Wales. All of these basins contain coal of Permian age Walker [1993]. Known hard coal resources further inland in the Cooper and Galilee Basins in Queensland have not been developed because they are too far from the coast. There is also significant production of Tertiary-age lignite in the Latrobe Valley of Victoria Thomas [2002].

Queensland and New South Wales accounted for more than 98 percent of Australia's hard coal production in the 2007 – 2008 fiscal year. The proximity of major coal resources to Australia's eastern seaboard has facilitated Australia becoming the world's largest coal exporter, see Footnote 2, accounting for about 20 percent of world steam coal exports and nearly 60 percent of metallurgical coal exports Anonymous [2009c].

Nine advanced coal mine developments in Queensland and New South Wales are expected to raise coal production capacity by around 7 million tonnes per year over the next three to four years. In order to handle this increased mine production, there were seven coal terminal expansions and five rail expansions either committed or under construction at the end of April 2009 Copeland [2009].

The best multi-Hubbert cycle fit of Australia's total coal production is shown in **Figures 4.43** and **4.44**. The production data for bituminous, subbituminous and lignite coals are from the Supplemental Materials to Mohr and Evans [2009]. We predict the peak of production in 2047, and the ultimate coal recovery of 77 Gt. Our estimate is below the "Reserves + Cumulative Production" ($R + C$ = 85.5 Gt) and is the "Best Guess" ($BG = 94$ Gt) in Table B.1 in Mohr and Evans [2009]. Note that this prediction requires more than doubling of the current rate of coal production, or extending it in time at some lower rate, by constraining the "natural" rate. In other words, the higher the peak rate, the steeper future decline will be.

The corresponding match of the rate and cumulative emissions of CO_2 in Australia is shown in **Figures 4.45** and **4.46**. The peak emissions of CO_2 of 2.1 Gt/y are predicted in the year 2042, and the ultimate emissions are 158 Gt of CO_2.

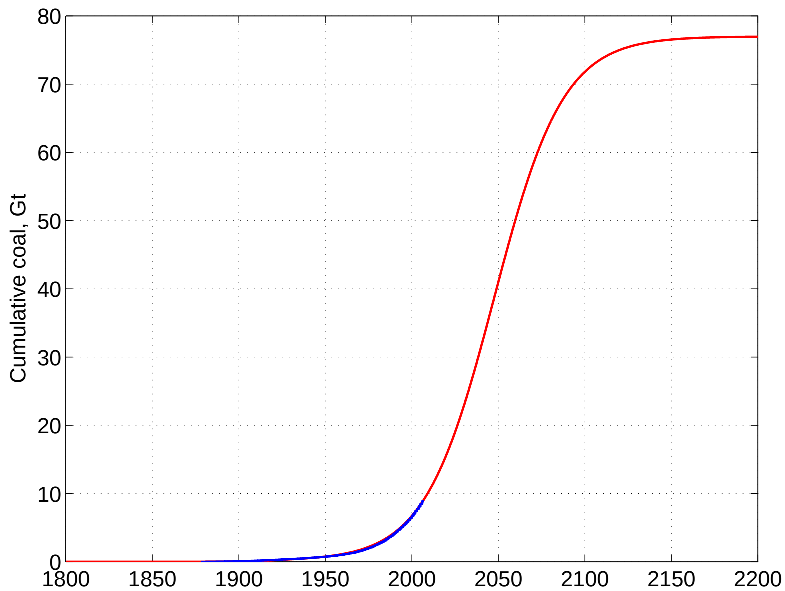

Figure 4.43: The best multi-Hubbert cycle match of the historical cumulative production of bituminous, subbituminous, and lignite coal in Australia. The year of peak production is 2047, and the ultimate coal production is 77 Gt. Data source: Supplemental Materials to Mohr and Evans (2009).

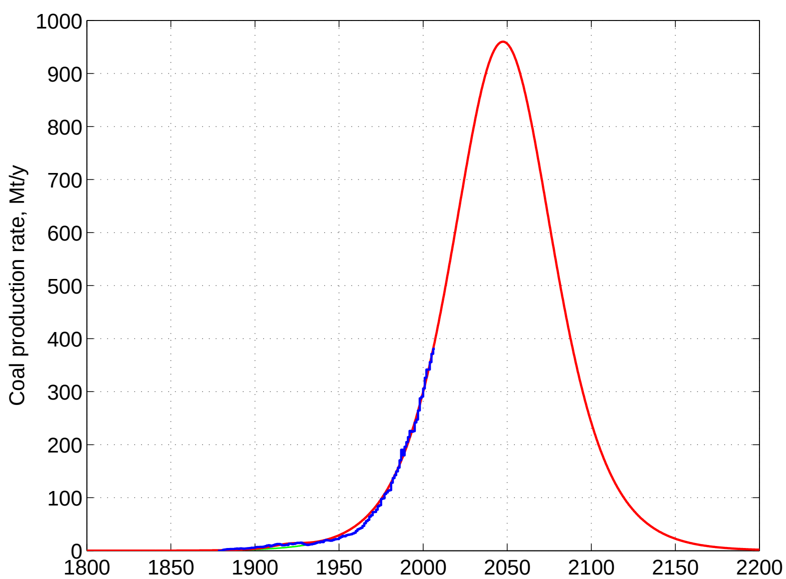

Figure 4.44: The best multi-Hubbert cycle match of the historical rate of production of bituminous, subbituminous, and lignite coal in Australia. Data source: Supplemental Materials to Mohr and Evans (2009).

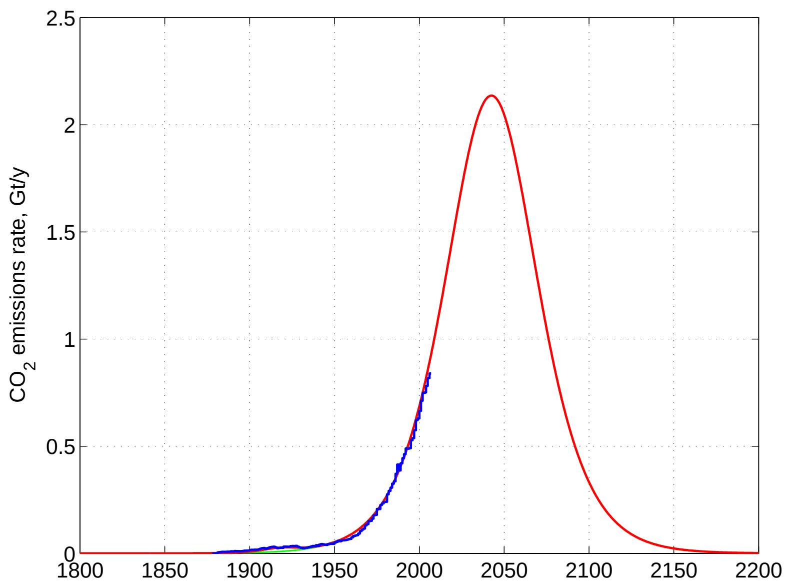

Figure 4.45: The best multi-Hubbert cycle match of the historical rate of CO_2 emissions in Australia. The predicted emission peak in the year 2042 is 2.1 Gt CO_2/y. Data source: Supplemental Materials to Mohr and Evans (2009).

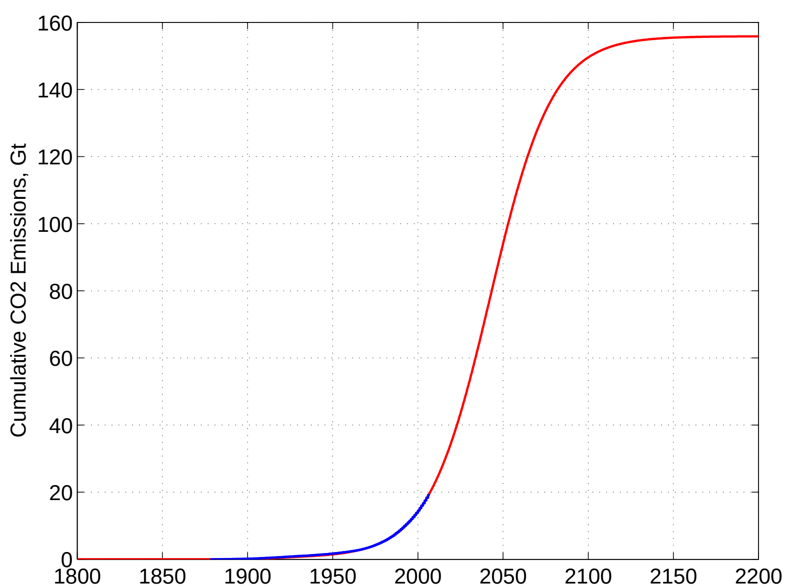

Figure 4.46: The best multi-Hubbert cycle match of the historical cumulative CO_2 emissions in Australia. The year of peak emissions is 2047, and the ultimate emissions are 158 Gt of CO_2. Data source: Supplemental Materials to Mohr and Evans (2009).

4.13.5 Former German Empire

Since Mohr and Evans lumped Germany and some of Poland's coal production data as "German Empire" (sic!), we follow their nomenclature, albeit very reluctantly.[11] Strictly speaking, most of the small Upper Silesian mines and many of the more important Lower Silesian mines, as well as those near the Czech Ostrava, were under German management before WWII.

Germany produces hard coal from the Carboniferous Ruhr, Saar and Aachen basins in the western part of the country. Ruhr is the most important of these, accounting for seven out of eight active hard coal mines. Lignite of Tertiary age is produced from the Rhein Basin in western Germany, as well as in the Leipzig and Lausitz areas. Seams are thick and undisturbed and the lignite is mined by open-cast methods Thomas [2002].

All of Germany's hard coal production is operated by Deutsche Steinkohle. Average working depth has reached 920 meters, resulting in high operating costs. Coal mining has been subsidized as part of Germany's energy security policy, but those subsidies are to be phased out by 2012 in Saarland and by 2018 in the rest of the country. It is anticipated that hard coal mining in Germany will cease at that time Anonymous [2009b]. Not so in Poland; coal production in Poland will continue for the foreseeable future Volkmer [2009].

Poland has three major coalfields; Upper Silesia, Lower Silesia and Lublin. Of these Upper Silesia is the most important, with numerous coal seams as much as 7 meters thick. The basin is structurally complex and coal rank has been increased locally by igneous intrusions Thomas [2002]. The Upper Silesian Basin accounts for more than 80 percent of Polish hard coal reserves, with 14 percent in the Lublin Coal Basin and less than 1 percent in the Lower Silesian Basin. The Lublin Basin was only discovered after 1960 because of thick overburden; coal seam depths there range from 360 to more than 1,000 meters Anonymous [2009d].

Tertiary lignite basins are present in central and southwestern Poland. The lignites range from Paleocene to Miocene in age, with middle Miocene deposits of the greatest economic importance Anonymous [2009e]. Ash and sulfur content is low and the lignite is mined by open-cast methods to supply local electric power plants. The reserves of Poland's four major lignite mines will be exhausted between 2017 and 2045, depending on the mine, but large undeveloped resources remain Volkmer [2009].

The best multi-Hubbert cycle fit of Germany and Poland's total coal production is shown in **Figures 4.47** and **4.48**. The production data for anthracite, bituminous, and lignite coals are from the Supplemental Materials to Mohr and Evans [2009]. Coal production in Germany and Poland peaked in 1987, and the ultimate coal recovery is 53 Gt. Our estimate is somewhat below the "Reserves + Cumulative Production" ($R+C=$ 64.2 Gt) and the "Best Guess" ($BG = 58$ Gt) in Table B.1 in Mohr and Evans [2009]. This makes sense because there is still plenty of producible coal left in Poland.

The corresponding match of the rate and cumulative emissions of CO_2 in the former German Empire is shown in **Figures 4.49** and **4.50**. The peak emissions of CO_2 of 1.4 Gt/y occurred in 1987, and the ultimate emissions are 100 Gt of CO_2.

[11] Patzek was born in a Silesian border mining town, Gliwice, where WWII started with a German provocation.

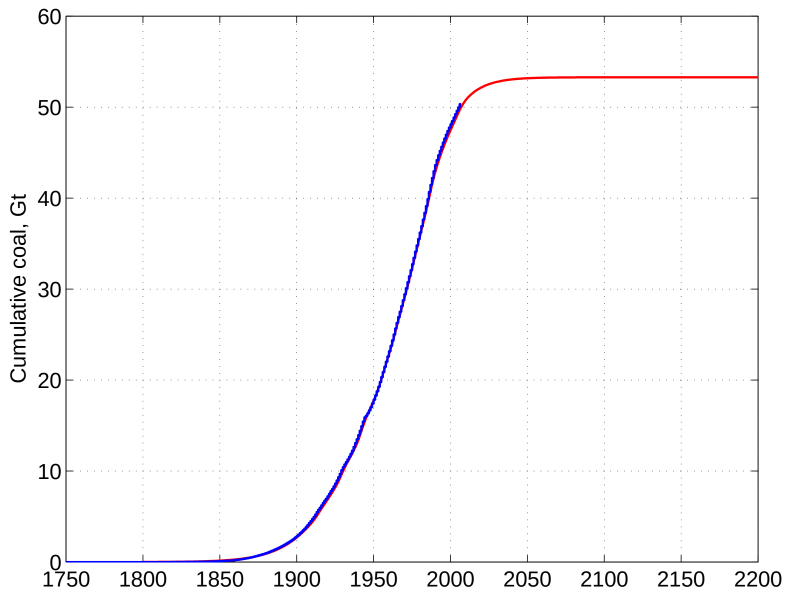

Figure 4.47: The best multi-Hubbert cycle match of the historical cumulative production of anthracite, bituminous and lignite coal in the former German Empire. The year of peak production was 1987, and the ultimate coal production is 53 Gt. Data source: Supplemental Materials to Mohr and Evans (2009).

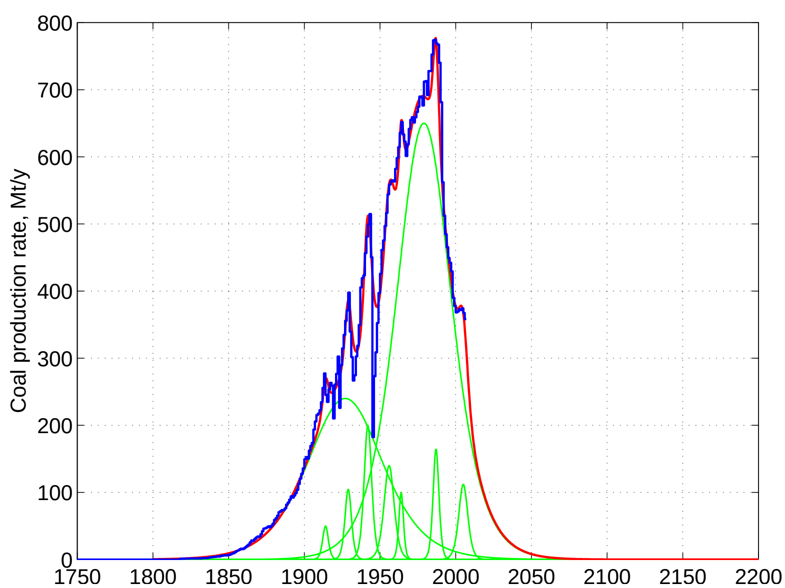

Figure 4.48: The best multi-Hubbert cycle match of the historical rate of production of anthracite, bituminous and lignite coal in the former German Empire. Data source: Supplemental Materials to Mohr and Evans (2009).

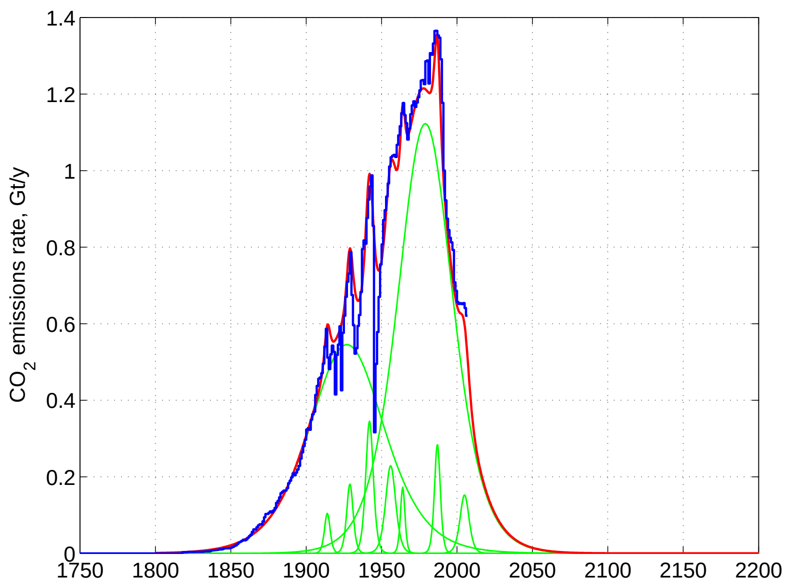

Figure 4.49: The best multi-Hubbert cycle match of the historical rate of CO_2 emissions in the former German Empire. The emission peak in the year 1987 was 1.4 Gt CO_2/y. Data source: Supplemental Materials to Mohr and Evans (2009).

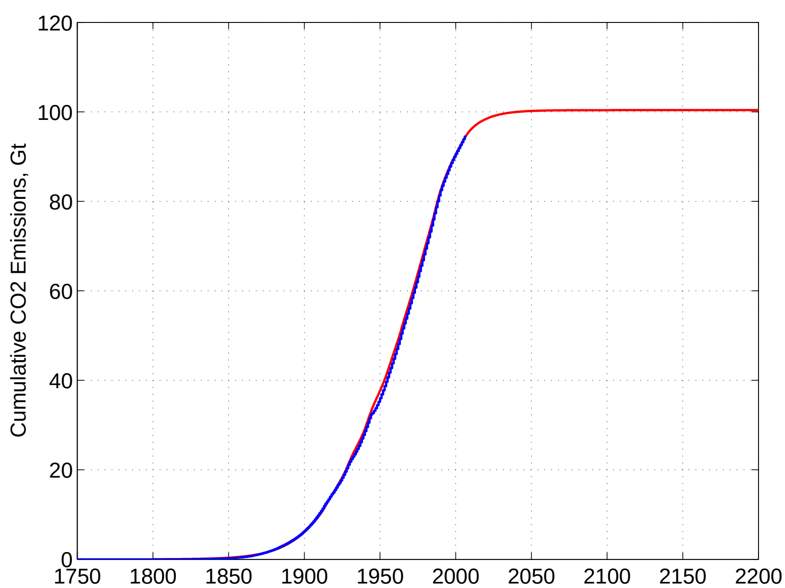

Figure 4.50: The best multi-Hubbert cycle match of the historical cumulative CO_2 emissions in the former German Empire. The year of peak emissions was 1987, and the ultimate emissions are 100 Gt of CO_2. Data source: Supplemental Materials to Mohr and Evans (2009).

4.13.6 The United Kingdom

The United Kingdom has several coal-producing areas. The coals are Carboniferous in age and are principally bituminous, with anthracite locally important in South Wales. Once the most important coal-producing region in the UK, South Wales produced anthracite and low-sulfur bituminous coals from seams 1.0 to 3.5 meters thick Thomas [2002]. The East Pennine coalfield, stretching from Leeds to Nottingham, contains at least 30 workable seams and is currently the most important coalfield in the U.K. It has a long history and was the source for a major coal export trade in the nineteenth century Walker [1993].

The best multi-Hubbert cycle fit of U.K.'s total coal production is shown in **Figures 4.51** and **4.52**. The production data for anthracite, bituminous, and lignite coals are from the Supplemental Materials to Mohr and Evans [2009]. The peak of production was in 1913, and the ultimate coal recovery is 28.3 Gt. This estimated ultimate recovery should be discounted by at least 1 Gt of coal because the numerous strikes of the British coal miners, and the ensuing production stoppages, cannot be captured by the Hubbert cycles. With this discount, our estimate is equal to the "Reserves + Cumulative Production" ($R + C = 27.3$ Gt) and the "Best Guess" ($BG = 27.4$ Gt) in Table B.1 in Mohr and Evans [2009]. Note that today the U.K. produces as much coal as it did in the year 1800.

The corresponding match of the rate and cumulative emissions of CO_2 in the U.K. is shown in **Figures 4.53** and **4.54**. The peak emissions of CO_2 of 0.7 Gt/y occurred in 1913, and the ultimate emissions are 68 Gt of CO_2.

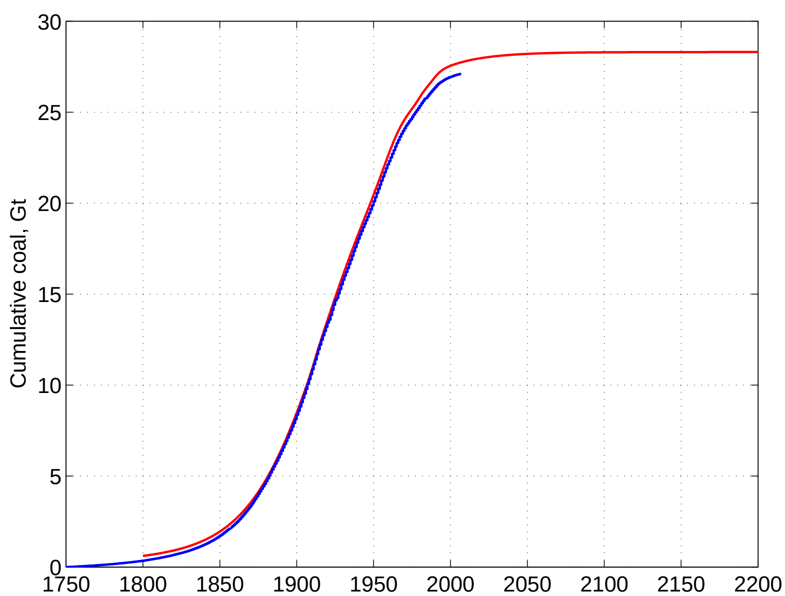

Figure 4.51: The best multi-Hubbert cycle match of the historical cumulative production of anthracite, bituminous and lignite coal in the U.K. The year of peak production was 1913, and the ultimate coal production is 28.3 Gt. Data source: Supplemental Materials to Mohr and Evans (2009).

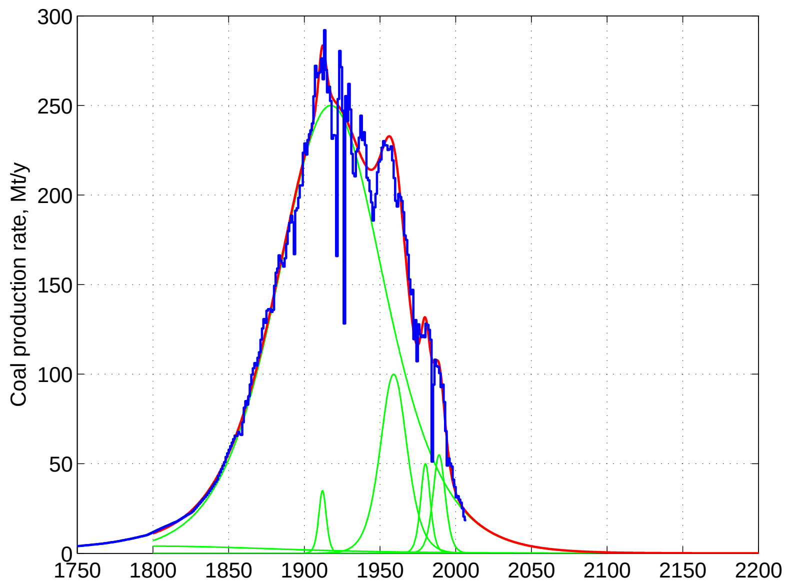

Figure 4.52: The best multi-Hubbert cycle match of the historical rate of production of anthracite, bituminous and lignite coal in the U.K. Note that the several abrupt production stoppages caused by strikes of the British coal miners cannot be captured by the Hubbert-cycle analysis. Data source: Supplemental Materials to Mohr and Evans (2009).

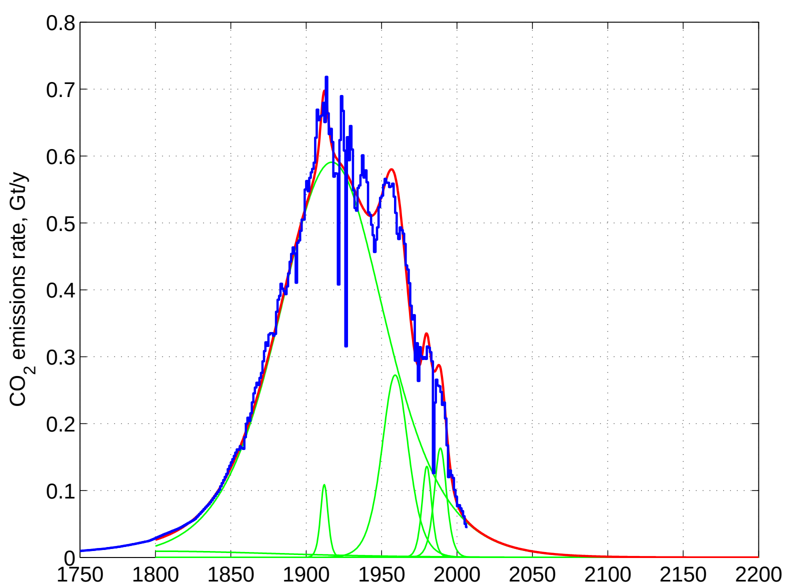

Figure 4.53: The best multi-Hubbert cycle match of the historical rate of CO_2 emissions in the former German Empire. The emission peak in the year 1913 was 0.7 Gt CO_2/y. Data source: Supplemental Materials to Mohr and Evans (2009).

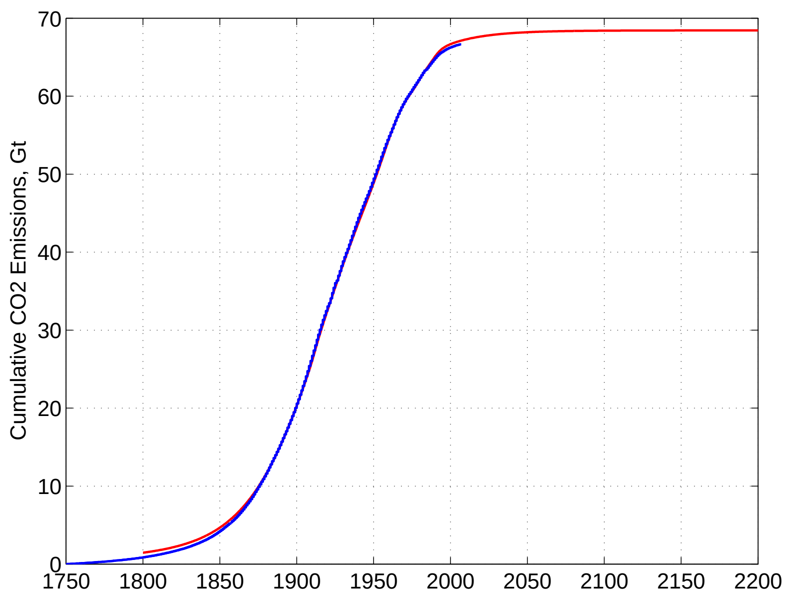

Figure 4.54: The best multi-Hubbert cycle match of the historical cumulative CO_2 emissions in the former German Empire. The year of peak emissions was 1913, and the ultimate emissions are 68 Gt of CO_2. Data source: Supplemental Materials to Mohr and Evans (2009).

4.13.7 India

More than 85 percent of India's coal production is produced by state-owned Coal India Limited (CIL), making it the world's largest coal company. According to its web site, CIL directly employs 425,000 people. The coal fields are in northeastern and east-central India, with 77 percent of proved reserves in the states of Jharkand, Orissa, Chattisgarh and West Bengal[12]. The most important producing area is the Raniganj Basin, north of Calcutta. Although Tertiary-aged coals exist in northeastern India, 99.5 percent of India's proven coal reserves are associated with Gondwana (Permo-Carboniferous) sediments, and the major coal measures are all of Permian age Walker [1993].

Unlike China, 81 percent of India's coal production comes from open-cast mines, but current plans are to increase the proportion of underground mining, see Footnote 12. India's coal production has been growing, but not rapidly enough to satisfy demand growth, see Footnote 1, so imports are increasing. This has resulted in concerns about the coal supply. According to Chikkatur et al [2009]:

> ... recent experiences have thrown into sharp relief the uncertainties and concerns regarding the adequacy of coal supplies to satisfy the growing hunger for power.

The best multi-Hubbert cycle fit of India's total coal production is shown in **Figures 4.55** and **4.56**. The production data for bituminous and lignite coals are from the Supplemental Materials to Mohr and Evans [2009]. We predict the peak of production in 2011, and the ultimate coal recovery of 32.6 Gt. The peak of the broad fundamental Hubbert cycle is in the year 2028. Our production-based estimate is 2 times less than the "Reserves + Cumulative Production" ($R + C$ = 66.7 Gt) and 3 times less than the "Best Guess" (BG = 104.5 Gt) in Table B.1 in Mohr and Evans [2009]. The latter two predictions are from the International Energy Agency.

The corresponding match of the rate and cumulative emissions of CO_2 in India is shown in **Figures 4.57** and **4.58**. The peak emissions of CO_2 of 1.2 Gt/y are predicted in the year 2011, and the ultimate emissions are 79 Gt of CO_2.

[12] Ministry of Coal, *Inventory of Coal Resources of India*, coal.nic.in/reserve2.htm.

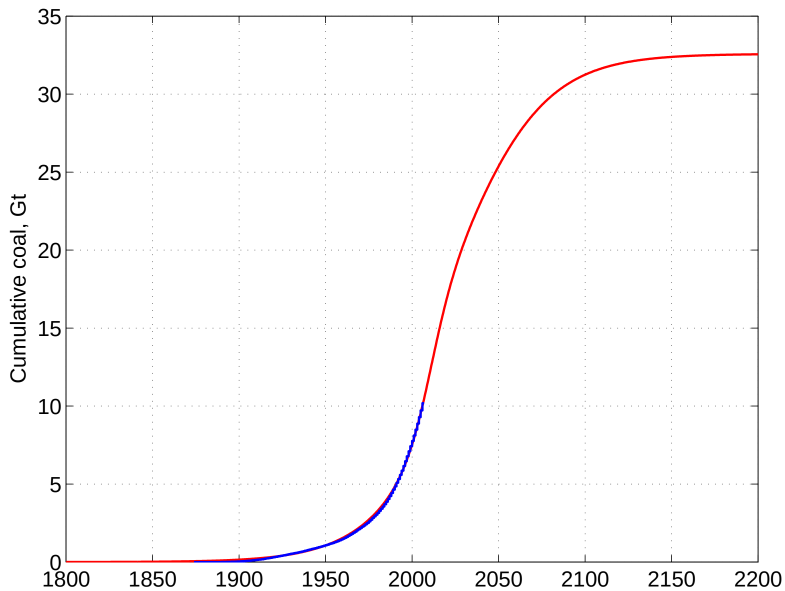

Figure 4.55: The best multi-Hubbert cycle match of the historical cumulative production of bituminous and lignite coal in India. The year of peak production is 2011, and the ultimate coal production is 32.6 Gt. The broad base peak is in the year 2019. Data source: Supplemental Materials to Mohr and Evans (2009).

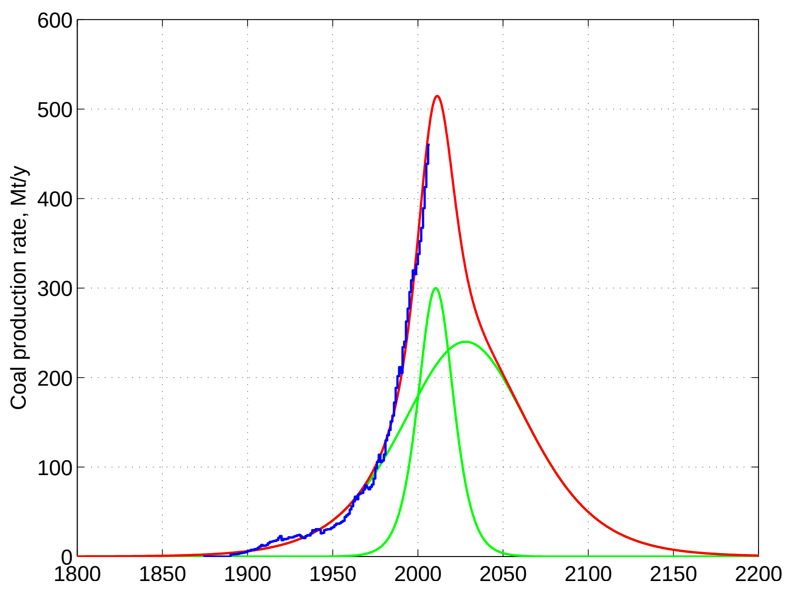

Figure 4.56: The best multi-Hubbert cycle match of the historical rate of production of bituminous, and lignite coal in India. Data source: Supplemental Materials to Mohr and Evans (2009).

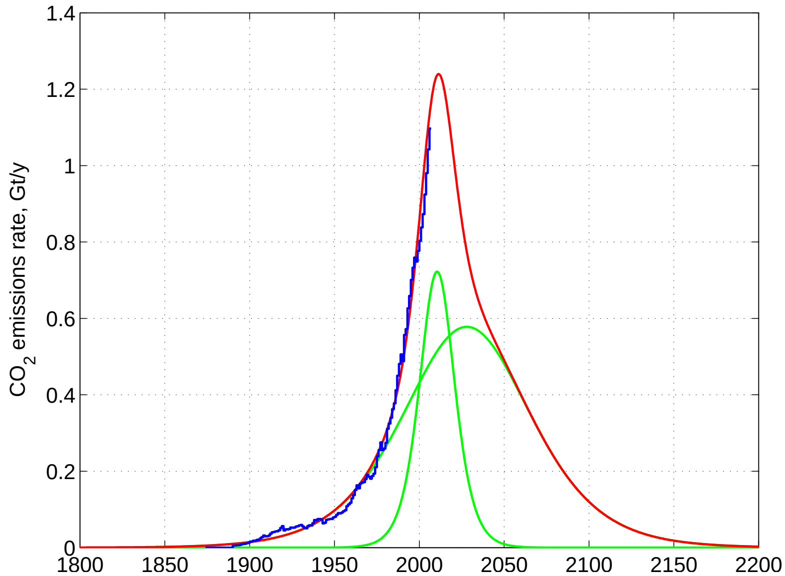

Figure 4.57: The best multi-Hubbert cycle match of the historical rate of CO_2 emissions in India. The predicted emission peak in the year 2011 is 1.2 Gt CO_2/y. Data source: Supplemental Materials to Mohr and Evans (2009).

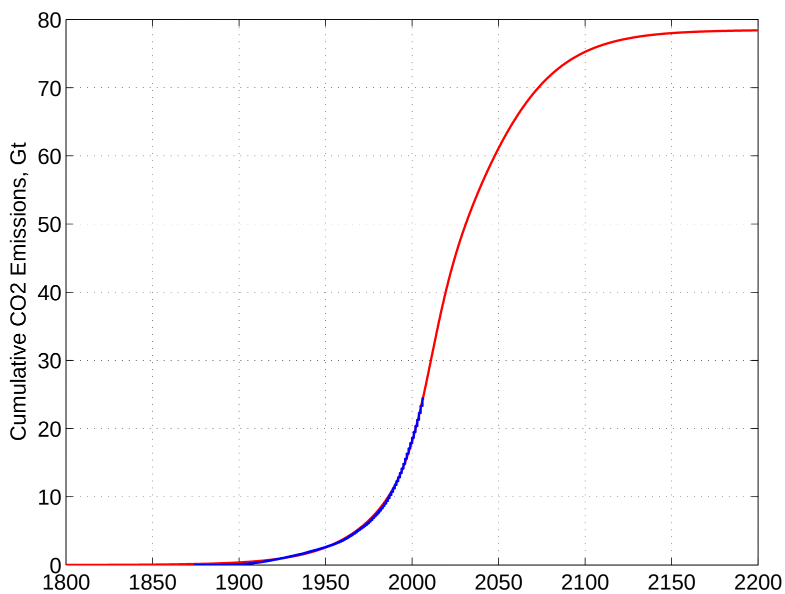

Figure 4.58: The best multi-Hubbert cycle match of the historical cumulative CO_2 emissions in India. The year of peak emissions is 2011, and the ultimate emissions are 79 Gt of CO_2. Data source: Supplemental Materials to Mohr and Evans (2009).

4.13.8 South Africa

South Africa's coal deposits are primarily located in Mpumalanga (formerly Transvaal) and to a lesser extent in KwaZulu-Natal and Free State. These areas are contiguous regions of the Karroo Basin. All reserves are hard coal and are located in the Karroo series of Permian age, which rests upon basement. The coal seams are thick, shallow, and nearly horizontal Thomas [2002]. An important geological point is that the coal deposits sit on basement and are shallow.

About 51 percent of South African coal mining is done underground and about 49 percent is produced by open-cast methods. The coal-mining industry is highly concentrated with five companies accounting for 85 percent of saleable coal production. These companies are Ingwe Collieries Limited (a BHP Billiton subsidiary), Anglo Coal, Sasol, Eyesizwe and Kumba Resources Limited. The eleven largest mines account for 70 percent of South Africa's coal output Anonymous [2009f].

Figures 4.59 – **4.60** are based on the data in the Supplemental Materials to Mohr and Evans [2009]. Our best multi-Hubbert cycle estimate shows the South African coal production already peaking and the ultimate coal recovery of 17.8 Gt. This estimate is identical to the "Linearized Hubbert" ($LH = 18.0$ Gt) estimate in Table B.1 in Mohr and Evans [2009]. A high, single Hubbert peak fit of the data results in the prediction of coal peak in 2035 and ultimate coal recovery of 38.6 Gt that is identical to the "Best Guess" ($BG = 38.7$ Gt) case in Table B.1. One may note, however, that the high case presented in **Figures 4.61** and **4.62** would require the doubling of current peak production in South Africa, or doubling the size and production of current mines there. Circumstantial evidence points to the contrary; most mines only go to about 300 meters depth at most, because the coal deposits sit on basement at that depth. Unlike many other hard coal-producing regions, there is no option of mining deeper seams in the same area. In 2008, the South Africans had to close some mines to save electricity because they had firm export contracts for more coal than they had surplus, resulting in a domestic shortage. As with China, all of the circumstantial evidence points to coal being less abundant than believed, see also Footnote 3.

The corresponding match of the rate and cumulative emissions of CO_2 in South Africa is shown in **Figures 4.63** and **4.64**. The peak emissions of CO_2 of 0.6 Gt/y are predicted in the year 2008, and the ultimate emissions are 44 Gt of CO_2.

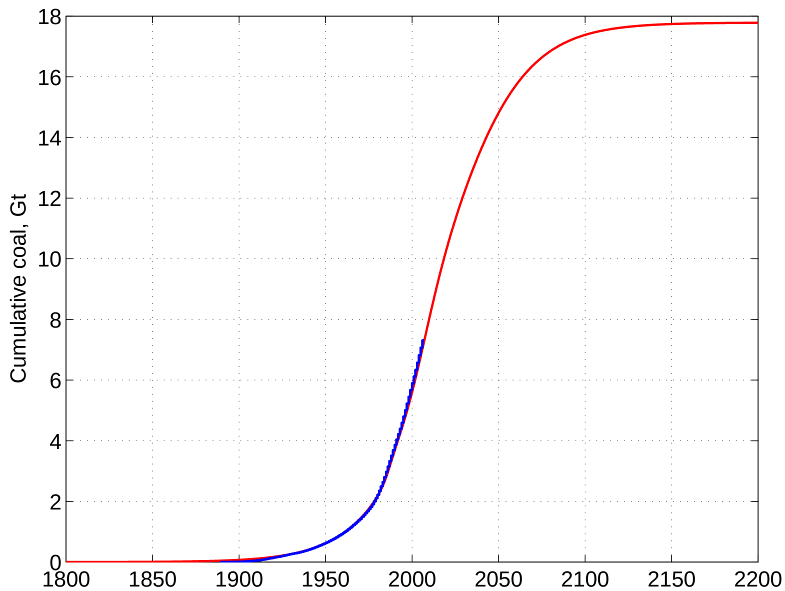

Figure 4.59: The best multi-Hubbert cycle match of the historical cumulative production of anthracite and bituminous coal in South Africa. The year of peak production is 2008, and the ultimate coal production is 18.2 Gt. The broad base peak is in the year 2022. Data source: Supplemental Materials to Mohr and Evans (2009).

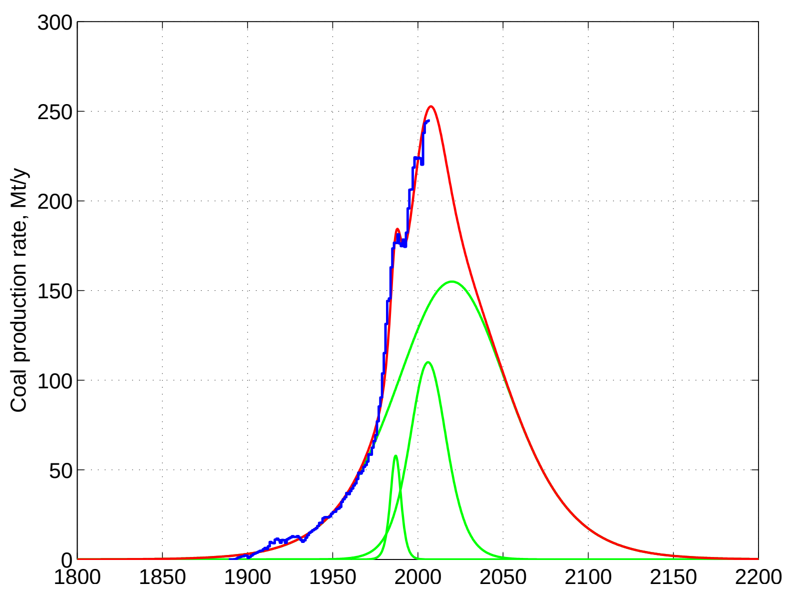

Figure 4.60: The best multi-Hubbert cycle match of the historical rate of production of anthracite and bituminous coal in South Africa. Data source: Supplemental Materials to Mohr and Evans (2009).

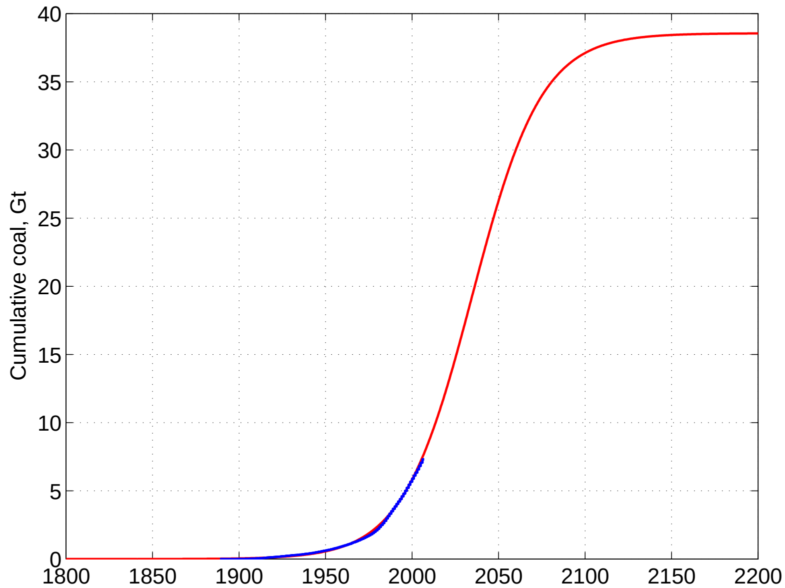

Figure 4.61: A high single-Hubbert cycle match of the historical cumulative production of anthracite and bituminous coal in South Africa. The year of peak production is 2035, the average logistic growth rate is 5 percent, and the ultimate coal production is 38.6 Gt. Given the geology of coal deposits in South Africa, this scenario seems to be impossible. Data source: Supplemental Materials to Mohr and Evans (2009).

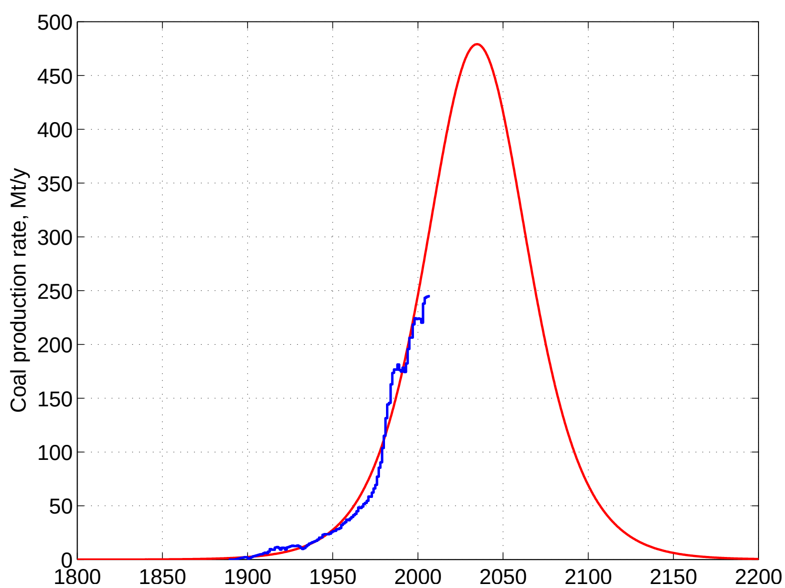

Figure 4.62: A high single-Hubbert cycle match of the historical rate production of anthracite and bituminous coal in South Africa. Data source: Supplemental Materials to Mohr and Evans (2009).

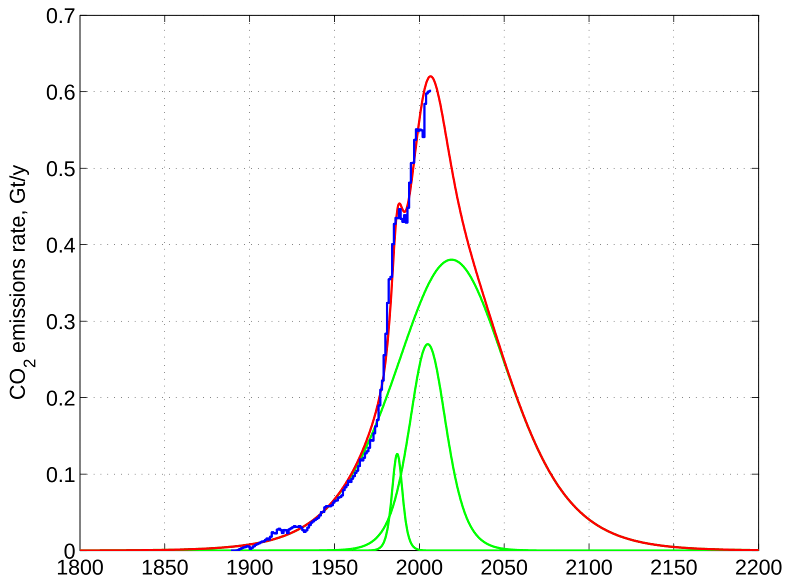

Figure 4.63: The best multi-Hubbert cycle match of the historical rate of CO_2 emissions in South Africa. The predicted emission peak in the year 2008 is 0.6 Gt CO_2/y. Data source: Supplemental Materials to Mohr and Evans (2009).

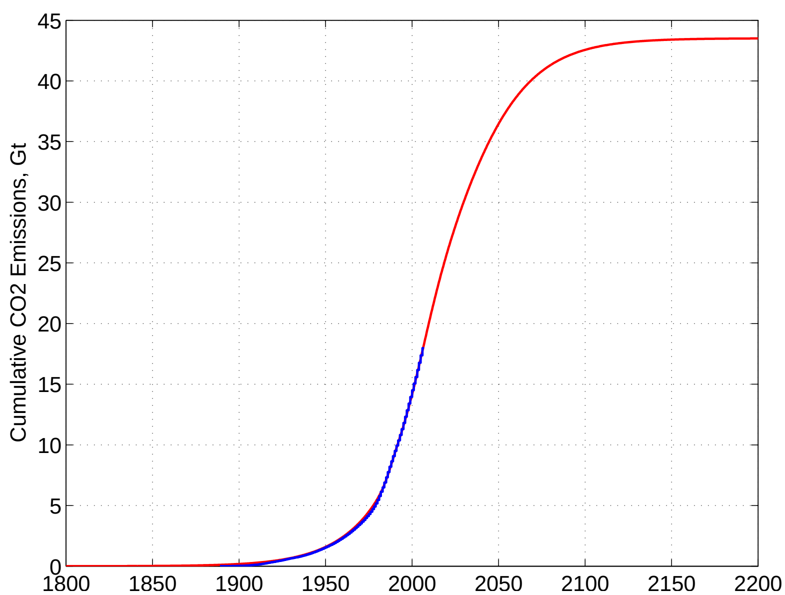

Figure 4.64: The best multi-Hubbert cycle match of the historical cumulative CO_2 emissions in South Africa. The year of peak emissions is 2008, and the ultimate emissions are 44 Gt of CO_2. Data source: Supplemental Materials to Mohr and Evans (2009).

4.13.9 Indonesia

Indonesia has two coal-producing regions, the islands of Sumatra and Borneo. Coal from Sumatra is largely consumed by power generation and coal from Kalimantan (the Indonesian part of the island of Borneo) is largely exported. The coal is entirely Tertiary in age and ranges from lignite to anthracite Walker [1993]. Seams are up to 10 meters thick in East and South Kalimantan, where igneous activity has locally increased the rank of the coal. Seams of sub-bituminous coal are up to 12 meters thick at Bukit Asam, southeastern Sumatra Thomas [2002].

Thick coal seems, shallow mining depths, and low labor costs make Indonesia a very low-cost coal producer. The presence of substantial low-cost coal reserves that are close to ports along a major shipping route has made Kalimantan a major source of thermal coal exports. Borneo Coal Indonesia exports five grades, ranging from 22 to 26 MJ per kilogram. All coals are less than 1 percent sulfur, and the 22 and 24 MJ/kg grades are less than 7 percent ash Anonymous [2009g].

The best single Hubbert cycle fit of Indonesia's total coal production is shown in **Figures 4.65** and **4.66**. The production data for anthracite and bituminous coals are from the Supplemental Materials to Mohr and Evans [2009]. We predict the peak of production in 2014, and the ultimate coal recovery of 5.6 Gt. Our estimate is identical to the "Reserves + Cumulative Production" ($R + C = 5.6$ Gt) and the "Best Guess" ($BG = 5.6$ Gt) in Table B.1 in Mohr and Evans [2009].

The corresponding match of the rate and cumulative emissions of CO_2 in Indonesia is shown in **Figures 4.67** and **4.68**. The peak emissions of CO_2 of 0.54 Gt/y are predicted in the year 2014, and the ultimate emissions are 12.2 Gt of CO_2.

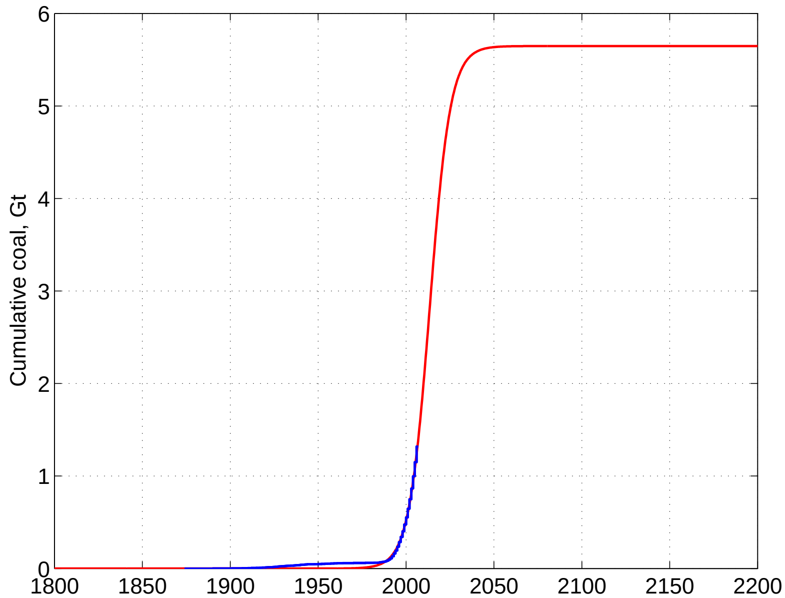

Figure 4.65: The best single Hubbert cycle match of the historical cumulative production of anthracite and bituminous coal in Indonesia. The year of peak production is 2014, and the ultimate coal production is 5.6 Gt. Data source: Supplemental Materials to Mohr and Evans (2009).

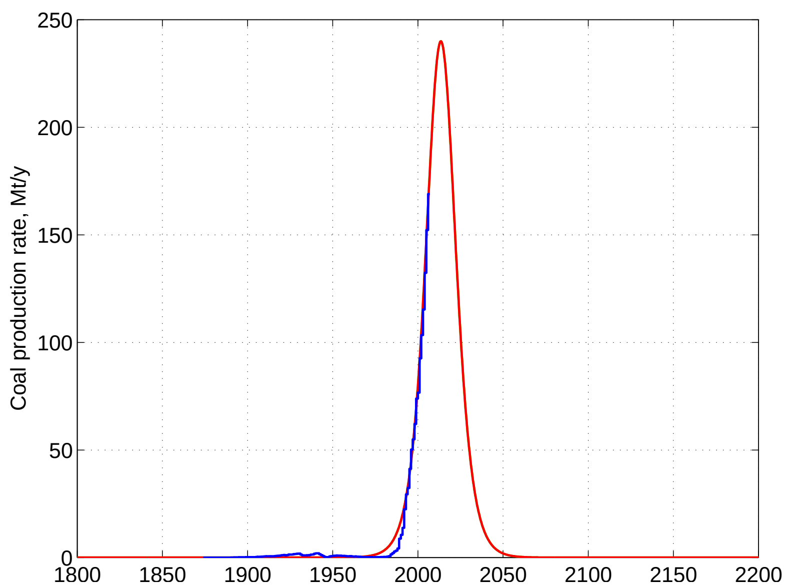

Figure 4.66: The best single Hubbert cycle match of the historical rate of production of anthracite and bituminous coal in Indonesia. Data source: Supplemental Materials to Mohr and Evans (2009).

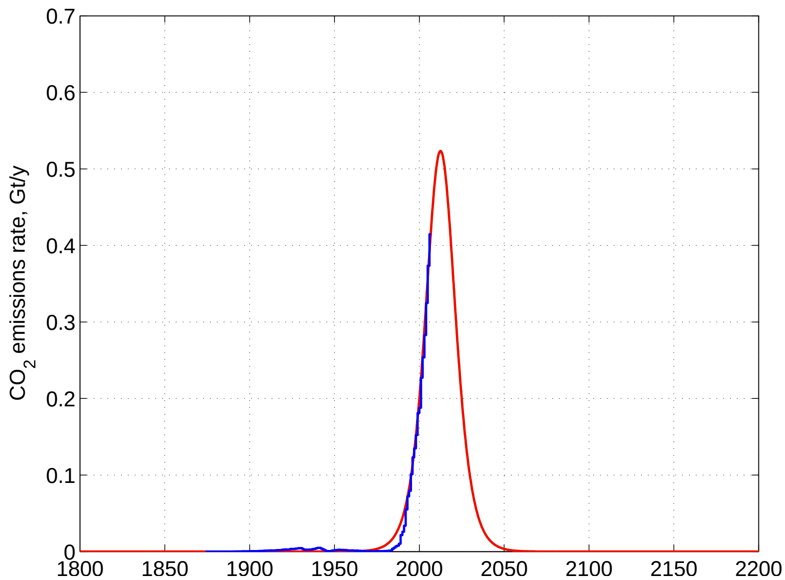

Figure 4.67: The best multi-Hubbert cycle match of the historical rate of CO_2 emissions in Indonesia. The predicted emission peak in the year 2014 is 0.54 Gt CO_2/y. Data source: Supplemental Materials to Mohr and Evans (2009).

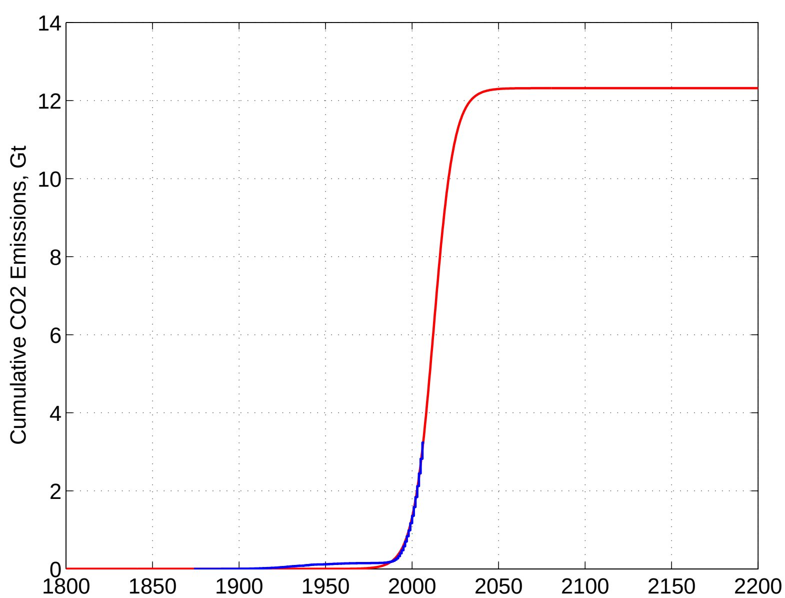

Figure 4.68: The best multi-Hubbert cycle match of the historical cumulative CO_2 emissions in Indonesia. The year of peak emissions is 2014, and the ultimate emissions are 12.2 Gt of CO_2. Data source: Supplemental Materials to Mohr and Evans (2009).

4.13.10 Mongolia

Most of Mongolia's coal resources are located in the north of the country. The Baganuur coal field in northern Mongolia contains low-sulfur, Cretaceous coals up to 25 meters thick. Other coalfields in northern Mongolia are Sharin Gol, Nalayh, Achit Nuur, and Khartarbagat. Also in northern Mongolia, highly tectonized Paleozoic coals are found in numerous small, isolated deposits. These are anthracite or low-volatile bituminous Thomas [2002].

The Tavan Tolgoi deposit in the Permian Southern Gobi Basin of southern Mongolia contains an estimated 6 billion tons of bituminous coal, about one-third of which is coking-quality, but its remote location prevented development until 2003. Production reached 1 million metric tons in 2007 and the coal is exported to China. The mine contains 16 major coal seams totaling 74.9 meters in thickness Anonymous [2009h].

The best multi-Hubbert cycle fit of Mongolia's total coal production is shown in **Figures 4.69** and **4.70**. The production data for bituminous and lignite coals are from the Supplemental Materials to Mohr and Evans [2009]. We predict the peak of production in 2100, and the ultimate coal recovery of 15.7 Gt. The peak of the small Hubbert cycle was in the year 1988. Our production-based estimate is 6 times less than the "Reserves + Cumulative Production" ($R{+}C = 100.2$ Gt) and is equal to the "Best Guess" ($BG = 15.2$ Gt) in Table B.1 in Mohr and Evans [2009]. The higher prediction is from an advertising section for Mongolia's Business Opportunities.[13]

The corresponding match of the rate and cumulative emissions of CO_2 in Mongolia is shown in **Figures 4.71** and **4.72**. The peak emissions of CO_2 of 0.3 Gt/y are predicted in the year 2100, and the ultimate emissions are 25 Gt of CO_2.

[13] *Mongolia: Business Opportunities for 2005, Special Advertising Section*, Fortune Magazine, www.timeinc.net/fortune/services/sections/fortune/intl/ media/2005_09mongolia.pdf, September 2005. Accessed on 07.04.2009.

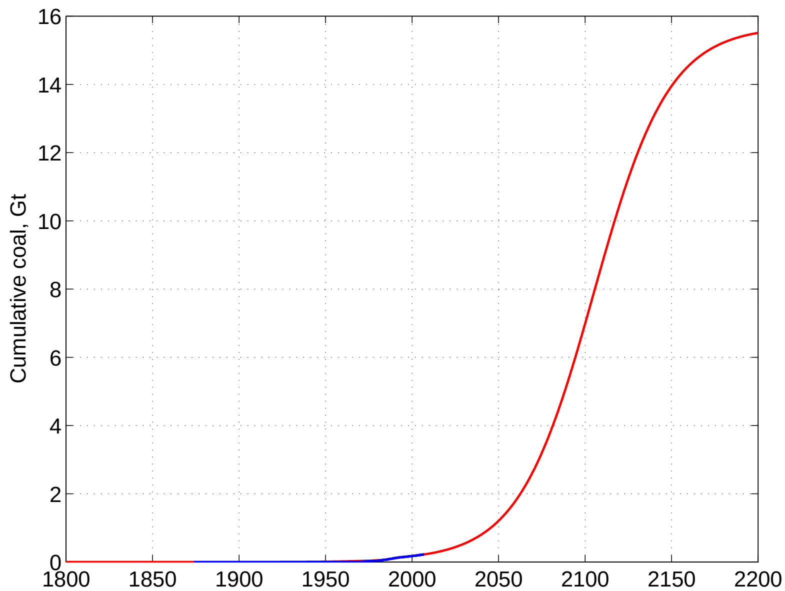

Figure 4.69: The best multi-Hubbert cycle match of the historical cumulative production of bituminous and lignite coal in Mongolia. The year of peak production is 2100, and the ultimate coal production is 15.7 Gt. Data source: Supplemental Materials to Mohr and Evans (2009).

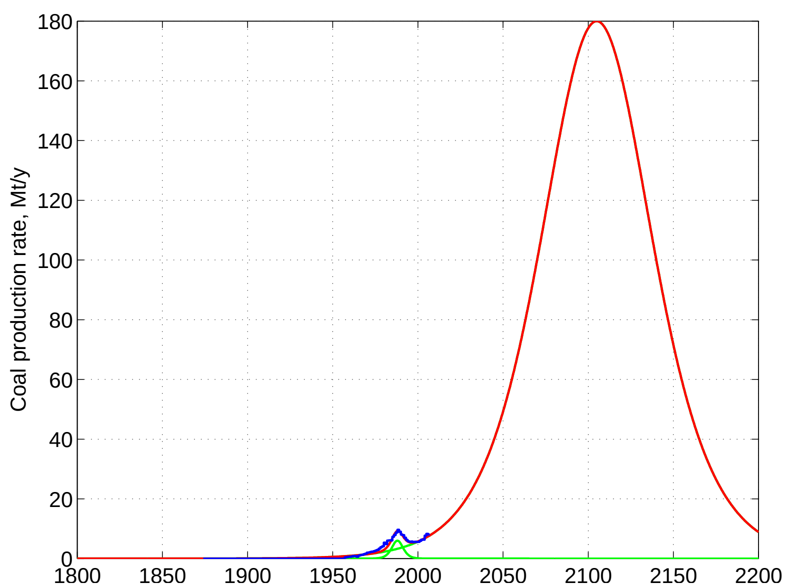

Figure 4.70: The best multi-Hubbert cycle match of the historical rate of production of bituminous, and lignite coal in Mongolia. The small peak is in the year 1998. Data source: Supplemental Materials to Mohr and Evans (2009).

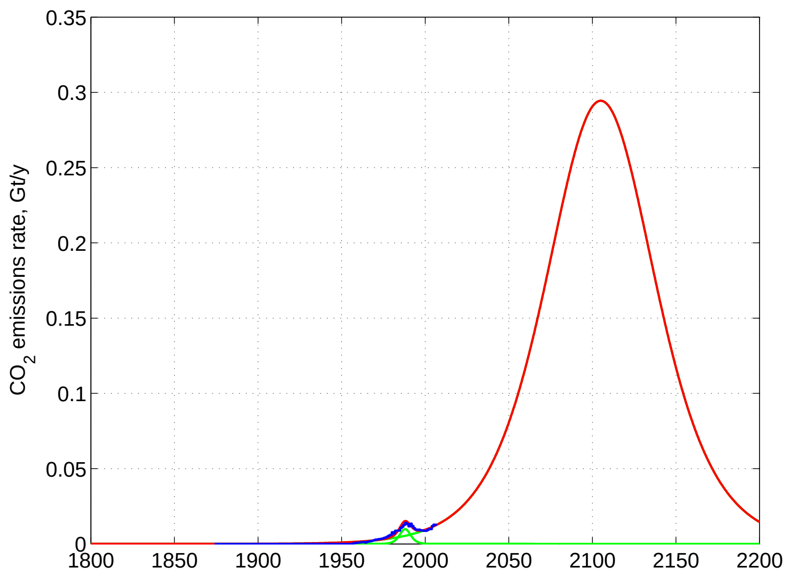

Figure 4.71: The best multi-Hubbert cycle match of the historical rate of CO_2 emissions in Mongolia. The predicted emission peak in the year 2100 is 0.3 Gt CO_2/y. Data source: Supplemental Materials to Mohr and Evans (2009).

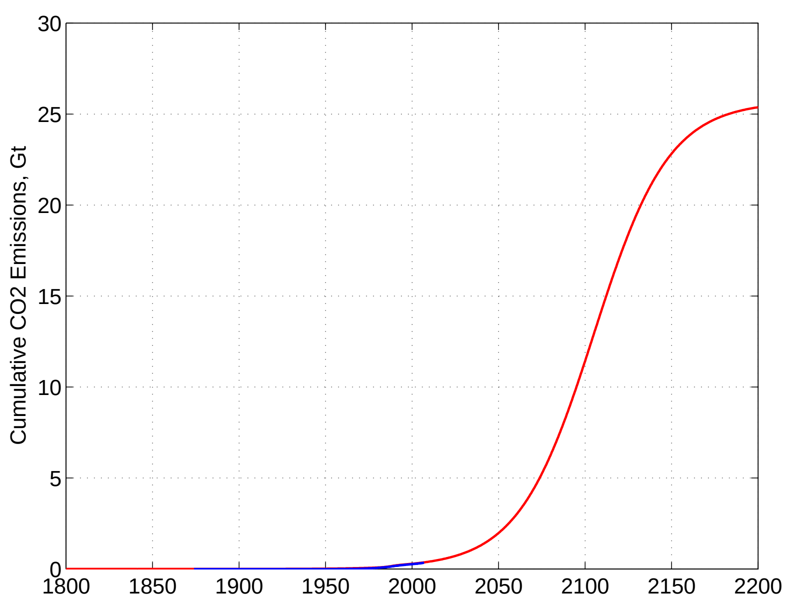

Figure 4.72: The best multi-Hubbert cycle match of the historical cumulative CO_2 emissions in Mongolia. The year of peak emissions is 2100, and the ultimate emissions are 25 Gt of CO_2. Data source: Supplemental Materials to Mohr and Evans (2009).

Chapter 5

Options for the Supply of Transportation Fuels to California

5.1 Abstract

Transportation in California is fueled by oil. Once an oil exporter, California now depends on imports for more than 60 percent of its oil supply. This paper examines the oil production outlook for each of California's major oil sources, including California itself. Oil production trends, published geological and engineering reports, and proposed developments in California's supply area are reviewed to define supply trends, especially for the medium-to-heavy, sour crudes that are processed in California's refineries. Refinery upgrading capacity is already highly developed in California, thus it is assumed that a competitive advantage in heavy, sour crudes will continue, although refining heavy oil releases more carbon dioxide.

About a quarter of California's imports are from Alaska, the rest from foreign sources including Saudi Arabia, Ecuador and Iraq. Before foreign sources became so important, California's refining industry processed California's own crudes and Alaska's North Slope crude. Like those crudes, oil from northern Saudi Arabia, southeast Iraq, and Ecuador is also sour and medium to heavy, ranging from 16 to 35 API and from 2 to more than 3 percent sulfur by weight. By far the most important sour crude development in California's supply area is Saudi Arabia's 900,000 BOPD Manifa project, originally slated for completion in 2011 but now facing delays. Manifa contains oil that ranges from 26 to 31 API and from 2.8 to 3.7 percent sulfur. Over the longer term, Alaska will continue to play an important supply role if the Chuckchi and Beaufort Seas live up to expectations.

Middle East production is not increasing, yet oil cargoes from the Middle East have to pass growing Asian markets to reach California. Alaska and Mexico also supply oil to the Pacific Basin, but are facing production declines. The effect of rising Asian demand on Pacific Basin oil markets is already visible, with significant amounts of oil coming to California from Atlantic Basin sources such as Angola, Brazil, and Argentina.

The US West Coast pipeline system is separate from the integrated East Coast, Gulf Coast and Midwest system, so energy security issues for the West Coast may differ from those of the country as a whole. There are policy options that could affect California's

oil supply security, including increased oil development in Alaska or offshore California, development of additional oil pipeline outlets on Canada's Pacific Coast or substituting natural gas for oil if possible. All of these policy options are currently the subject of political debate.

5.2 Historical Oil Production Trends in California's Supply Area

Historical oil production trends are of interest because, unlike reserve estimates, they are readily verifiable factual information. Another issue with published reserve data is the quality of the supporting information; Alberta produces a detailed annual reserves report, while Saudi Arabia and Iraq publish only national aggregate figures. All of the oil production volumes reported in this section are from the annual production survey of the Oil and Gas Journal or the annual report of the Alaska Division of Oil and Gas and do not include natural gas plant liquids.

Iraq's oil production peaked in 1979 at 3.43 million BOPD. In 2007 it was 2.09 million BOPD, but production levels had been affected by internal instability and were higher in 2008.

Saudi Arabia's oil production peaked in 1981 at 9.64 million BOPD. The Saudis have consistently claimed a productive capacity substantially greater than this, but have not produced as much since, even in times of high oil prices. In 2007 Saudi oil production was 8.63 million BOPD.

California's own oil production peaked in 1985 at 1.1 million BOPD. By 2006 it had declined to 685,000 BOPD. California's heavy oil fields have been intensively developed and production from them is expected to decline further.

Alaska's oil production peaked in 1988 at 2.14 million BOPD; in 2007 it was 756,000 BOPD. Alaska's oil production is dominated by the Prudhoe Bay Field, which is at an advanced stage of decline, but substantial exploration potential remains, both onshore and offshore.

Oil production in Mexico peaked in 2004 at 3.38 million BOPD; in 2007 it produced 3.08 million BOPD. Mexico's oil production is expected to continue to decline because of the increasing maturity of the offshore oil fields in the Gulf of Campeche.

Ecuador's oil production was 535,000 BOPD in 2006, but in 2007 it was only 499,000 BOPD. One year of declining production may be a result of many factors, and is not necessarily indicative of near-term supply problems.

The oil production levels of Angola, Brazil, and Canada are currently at all-time highs due to increased heavy oil development in Canada, and to deep offshore discoveries in Brazil and Angola. These 'ABC' countries are likely to play an increasing role in California's oil supply.

5.3 California's Oil Production

Although California's oil production did not peak until 1985, its importance in the world of oil was greatest around 1925, when California accounted for more than 22 percent of world oil production American Petroleum Institute [1993]. This was the peak of development of the Los Angeles Basin oil fields, but before the discovery of the East Texas Field or the development of the Permian Basin. Figure 5.1 shows the relative importance of different oil-producing regions in 1925.

Because of California's history as an oil producing and exporting province, its refining industry was originally built to process local crudes. Table 5.1 shows the API gravity and sulfur content of two of the most important California crude streams.

Table 5.1: California oil properties, Selected Crudes
Guerard [1984]

Field	Kern River	Wilmington
API Gravity	12.6	19.4
Sulfur Content	1.19 %	1.59 %
Viscosity@100F	6,000 cp	470 cp

California produced 683,000 BOPD in 2006. Of this production, 409,000 BOPD was heavy oil, and 113,000 BOPD of the total was produced offshore California Division of Oil and Gas [2006].

California's Heavy Oil Production is dominated by four large, steam-enhanced oil production projects in Kern County. These are the Midway-Sunset, Kern River and Cymric Fields, and the Tulare Sand in South Belridge Field. These four projects accounted for about 69 percent of California's heavy oil production in 2006. All of these are declining except for Cymric, which has had its life extended by the development of a deeper reservoir, the Etchegoin. The recent production history of these four projects is shown in Figure 5.2. Note that the values shown in the figure for South Belridge are for the Tulare sand only and do not include the light oil production from the Belridge Diatomite. Although the production of large amounts of incremental heavy oil from these reservoirs is a great technical accomplishment, that same success now makes further production declines inevitable because about half of the OOIP has already been produced.

Other known heavy oil and tar sand deposits in California have not been developed because the oil is too viscous. The largest of these, the Foxen Tar Sand in the Santa Maria Basin, is estimated to have 2 billion barrels of OOIP while other known tar sands at Oxnard, Arroyo Grande and Paris Valley have less than 1 billion barrels of OOIP in aggregate Hallmark [1982]. This compares to estimated OOIP of 6.2 billion barrels for the Midway-Sunset Field and 4.1 billion barrels for the Kern River Field Roadifer [1986]. The conclusion is that these undeveloped oil accumulations are smaller than existing major projects and are not likely to arrest onshore production declines. The greatest potential for increasing California's oil production probably lies offshore.

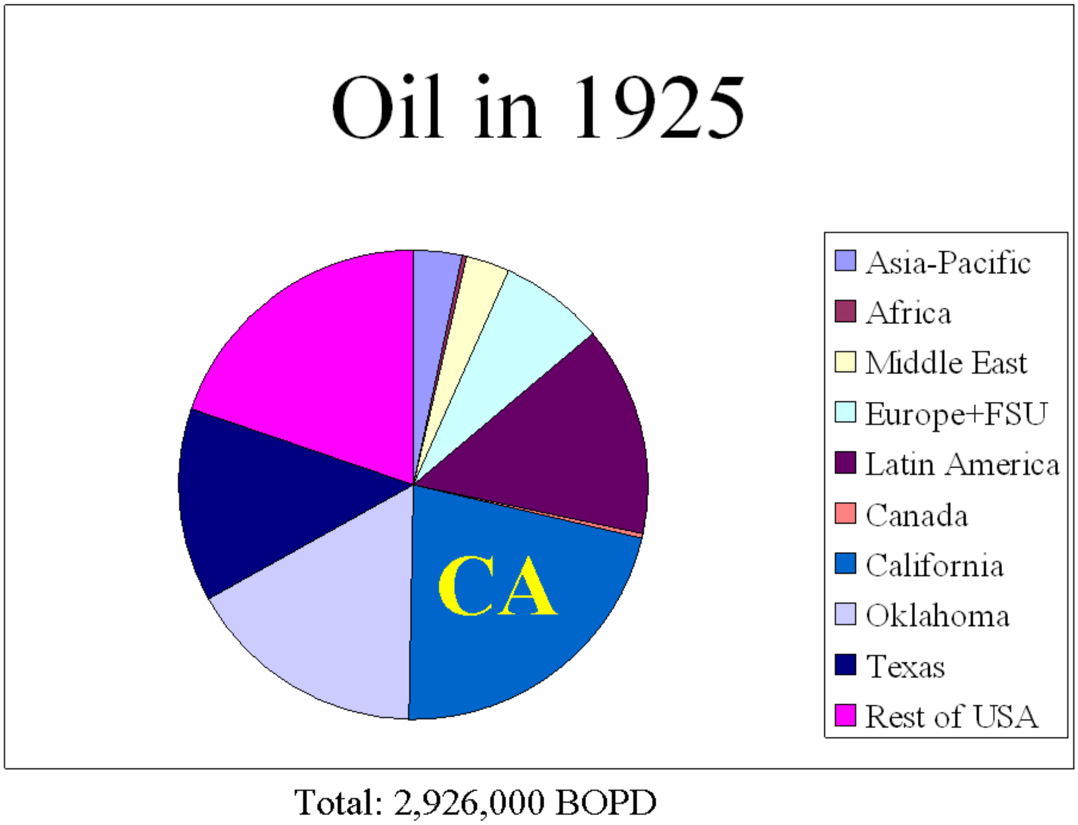

Figure 5.1: World Oil Production in 1925
Data source: API.

5.3.1 Offshore California

One of the few areas in the world that has large, undeveloped oil reserves is offshore California. Offshore oil production from wooden piers began at Summerland around 1890. There were concerns about the impact of offshore drilling even early in its history, so a compromise was reached in which all of the state offshore royalties were dedicated for many years to the Department of Beaches and Parks.

A major oil spill in 1969 strengthened opposition to offshore drilling and today there is in practice a ban on new platform installations. This has not prevented all new field developments; Bonito and Sword are recent extended-reach developments from existing platforms. Large heavy oil fields north of Point Sal are far from existing infrastructure and remain undeveloped. Figure 5.3 shows developed and undeveloped oil fields around Santa Barbara County. The offshore field outlines in the figure are from MMS and the onshore field outlines are from the California Division of Oil and Gas. Although only a small part of the California Coastline is shown in the figure, it includes most of the known offshore oil reserves of the state. These were estimated at 303 million barrels of remaining proved reserves, 1.166 billion barrels of remaining unproved reserves, and 149

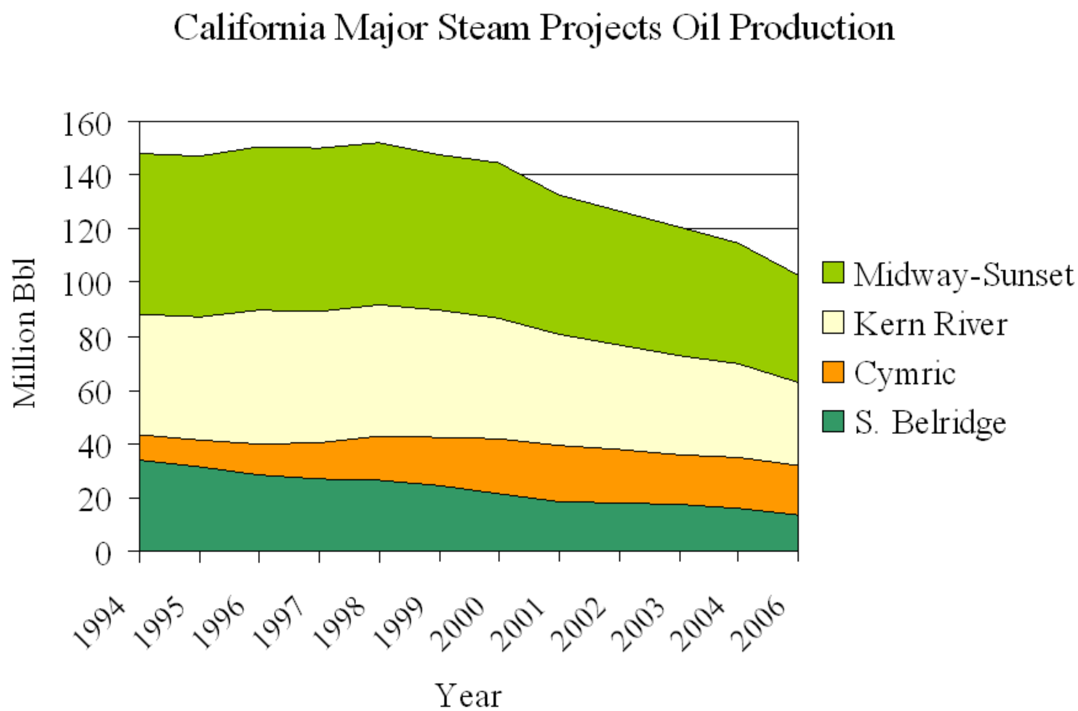

Figure 5.2: California Major Steam Projects Oil Production
California Division of Oil and Gas [2006]

million barrels of known resources on expired leases at yearend 2003 (Syms and Voskanian [2007]).

In addition to these known fields, there is considerable exploration potential offshore California. That potential is greatest offshore Southern California, but is also significant offshore Central and Northern California. At a 46 dollar per barrel price assumption, the undiscovered economically recoverable oil resources offshore Southern, Central and Northern California are estimated at 3.9, 1.9 and 1.5 billion barrels respectively Minerals Management Service [2006]. This 7.3 billion barrel total rises to 8.6 billion barrels in the 80 dollar per barrel case. Resources of this magnitude could represent a significant addition to California's oil supply.

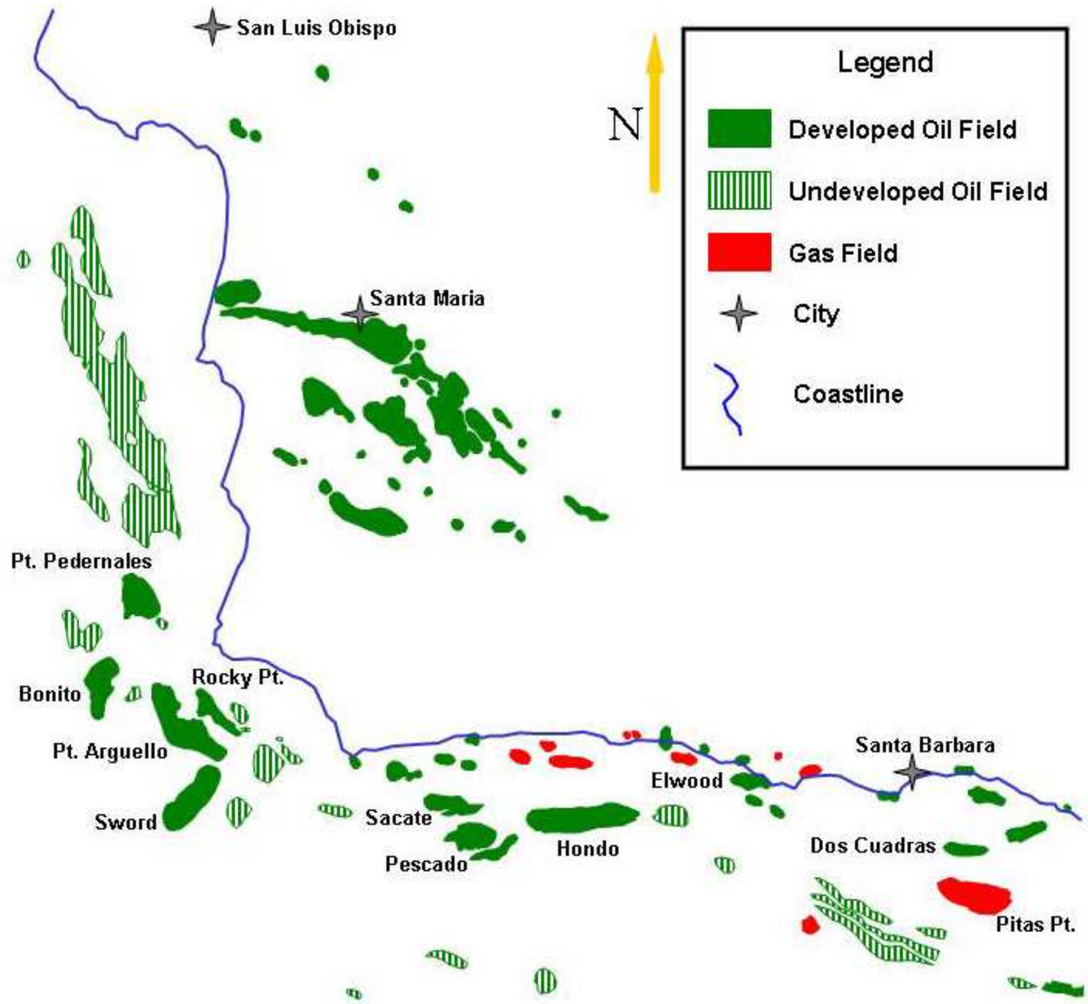

Figure 5.3: Offshore California Index Map

5.4 Alaska

Alaska's oil production is currently about a third of its 1988 peak. Alaska is a very high cost area, so low oil prices discouraged development from 1986 until about 2005. In addition, the Trans-Alaska Pipeline partners benefit from the substantial tariff, which gives them a competitive advantage. Figure 5.4 shows the history and projections for North Slope oil production. This figure is based on remaining reserves in existing fields. The important observation is that existing and proposed Alaskan developments are not likely to provide a major increase in Alaskan oil supply; major new developments would be needed.

Much of the discussion of oil development on Alaska's North Slope centers on the coastal plain of the Arctic National Wildlife Refuge. The area in question is only a very small part of the North Slope, and an important structure within it was tested by an exploratory well in 1986 - 1987. The well was drilled on a native inholding in the 1002 area. The results of this well and several others were not used by the USGS in its assessment of ANWR potential for confidentiality reasons.

The Chukchi and Beaufort Seas have large oil potential, as evidenced by the number of tracts receiving bids in recent federal lease sales. Chukchi Sea lease sale 193 in 2008 received 2.66 billion dollars in winning bids on 488 blocks Minerals Management Service [2008]. In the Beaufort Sea, 2007 lease sale 202 received 42 million dollars in winning bids on 92 blocks Minerals Management Service [2007] and 2005 lease sale 195 received 47 million dollars in winning bids on 121 blocks Minerals Management Service [2005]. These tracts could contain sufficient resources to offset the projected declines shown in Figure 5.4. The undiscovered economically recoverable oil resources in federal waters offshore Alaska are estimated at 8.35 billion barrels at a 46 dollar per barrel price assumption, and 21.5 billion barrels in the 80 dollar per barrel case Minerals Management Service [2006]. Note that the offshore Alaska resource estimates are more sensitive to oil prices than those offshore California.

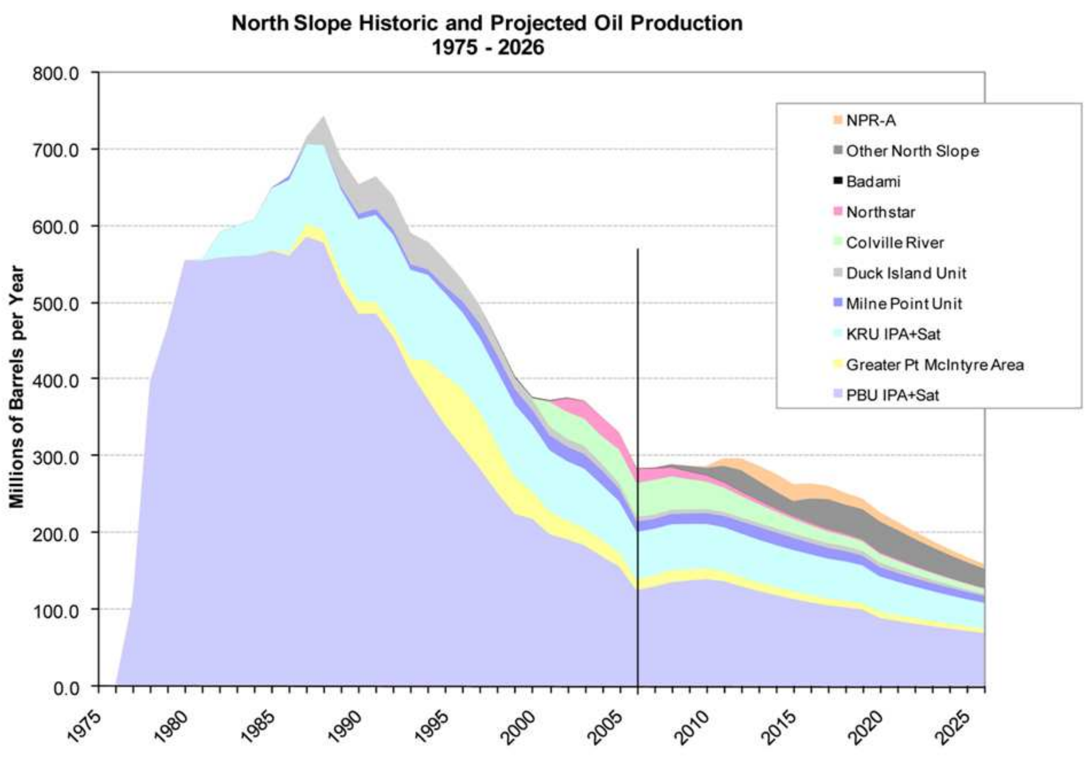

Figure 5.4: Projection of North Slope Production
Alaska Division of Oil and Gas [2008]

5.5 Foreign Sources of Oil to California

Figure 5.5 shows the countries of origin for California's foreign crude receipts from 2000 through 2005. Note the dominance of Saudi Arabia, Ecuador and Iraq, with Mexico coming in a distant fourth in oil supply to California. Another important development is the appearance of Angola, Brazil and Canada as significant suppliers in 2005.

California's oil sources are the main suppliers of heavy, sour crudes to the Pacific Basin. For this reason, California competes directly with other Pacific Rim consumers that have the ability to process these heavier oils.

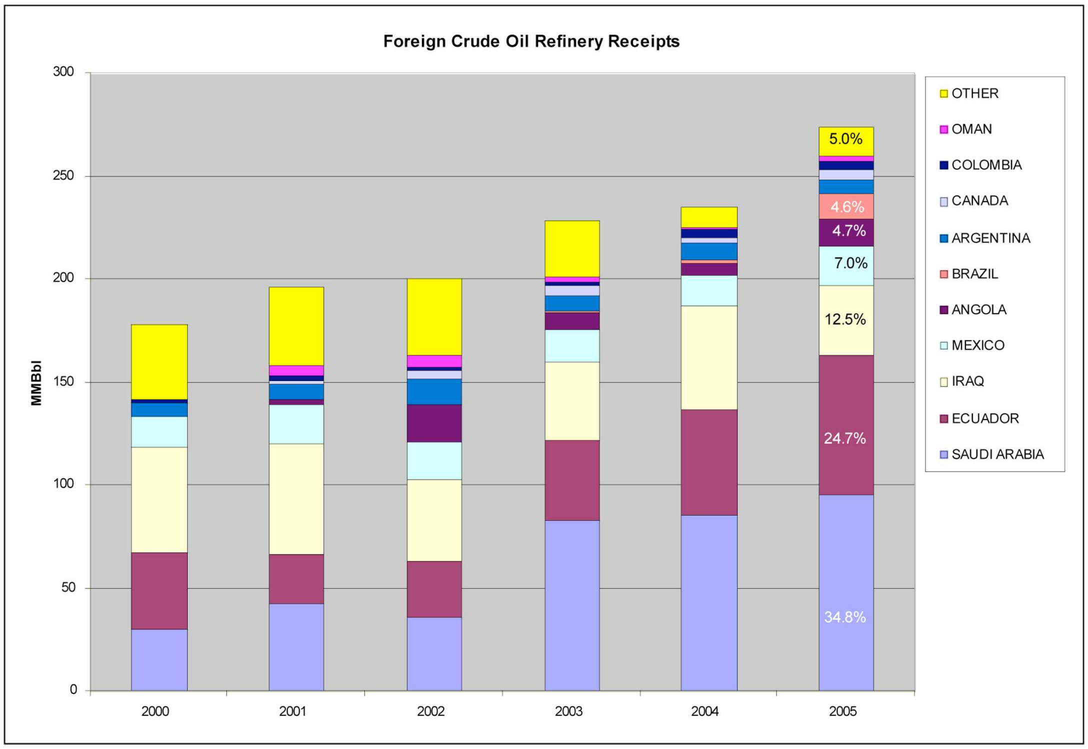

Figure 5.5: Foreign Crude Receipts
California Energy Commission [2007]

5.5.1 Saudi Arabia and Iraq

Most Saudi production comes from older onshore fields, but the Arab Medium and Heavy grades used by California refineries are primarily produced offshore northernmost Saudi Arabia. The oil fields of southeast Iraq, Kuwait and northernmost Saudi Arabia produce primarily from sandstone reservoirs of Cretaceous age. These fields are characterized by multiple pay zones and strong natural water drives. Cretaceous carbonate reservoirs and shallow heavy oil are also present.

The Safaniya Field was discovered in 1951 and is the world's largest offshore oil field.

Table 5.2: Safaniya Field, Saudi Arabia, Reservoir Parameters

Reservoir	Safaniya	Khafji
Net Thickness	136 feet	137 fet
Oil Gravity	27	27
Viscosity@100F	6,000 cp	470 cp
Sulfur Content	2.93 %	2.84 %
Porosity	26 %	25 %
Permeability	5700 md	6250 md

Production of Arab Heavy crude comes from two major sands, the Safaniya and the Khafji. Peak historical production was about 1.8 million BOPD in 1981. Table 5.2 above shows that these reservoirs combine excellent permeability with low oil viscosity at reservoir conditions so this is a conventional production operation even though we call the oil Arab Heavy.

The Zuluf Field was discovered in 1965. Production of Arab Medium crude comes from the Khafji sand. Production capacity was increased to 1.1 million BOPD in 1993.

The northern Saudi oil fields are becoming mature, but Qatif and Abu Safah of the southern Saudi fields were expanded in 2004 and produce Arab Medium. There is also a proposed 900,000 BOPD heavy oil development of the Manifa Field, but it has recently been delayed from its completion date of yearend 2011 Saudi Aramco cancels Manifa Contract [2008]. Manifa lies between the northern and southern producing areas and produces Arab Heavy from carbonate reservoirs of Cretaceous age. Table 5.3 gives parameters of the three most important reservoirs in Manifa Field.

The southern Saudi fields produce mostly Arab Light from carbonate reservoirs of Jurassic age. These reservoirs do not have natural water drives and are waterflooded for that reason. Horizontal drilling is now used extensively in Saudi oil projects.

Table 5.3: Manifaa Field, Saudi Arabia, Reservoir Parameters

Reservoir	U. Ratawi	L. Ratawi	Manifa
Net Thickness	50 feet	188 fet	71 feet
Oil Gravity	31	26	29
Viscosity@Reservoir	2.6 cp	4.4 cp	2.8 cp
Sulfur Content	2.77 %	3.66 %	2.97 %
Porosity	17 %	22 %	20 %
Permeability	50 md	600 md	300 md

About 80 percent of Iraq's oil production comes from the southeast. Northern Iraq's oil production is exported to the Mediterranean via Turkey and does not supply California. Further Iraq development depends on political stability and investment levels, which are difficult to predict at this time. Project Kuwait, which is a redevelopment of the fields in northern Kuwait, has been repeatedly delayed. For these reasons, future production levels are difficult to predict.

5.5.2 Latin America and West Africa

Ecuador was the source of a quarter of California's foreign imports in 2005. Nearly all of Ecuador's oil production comes from the Oriente Basin, which is located east of the Andes. Unlike the Middle East, where production is dominated by a small number of very large fields, oil production in Ecuador comes from numerous fields. Although Ecuador's production was less in 2007 than in 2006, several additional heavy oil fields could be developed including Pungarayacu, which is estimated to contain between 4.5 and 7 billion barrels of oil in place. Ecuador's Giant Pungarayacu to See Heavy Oil Appraisal [2008].

Mexico has been a significant supplier to California in the past, but is facing major production declines Watkins [2008]. Mexico's oil production has been dominated by the Cantarrell Complex that came onstream in 1980, and further production gains were achieved with nitrogen injection, but now the field is in decline.

Brazil supplies some oil to California and production is increasing due to deep-water developments. Perhaps the most exciting current development in oil supply anywhere is the series of recent discoveries in the presalt sediments of the Santos Basin. If recent government estimates of 50 to 80 billion barrels of oil prove accurate, this will have a major effect on the world oil trade and is likely to greatly increase the volume of oil shipped from the Atlantic to the Pacific Basin.

Argentina, Venezuela and Angola also supply some oil to California. It is not anticipated that Agentina's oil exports will grow significantly in the near future. Venezuela has huge heavy oil reserves. It is not currently a major supplier of oil to California, but eventual development of these resources could change that. Angola is now a supplier to California, its oil production is increasing and it has joined OPEC.

5.5.3 Canada as a Supplier to California

The heavy oil resources of Venezuela and Canada are the World's largest hydrocarbon accumulations. Figure 5.6 shows the world's eight largest hydrocarbon accumulations by oil in place. The source for this information dates to 1986, but such tabulations are difficult to find.

The economics of oil sands production recently became highly favorable and development is proceeding much more rapidly in Canada than in Venezuela. Canada has become the largest supplier of oil to the US and Canadian heavy oil dominates Midwest supply now. The Canadian Association of Petroleum Producers claims that production from the oil sands in Alberta will be 3.3 to 4.0 million BOPD in 2020.

Pipelines from the oil sands to Kitimat or Prince Rupert on the Pacific Coast have been proposed, and could supply California. There is an existing pipeline to Burnaby in British Columbia that has recently been expanded to 200,000 BOPD.

Oil sands production is more carbon-intensive than conventional oil. This carbon comes primarily from two processes; steam generation for bitumen extraction and production of hydrogen for refinery upgrading processes.

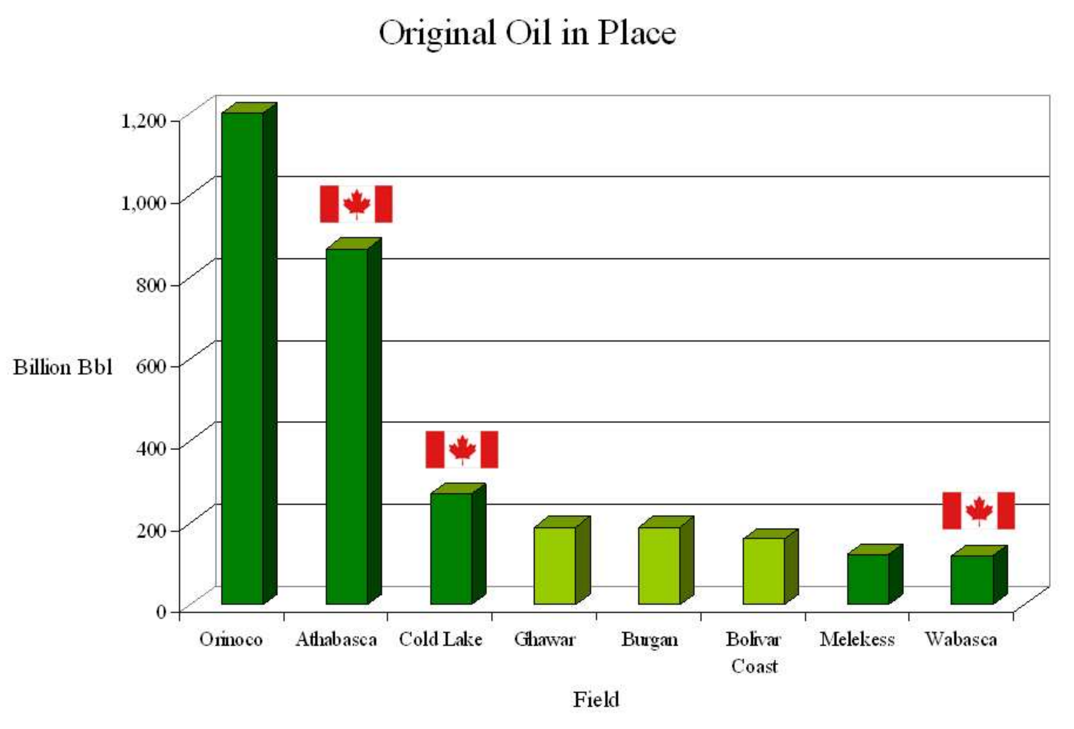

Figure 5.6: World's Eight Largest Hydrocarbon Accumulations
Data from Roadifer,1986

5.6 California's Refining Capacity

California refineries have evolved from processing California oil to processing a mix of California crudes, Alaska North Slope, Arab Heavy, and Ecuador Oriente, among others. Because of this history, California refineries are designed to process heavy oil.

Refineries designed to process heavy crude typically have three stages; distillation, cracking and coking. The ratio of coking capacity to crude distillation capacity gives an approximation of the extent to which a region's refineries have been designed to process heavy crude. Figure 5.7 shows that coking capacity in California is 25 percent of primary crude distillation capacity, as compared to 2.0 percent in Japan and 0.7 percent in Korea. This illustrates that enormous investments have already been made in heavy oil refining capacity in California.

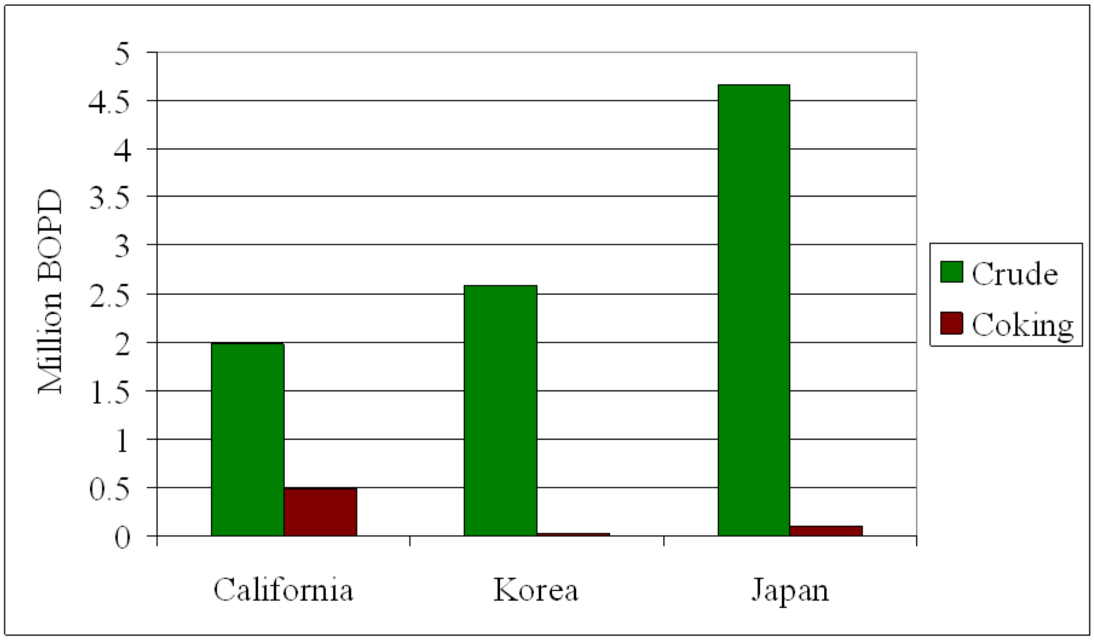

Figure 5.7: Crude Distillation versus Coking Capacity for Major Pacific Oil Markets
Data from Nakamura, 2007

5.7 Energy Security Considerations and the Low Carbon Fuel Standard

Concerns about energy security in California mostly revolve around oil. Because the waterborne crude market is global, regional oil price differentials are a function of freight rates if the market is in equilibrium. The problem is that oil supply disruptions are not equilibrium situations almost by definition. During disruptions energy security is an issue. The time required for markets to reach equilibrium is the time required to rearrange marine supply chains, which is to say that long supply lines decrease security. Diversification of oil supply sources increases security because it is unlikely that multiple sources would be disrupted at the same time. Substitution increases energy security as long as the supply of the substitute is independent of the supply of oil.

Concerns about climate change have led California to propose a low-carbon fuel standard. The goal is to reduce carbon equivalent emissions per unit of fuel energy by 10 percent by 2020 (Farrell and Sperling [2007]). The problem with this approach is that it does not address the actual problem, which is total emissions, while working against California's competitive strength in the refining of heavy oil.

5.8 Fuel Substitution Possibilities

Oil is used primarily for transportation fuel in California. Alternative vehicle fuels include natural gas, propane, biofuels and electricity.

Natural gas is the least environmentally damaging transportation fuel, but storage is more difficult than for liquid hydrocarbon fuels. California's natural gas currently comes from the U.S. and Canada. Natural gas has several desireable aspects; it is cheaper than oil, large new resources have been found in the U.S. lower-48, and Alaska also has very large volumes of undeveloped natural gas. Natural gas vehicles also do not have the toxic aromatic compounds that are a problem with gasoline and Diesel fumes.

Since 1977, the Energy Information Administration has published figures for associated and non-associated gas production. Figure 5.8 is an approximate comparison between the energy yielded from oil wells and that from gas wells over time in the United States. Oil production was converted at 5.95 GJ per barrel, marketed dry gas at 1025 btu per cubic foot and gas liquids at 4.525 GJ per barrel, which is the value for propane. In order to adjust for the fact that a significant proportion of gas comes from oil wells, the energy curves labeled Oil and Gas in Figure 9 were calculated by the following approach:

$$Oil = energyoil + energyassocgas + energyNGL \times \frac{volumeassocgas}{volumegas} \tag{5.1}$$

$$Gas = energynonassocgas + energyNGL \times \frac{volumenonassocgas}{volumegas} \tag{5.2}$$

Propane, biofuels and electric cars raise more difficult questions. Propane supplies are limited and it is an essential feedstock for the petrochemical industry. With biofuels, once again supplies are limited and biofuels compete with the food supply for land, water and fertilizer. Electricity comes from a variety of sources in California and it can be considered secure because nearly all of these sources are domestic. Electric cars are politically popular, but have an energy storage problem which limits their range. This is the reason that an earlier attempt to mandate electric cars in California was not successful. For the purposes of this paper, electric cars will not be considered current technology.

Of the currently available alternatives, natural gas appears to have the greatest potential for replacing a portion of California's oil usage in the transportation sector. Thailand, a nation which faces a similar choice between locally-produced gas and Pacific Basin oil markets, has embarked on a program to increase the number of natural gas vehicles on its roads from 122,375 in 2008 to 332,000 in 2012. Their goal is to replace 20 percent of oil imports by 2012 (Petroleum Authority of Thailand [2008]).

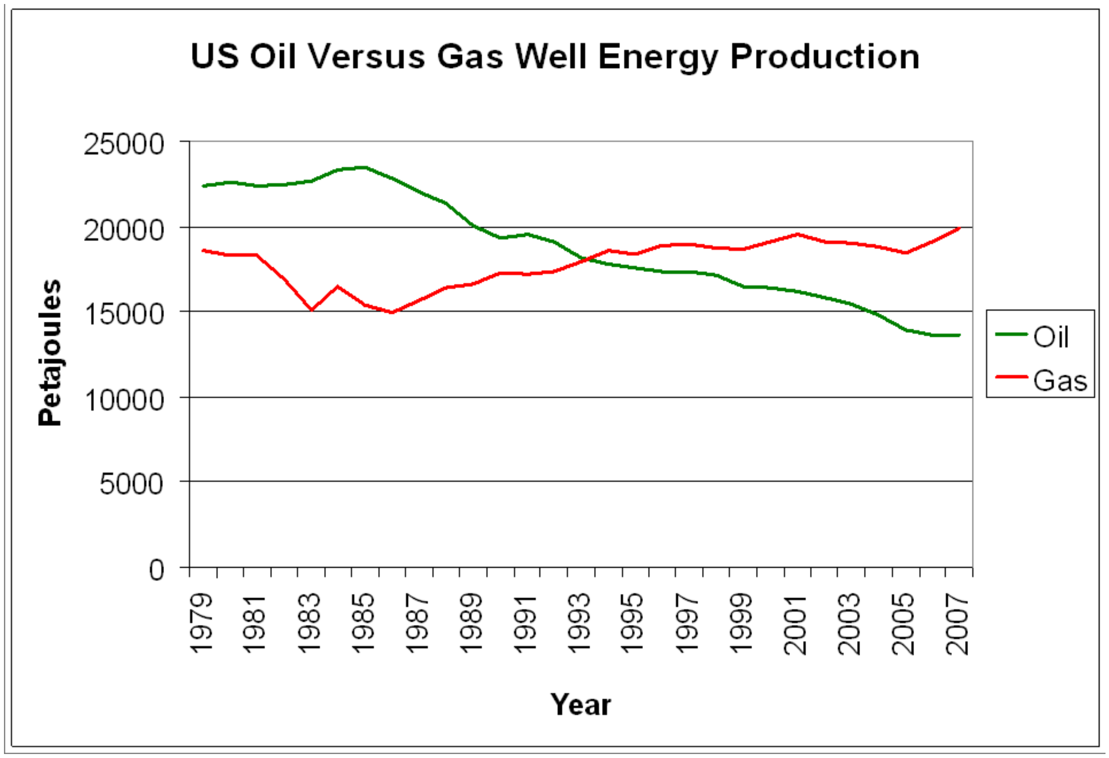

Figure 5.8: US Oil and Gas in Energy Units
Data source DOE/EIA

5.9 Conclusions

1. California is increasingly dependent on oil from the Middle East and Ecuador. This means the state is affected by factors outside of local control, such as the Manifa Field delay in Saudi Arabia. An additional concern about these areas is that reserves are reported without supporting information, leaving future supplies uncertain.

2. California's refining industry is built for heavy, sour crude oil. This capability represents an enormous cumulative investment in a technology that gives us an energy security advantage.

3. Canada is the most promising oil source for California in the long term. It has very large reserves of the heavy oils that California's refining industry is built for. Canada's reporting of reserves is highly transparent, removing uncertainty over the magnitude of its resources.

4. Environmental concerns restrict oil development offshore California. Another environmental regulation, the low-carbon fuel standard, reduces California's energy security by discouraging oil from Canada and onshore California.

5. Substitution of compressed natural gas for liquid fuels in a portion of the vehicle fleet improves transportation fuel security.

Bibliography

Alaska Division of Oil and Gas, *2007 Annual Report*, Alaska Division of Oil and Gas, Anchorage, AK 2008

American Petroleum Institute 1993, *Basic Petroleum Data Book*, Volume XIII, Number 2, American Petroleum Institute, Washington DC

California Division of Oil, Gas, Geothermal Resources, *Annual Report of The State Oil and Gas Supervisor, 1994 through 2006*, California Division of Oil, Gas, and Geothermal Resources, Sacramento CA

California Energy Commission, *2007 Integrated Energy Policy Report*, CEC-100-2007-008-CMF, California Energy Commission, Sacramento CA

Energy Information Administration, *Historical Production of Oil*, http://tonto.eia.doe.gov/dnav/pet/hist/mcrfpus1m.htm Department of Energy, Washington DC

Energy Information Administration, *US Natural Gas Marketed Production*, http://tonto.eia.doe.gov/dnav/ng/hist/n9050us2a.htm Department of Energy, Washington DC

Energy Information Administration, *US Crude Oil, Natural Gas and Natural Gas Liquids Reserves Report*, http://www.eia.doe.gov/oil_gas/natural_gas/-data_publications /crude_oil_natural_gas_reserves/cr.html
Department of Energy, Washington DC

Ecuador's Giant Pungarayacu to See Heavy Oil Appraisal, Oil and Gas Journal, October 27, 2008, pp 41-42 Pennwell Publishing, Tulsa OK

Farrell, Alexander E. and Sperling, Daniel, *A Low-Carbon Fuel Standard for California, Part 1: Technical Analysis, 2007*, University of California, Berkeley CA

Guerard, William F., *Heavy Oil in California, 1984*, California Division of Oil, Gas, and Geothermal Resources, Sacramento CA

Hallmark, Fred O., *Unconventional Petroleum Resources in California, 1982*, California Division of Oil, Gas, and Geothermal Resources, Sacramento CA

Minerals Management Service, *Beaufort Sea Lease Sale 195 Bid Recap, 2005*, Minerals Management Service, Washington DC

Minerals Management Service, *Planning Area Resources Addendum to Assessment of Undiscovered Technically Recoverable Oil and Gas Resources of the Nation's Outer Continental Shelf, 2006*, Minerals Management Service, Washington DC

Minerals Management Service, *Beaufort Sea Lease Sale 202 Bid Recap, 2007*, Minerals Management Service, Washington DC

Minerals Management Service, *Chukchi Sea Lease Sale 193 Bid Recap, 2008*, Minerals Management Service, Washington DC

Nakamura, David N., *Worldwide Refining Survey, 2007*, Oil and Gas Journal, December 24, 2007, Pennwell Publishing, Tulsa OK

Petroleum Authority of Thailand, *NGV Expansion Target*, http://pttweb2.pttplc.com/webngv/en/nw_pi.aspx Petroleum Authority of Thailand, Bangkok 2008

Roadifer, R. E., *How Heavy Oil Occurs Worldwide*, Oil and Gas Journal, March 3, 1986, Pennwell Publishing, Tulsa OK

Saudi Aramco cancels Manifa Contract, Oil and Gas Journal Online, November 19, 2008, Pennwell Publishing, Tulsa OK

Syms, Harold E. and Voskanian, Armen, *Estimated Oil and Gas Reserves Pacific Outer Continental Shelf*, OCS Report MMS 2007-012, 2007, Minerals Management Service, Washington DC

United States Geological Survey, *Arctic National Wildlife Refuge, 1002 Area, Petroleum Assessment, 1998, Including Economic Analysis*, USGS Fact Sheet FS-028-01, 2001, United States Geological Survey, Washington DC

Watkins, Eric, *Mexican production continues downward spiral*, Oil and Gas Journal, September 26, 2008, Pennwell Publishing, Tulsa OK

Chapter 6

Conclusions

A multi-Hubbert cycle analysis was performed on historical time series of U.S. coal extraction rates, resulting in an estimate of U.S. coal reserves that is much lower than the estimated recoverable coal reserves published by the U.S. Energy Information Administration. This approach differs from that used in Hook and Aleklett [2009] in being independent of reserve estimates. The difference is large enough to support the argument that there is no large surplus of coal to supply a coal-to-liquids industry.

A limited supply of coal will be diverted to its most valuable use. Electric power generation is the most valuable use of most grades of coal and will discourage coal-to-liquids conversion without an ongoing subsidy. This will remain the case as long as natural gas competes with coal in electric power generation. This analysis differs from other published work on coal-to-liquids conversion by addressing the relative cost of natural gas versus coal conversion as a source of transportation fuel, and how that cost is affected by interfuel competition in the power generation sector.

In Chapter 4, a multi-Hubbert cycle analysis was performed on global coal production data. The resulting base case of coal-generated carbon emissions is significantly below 36 of the 40 carbon emission scenarios from the IPCC. We conclude that the global peak of coal production from existing coalfields should occur close to the year 2011. The peak coal production rate calculated here is 160 EJ/y, and the associated peak carbon emissions from coal burning are 4.5 Gt C per year. After 2011, the production rates of coal and CO_2 decline, reaching 1990 levels by the year 2037, and reaching 50% of the peak value in the year 2047. It is unlikely that future mines will reverse the trend predicted in the base case scenario here, and current efforts to sequester carbon should be reexamined. This work differs from Mohr and Evans [2009] and Rutledge [2009] by using a multi-Hubbert cycle approach and by including qualitative geologic information as a check on results.

The last chapter examines the constraints on oil production from the Middle East and Ecuador, the principal foreign sources of oil to California, and concludes that heavy oil from Canada may be the most desirable future source of transportation fuels for California. The oil sources that are most attractive from an energy security standpoint are offshore California, arctic Alaska and the Alberta oil sands. All of these options are associated with environmental concerns. This chapter differs from other published work on the impact of future oil shortages by specifically addressing the impact on the state of California.

Given the critical economic importance of oil and coal resources, and the volume of evidence supporting the contention that they are less abundant than published reserve figures indicate, improvements in efficiency are urgent. California's oil supply is particularly vulnerable, its refineries are designed to process heavy oil and Alberta is the heavy oil source of the future. It would be foolish to exclude supplies that have about the same carbon intensity as California heavy oil. The urgency of the energy supply issue needs to be appreciated both in the state of California and in the University of California.